Max-Planck-Institut für Astronomie

Heidelberg-Königstuhl

Annual Report 1998

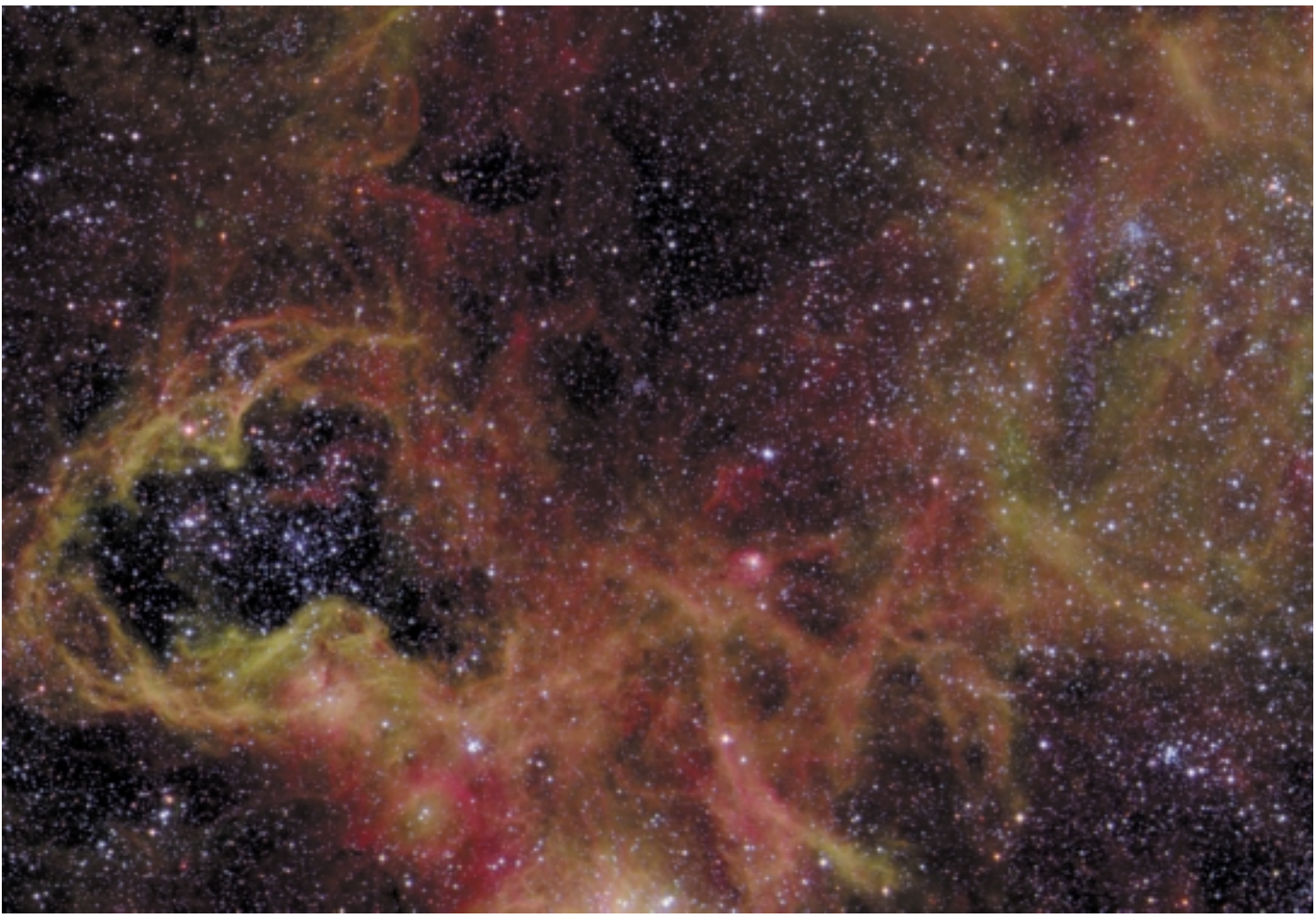

Max-Planck-Institut für Astronomie

Heidelberg-Königstuhl

Annual Report

Das Max-Planck-Institut für Astronomie

Managing Directors:
Prof. Steven Beckwith (until 31. 8. 1998), Prof. Immo Appenzeller (as of 1.8.1998)

Academic Members, Governing Body, Directors:
Prof. Immo Appenzeller (as of 1.8.1998, temporary),
Prof. Steven Beckwith, (on sabbatical leave as from 1. 9. 1998),
Prof. Hans-Walter Rix (as of 1. 1. 1999).

Emeritus Academic Members:
Prof. Hans Elsässer, Prof. Guido Münch

External Academic Members:
Prof. Immo Appenzeller, Prof. Karl-Heinz Böhm, Prof. George H. Herbig

Scientific Oversight Committee:
Prof. R. Bender, Munich; Prof. R.-J. Dettmar, Bochum; Prof. G. Hasinger, Potsdam; Prof. P. Léna, Meudon; Prof. M. Moles Villamante, Madrid; Prof. F. Pacini, Florence; Prof. K.-H. Schmidt, Potsdam; Prof. P.A. Strittmatter, Tucson; Prof. S.D.M. White, Garching; Prof. L. Woltjer, St. Michel l'Observatoire.

The MPIA currently employs a staff of approximately 160, including 43 scientists, 37 junior and visiting scientists, together with 80 technical and administrative staff. Students of the Faculty of Physics and Astronomy of the University of Heidelberg work on dissertations at degree and doctorate level in the Institute. Apprentices are constantly undergoing training in the Institute's workshops.

Anschrift: MPI für Astronomie, Königstuhl 17, D-69117 Heidelberg.
Telephone: 0049-6221-5280, Fax: 0049-6221-528246.
E-mail: Name@mpia-hd.mpg.de, *Anonymous ftp*: ftp.mpia-hd.mpg.de
Isophot Datacenter: phthelp@mpia-hd.mpg.de.
Internet: http://www.mpia-hd.mpg.de

Calar Alto Observatory

Address: Centro Astronomico Hispano Aleman,
Calle Jesus Durbán Remón 2/2, E-04004 Almería, Spain
Telephone: 0034-50-230988, -632500, Fax: 0034-50-632504,
E-mail: name@caha.es

Publication Information

Printed in Germany
Editors: Dr. Jakob Staude, Prof. Dr. Immo Appenzeller
Text: Dr. Thomas Bührke
Illustrations: MPIA and others
Graphics and picture editing: Dipl. Phys. Axel M. Quetz
Layout: Josef Hegele, Dossenheim
Printing and Production: Colordruck, Leimen
ISSN 1437-2924

Contents

I General

The MPIA's Research Goals

In 1967, the Senate of the Max Planck Society decided to establish the Max Planck Institute for Astronomy in Heidelberg with the aim of restoring astronomical research in Germany to a leading global position after the major setbacks it had suffered due to two World Wars. Two years later, the Institute commenced its work in temporary accommodation on the Königstuhl, under the direction of Hans Elsässer. The Institute moved into its new building in 1975 (Figure I.1). A long-term goal of the newly established MPIA was to build up and operate two high-performance observatories, one in the northern hemisphere and one in the southern hemisphere. In 1970, after an intensive search for a location, the choice for the northern hemisphere was made in favour of Calar Alto Mountain (height: 2168 metres) in the province of Almería, southern Spain. This European location offers good climatic and meteorological conditions for astronomical observations. 1972 saw the establishment of the »Deutsch-Spanisches Astronomisches Zentrum / German-Spanish Astronomical Centre« (DSAZ), known in short as the Calar Alto Observatory.

The complex technological problems associated with the planning and construction of the telescopes were solved in cooperation with Carl Zeiss of Oberkochen and other companies. In this way, a large number of firms have acquired know-how which has helped them to secure leading positions on the world market.

Between 1975 and 1984, the 1.2 metre reflector financed by the Deutsche Forschungsgemeinschaft as well as the 2.2 metre and 3.5 metre telescopes started operation on Calar Alto. The 80 centimetre Schmidt reflector was transferred from the Hamburg Observatory. There is also a Spanish 1.5 metre telescope on the site, operated by the Observatorio Nacional de Madrid. Figure I.2 shows a view of the telescope domes on Calar Alto. The original plans to construct a southern observatory on the Gamsberg in Namibia could not be implemented for political reasons. The 2.2 metre telescope which was intended for this purpose has been loaned to the European Southern Observatory for 25 years. Since 1984, it has been in operation on La Silla Mountain in Chile, with 25 % of its observing time available to the astronomers of the Max-Planck Society.

At present the operation of the Calar Alto Observatory is a central task for the MPIA. This includes the constant optimisation of the telescopes' capabilities: now that the ALFA adaptive optical system has become operational, the 3.5 metre telescope is once again at the forefront of technological development (Chapter III). Other aspects include the development of new measuring instruments in Heidelberg, the preparation of observation programmes and the subsequent data analysis. A substantial part of the Institute's work is devoted to building new instruments for the telescopes (Chapter III). The MPIA is equipped with

Figure I.1: The Max Planck Institute of Astronomy on the Königstuhl in Heidelberg.

Figure I.2: View from the south of the Calar Alto Observatory in southern Spain, with its five telescope domes. From left to right: the building for the Spanish 1.5 metre telescope, the Schmidt reflector, the 1.23 metre telescope, the 2.2 metre telescope, and the 43 metre high dome of the 3.5 metre telescope.

high-tech precision mechanics and electronics workshops for this purpose. With the Calar Alto Observatory, the MPIA has one of the two European observatories with the highest performance. Research concentrates on the »classical« visible region of the spectrum and on the infrared region.

In addition, the MPIA has been engaged in space-based research ever since it was established. This was associated with an early start on infrared astronomy which has played a particularly important part in the Institute's later development as a whole. In the 1970's, two photometers were developed and built at the MPIA, which flew on board the two solar probes Helios 1 and Helios 2, where they worked faultlessly. The fact that the measurements obtained at that time contain information that is still valuable today is shown by a recent data analysis which led to the detection of fluctuations in the solar wind (Chapter IV.3). A more or less parallel development to the Helios mission involved the THISBE balloon gondola (Telescope of Heidelberg for Infrared Studies by Balloon-borne Experiments). This altitude research balloon was designed to carry telescopes and equipment weighing as much as 400 kilograms up to a height of 40 kilometres, where long wavelength infrared observations are possible. Four telescopes with apertures of 6 to 20 centimetres were built in the workshops of the MPIA and were deployed on THISBE. Scientific aspects deserving particular emphasis here include the first observation of the central region of the Milky Way at a wavelength of 2.4 μm wavelength, and the measurement of the airglow, due to the emission of the OH-radical in the atmosphere.

The MPIA currently has a substantial involvement in the ISO project (Infrared Space Observatory, Figure I.3) of the European Space Agency ESA (Chapter II.3): ISOPHOT, one of four measuring instruments on ISO, was developed under the leadership of the Institute. ISO was switched off on 8. 4. 1998, after its supply of coolant had been exhausted. Since then, the observations with ISO have formed the basis for extensive work in all areas of astronomy (Chapters II.1, II.2, IV.2, and IV.3). These projects attest to the successful performance of this space telescope.

Summer 1998 saw the start of the three year postoperative phase. During this phase, the data must be carefully calibrated and archived; in this instance, particular importance is attached to a clearly arranged archive classified by objective criteria. This task was accomplished when ESA set up a central archive at its station in Villafranca, Spain, in 1998, and the four institutes responsible for the measuring instruments each built up a data centre in addition.

According to an agreement with ESA, the ISOPHOT Data Centre at the MPIA is one of the nodes in this international network totalling seven ISO data centres (Figure I.4). In cooperation with the ISO Science Operations Center, Madrid, the standard »PHT Interactive Analysis« software (PIA) has been developed at the MPIA to evaluate the raw data supplied by the satellite. In the year 1998,

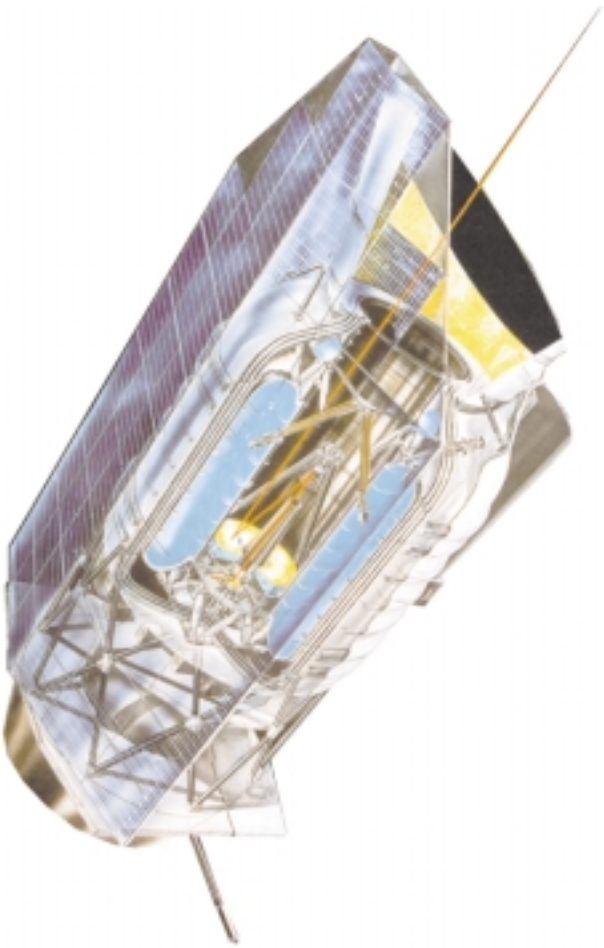

Figure I.3: Sectional drawing of ISO, the European Infrared Satellite Observatory cooled by liquid helium, in which the MPIA has a major involvement.

work started on a new, improved automatic analysis software (»Pipeline«), which will supply accurate data for the scientific archive.

In addition to the archiving and recalibration, the Heidelberg Data Centre also acts as a service facility for astronomers from other institutes. In 1998, more than 40 guest scientists visited the data centre, to receive support with data reduction over periods of several days (and several weeks on occasions). This facility is financed until the end of 2001 and it will be concentrating on the ISOPHOT data. The aim of all these efforts is the scientific interpretation of the data gathered during the ISO mission.

The experience gained with ISOPHOT was a decisive factor in the MPIA's major involvement in the construction of the PACS Infrared Camera. This will operate on board the Far-Infrared and Submillimeter Telescope (FIRST) of ESA (Chapter III). The launch of this 3.5 metre space telescope is planned for the year 2007.

Participation in international groundbased observatories and projects is also of major importance. For example, the IR camera MAX (Mid-Infrared Array eXpandable), built at the MPIA together with an associated tip-tilt secon-

dary mirror, has been working for some years at UKIRT (United Kingdom Infrared Telescope), the British 3.9 metre telescope in Hawaii – one of the largest telescopes in the northern hemisphere (Figure I.5). In return for these activities, the MPIA astronomers receive a fixed proportion of the observation time at this telescope.

The MPIA is coordinating the development of the high-resolution infrared camera CONICA for the ESO's Very Large Telescope (VLT), which is the world's largest telescope, on Cerro Paranal in Chile. Work has already started on the development and construction of MIDI, an interferometry instrument for the VLT. In 2000, this pioneering instrument should make it possible to couple two large telescopes interferometrically in the infrared (Chapter III) for the first time. Above and beyond this, as from the year 2002, the MPIA will be substantially involved in the Large Binocular Telescope (LBT, Figure I.6), another of the new generation of telescopes. The LBT is currently being built by an American-Italian-German consortium on Mount

Figure I.5: The MPIA participates in the UKIRT infrared telescope in Hawaii with a sensitive infrared camera.

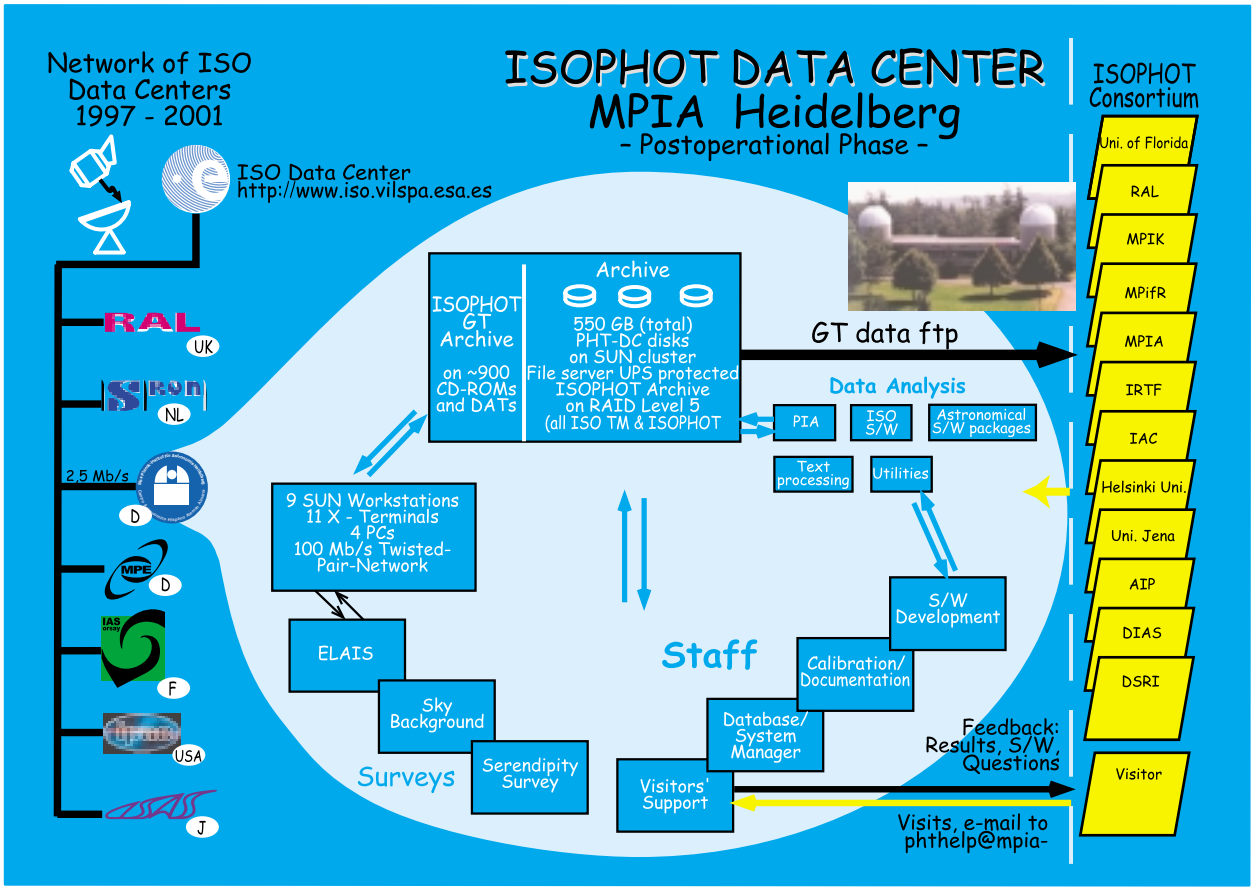

Figure I.4: After the end of the ISO mission, the data centres (left) handle the important task of archiving and recalibrating the collected data. The ISOPHOT data centre at the MPIA also acts as a service facility for visiting scientists.

Graham in Arizona, USA. It will be the most powerful telescope in the northern hemisphere. In conjunction with the MPI for Extra-Terrestrial Physics in Garching, the MPI for Radio Astronomy in Bonn, the Potsdam Astrophysical Institute and the Heidelberg State Observatory, the MPIA will probably have a 25% share in the costs and use of the LBT.

Aided by this wide and varied range of instruments, the MPIA will be able to go on making a major contribution towards astronomical research in the 21st century.

Thanks to its location in Heidelberg, the MPIA has the opportunity of working in a particularly active astronomical environment: there has constantly been a rich variety of cooperation with the State Observatory, the Astronomisches Rechen-Institut, the University's Institute of Theoretical Astrophysics and the Astrophysics Department at the MPI for Nuclear Physics. One particularly striking and effective aspect of this cooperation comprises the "Sonderforschungsbereiche", special research areas funded by the Deutsche Forschungsgemeinschaft over periods of many years: these are the Sonderforschungsbereich number 328 (»Evolution of Galaxies«, 1987–1998) and number 1700 (»Galaxies in the Young Universe«, from 1999 onwards), in which all the Heidelberg Institutes mentioned above are involved, with major proportions of their resources.

The Institute's tasks also include informing an extensive public audience about the results of astronomical research. Accordingly, members of the Institute give lectures in schools, adult education centres and planetariums, and they appear at press conferences or on radio and television programmes, especially when there are astronomical events which attract major attention from the public. Numerous groups of visitors come to the MPIA on the Königstuhl and to the Calar Alto Observatory. Since 1976, the premises of the MPIA have been the setting for a regular one week teacher training course held in the autumn, which is very popular among teachers of physics and mathematics in Baden-Württemberg.

Finally, the monthly journal Sterne und Weltraum (Stars and Space), co-founded by Hans Elsässer in 1962, is published at the MPIA. This journal is aimed at the general public and it offers a lively forum both for specialist astronomers and for the large body of amateur astronomers.

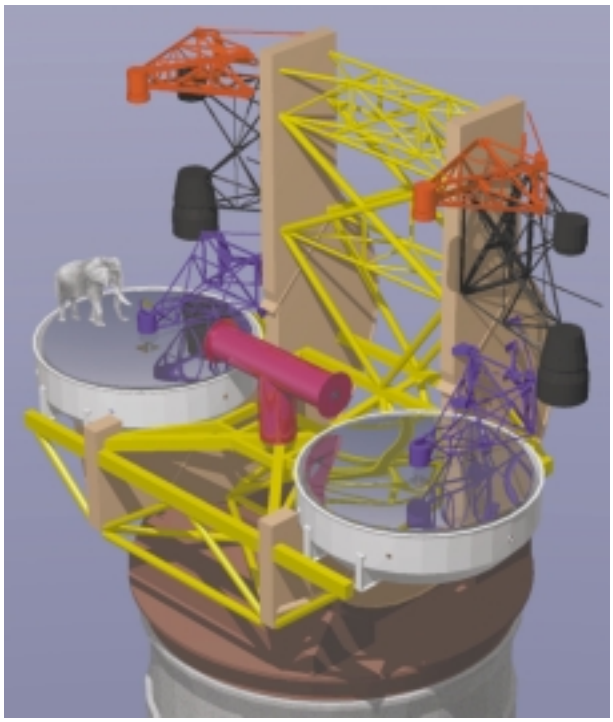

Figure I.6: Development drawing of the Large Binocular Telescope. It will have two 8.4 metre mirrors which will be carried on a joint mount.

Scientific Questions

The central question of all cosmological and astronomical research deals with the formation and evolution both of the universe as a whole, and of the stars, the galaxies, the sun and its planets. The MPIA's research program is oriented around this question. In the field of galactic research, the Institute concentrates on the formation of stars in large interstellar clouds made of gas and dust. In the field of extra-galactic astronomy, the focus is on the question of the large-scale structure of the cosmos, the search for the protogalaxies and research into active galaxies and quasars. These are remote stellar systems with an enormous radiation power. The observational astronomers are supported by a theoretical group, which uses sophisticated computer simulations to recreate processes in the universe extending over tens of thousands or millions of years. In this way, the MPIA achieves a fruitful synthesis of observation and theory.

Galactic Research

One important aspect of galactic research at the MPIA concerns the formation of new stars. The very first phases of this process unfold in the interior of the interstellar gas and dust clouds, which means that they remain hidden from our view in visible light. However, infrared radiation is capable of penetrating the dust, which is why this wavelength range is preferable for studying the early stages of the star formation.

The newly born star is surrounded by a dense equatorial dust disk in which the material can condense either to form more stars or to form planets. After a few million years, the disk finally disintegrates. This is also how astronomers imagine the birth of our solar system, 4.5 billion years ago. Empirical evidence for the actual existence of the protoplanetary disks began to be assembled more intensively during the 1980's, thanks in particular

to a great deal of work carried out at the MPIA. Presently, the following questions are at the forefront of this Institute's activities: how many of the young stars form a disk around themselves, and for how long can such a disk exist? Which factors decide whether one or more stars – or on the other hand planets – will form in a dust disk of this sort? Over what time scale do the disks disintegrate? (Chapter II.1)

One interesting phenomenon whose causes are related to the dust disks is that of the collimated gas jets which shoot out into space at high speed perpendicularly to the disk. These so-called jets, the cause of which has so far not been completely clarified, are among the bipolar flows – short-lived but fundamental phenomena in the birth of stars – which have been studied intensively and with great success at the MPIA since the start of the 1980's (Chapter IV.1). In every case, the equatorial dust disk mentioned above forms the plane of symmetry to the flows and the bright gas nebulae. The MPIA's astronomers are seeking answers to some important questions such as: how are the particles accelerated? How long does the bipolar phase last? Does every newly born star generate flows of this sort, and what role does this phenomenon play in the evolution of young stars?

The later stages of stellar evolution are also being investigated at the MPIA. Stars which are substantially more massive than the sun explode as Type II supernovae at the end of their lives. What happens in the last ten thousand years before the explosion? We are now familiar with a class of stars which are probably in this pre-supernova stage: the Luminous Blue Variables. Evidently they too are already casting off parts of their outer shell as they create a gas cloud around themselves. Probably the most fascinating example is provided by the star Eta Carinae with the Homunculus nebula which surrounds it. It formed the subject of a theoretical study which was devoted to the evolution of this object in the more recent past.

Extragalactic Research

It is a cosmologist's dream to be able to look back into the era of the universe when the first galaxies were being formed. However, the protogalaxies are so remote, and the light from them is consequently so faint, that it has so far been impossible to discover them. In order to achieve this goal, astronomers must use sensitive detectors working at the limits of the most powerful telescopes, and they also need to develop ingenious search strategies. Since the mid-1990's, the CADIS (Calar Alto Deep Imaging Survey) observational programme has been running on the 3.5 metre telescope at Calar Alto, with the aim of searching for the first galaxies in the universe (Chapter IV.2). CADIS is intended to run for at least five years and it is currently one of the MPIA's key projects.

Another topic of current interest is the development of a unified model for the large number of known active galaxies. These include radio galaxies, from whose centres two opposed jets of material shoot out, as well as quasars, the most luminous objects in the universe. At first sight, these two types of galaxies seem to have little in common with each other. However, for about ten years now there has been discussion of a model according to which the centre of these stellar systems contains a black hole surrounded by a dense dust ring. Depending on the observation angle, this ring conceals the central area around the black hole more or less completely. So, the galaxies then appear to us as quasars or radio galaxies. An extended ISO study at the MPIA is devoted to this question (Chapter II.2).

Less spectacular, but equally important for an understanding of how galaxies evolve, are the dwarf galaxies. These show certain features which it has not yet been possible to explain unambiguously. One of these characteristics is the unusual paucity of heavy elements in many dwarf galaxies. The theoretical group at the MPIA has investigated this problem with the help of extensive computer simulations, involving close examination of the role of supernovae in particular (Chapter II.3).

The Solar System

The solar system is not among the primary subjects dealt with at the MPIA. Only the zodiacal light has been the subject of detailed studies since the founding of the Institute. The zodiacal light owes its origins to a fine dust component which is distributed throughout the entire planetary system. Thanks to ISOPHOT, it has now become possible to examine the radiation of this interplanetary dust at wavelengths of about 200 μm for the first time. This allows some conclusions to be drawn about the composition and size of these particles.

However, when important current events have taken place within the solar system, the telescopes on Calar Alto have been able to demonstrate their capabilities time and time again. In 1994, images from the Calar Alto Observatory went around the world, showing the impact of debris from comet Shoemaker-Levy 9 on Jupiter.In 1997, Comet Hale–Bopp was the focus of a great deal of attention on the part of the public. With the Schmidt telescope on Calar Alto, it was possible to obtain detailed photographs showing the rare phenomenon of the striae.

Two pieces of work deserve emphasis during the year under report. On the one hand, a reliable thermal model for asteroids was successfully compiled for the first time. This makes it possible to use these small celestial bodies as infrared standards in the future. ISO data played a vital role in this undertaking (Chapter IV.3). Another productive study involved a new analysis of Helios data from the 1970s. This showed that the intensity of the solar wind was fluctuating at that time: an important contribution to the understanding of solar-terrestrial relationships, whose study is still in its infancy.

II Highlights

II.1 Disks around Young and Old Stars

The Vega Phenomenon

During observations with the IRAS space telescope in the mid-1980s, astronomers chanced upon unexpectedly intense infrared radiation from the stars Vega, Fomalhaut and Beta Pictoris. Subsequent investigations showed that it was not the stars themselves which are emitting this radiation, but rather the dust disks which surround them. The discovery of this Vega phenomenon, as it is known, came as a great surprise at the time. Admittedly, dust disks of this sort had been expected in the case of young stars, because they are a natural consequence of the birth of the star (see Chapter IV.1.). But Vega, Fomalhaut and Beta Pictoris are main sequence stars. They were formed as long ago as several tens or hundreds of millions of years, and they are now – like our Sun – in hydrostatic equilibrium, a condition of long-term stability.

The origin of the disks around main sequence stars has not been clarified at all. On the one hand, they could still be left-overs from the time when the central stars were formed. On the other hand, it is also possible that the supply of dust particles is continuously replenished, so that the disks are constantly being renewed. A fact which argues in favour of the second possibility is that several forces act on the particles, constantly destroying the disks:

- the stellar wind pushes the dust particles away from the star. If these particles are electrically charged, they will also be carried along by the interplanetary magnetic field.
- due to radiation pressure, the stellar light also pushes very small particles (with diameters of less than 1 μm) away from the star.
- at the same time, the stellar light transfers a momentum to the particles. On account of the dust's movement relative to the photons, this momentum not only has a component which is directed radially away from the star, but also a small component opposed to the direction of movement of the dust particle. Due to this so-called Poynting-Robertson effect, the particle is slowly decelerated, so that it approaches the star on a helical path and ultimately vaporizes close to it. In the case of particles with diameters of more than about ten micrometers to about one centimetre, the Poynting-Robertson effect dominates over the pressure of radiation.
- as a result of collisions between the particles, they become smaller and smaller, so that both the forces mentioned initially can act more effectively.
- in the case of »soft« collisions, the particles may remain stuck to one another and, if the particle density in the disks is sufficiently high, they can form larger objects (planetesimals). These are then able to combine to form large planets, due to gravitational force.

In actual fact, our Sun is also surrounded by a thin disk of dust. Since the particles are scattering solar light, this disk can be detected on the western horizon in the eve-

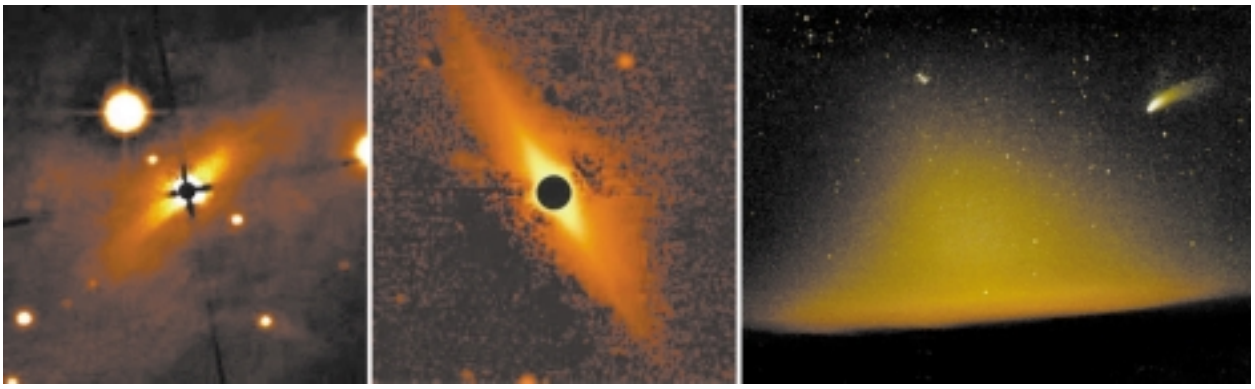

Figure II.1: The sun is surrounded by a thin cloud of dust which can be recognised on the horizon as a faintly shimmering cone of Zodiacal light (right). Other stars such as BD +31°643 (left), and β Pictoris (centre), also have a circumstellar disk.

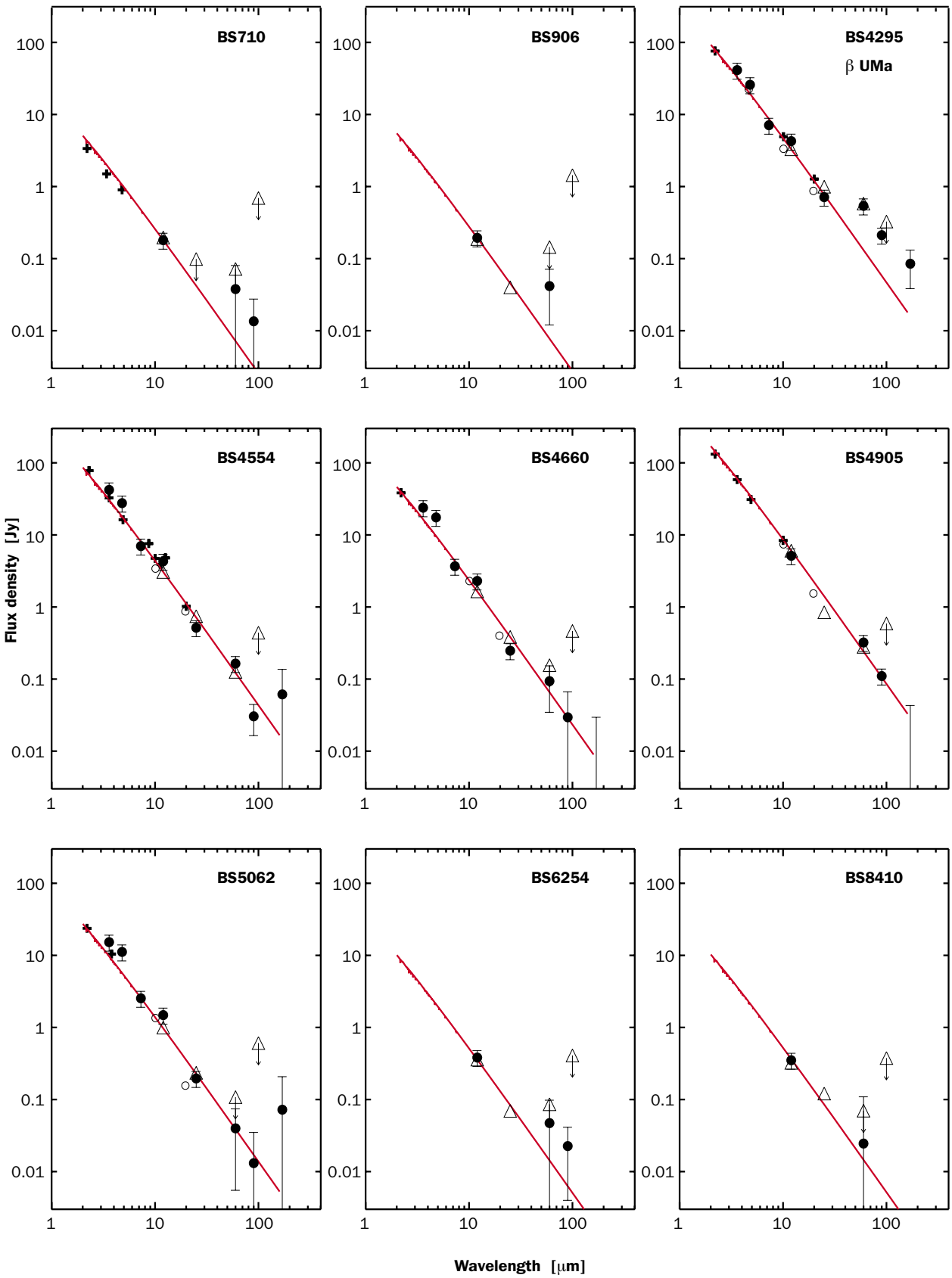

Figure II.2: The infrared fluxes of the observed stars in the Ursae Majoris cluster. Only β UMa (top right) shows a significant infrared excess which suggests a circumstellar dust disk.

nings and on the eastern horizon in the mornings, close to the ecliptic. This phenomenon is called the Zodiacal light (Figure II.1; see also Chapter IV.3). Because of the effects just cited, a dust disk of this sort is constantly losing matter. In our solar system, an additional factor is that dust particles are colliding with the planets and planetoids. In this case, the loss rate is estimated at about 10^{12} kilograms per year. If (as astronomers assume) the interplanetary dust disk of the sun is not a temporary phenomenon, the supply of this matter has to be constantly replenished.

There are good reasons for assuming that approximately $^2/_3$ of the interplanetary dust particles in the solar system are formed during collisions between planetoids, while comets supply the remainder. Now, if other main sequence stars such as Vega are surrounded by dust disks, does this mean that they too have planetoids and comets which continue to supply the dust? Or do their disks date back to the star formation phase?

This important question may be approached in different ways. For example, it is very important to know whether the masses of the disks decrease as the age of the stars increases. This is why astronomers from the MPIA, in conjunction with colleagues from the Konkoly Observatory, Hungary, and the Jena Observatory, have been using the ISO infrared observatory to study nine stars in the so-called Ursae Majoris group.

The rule or the exception?

All of these stars are approximately at the same distance of 80 light years, and they are all about 300 million years old. They originally belonged to an open star cluster, which has since dispersed. Only the central part has remained together. Like Vega, Fomalhaut and Beta Pictoris, the objects that were examined are A-stars.

Observations in the visible range are not suitable for determining the dust masses. In this case, all that is actually seen is the stellar light reflected from the dust particles. Moreover, since the disks are opaque in the visible range, it is only the particles from the outer zones of the disk which reflect. In the infrared and submillimetre ranges however, where the disks are transparent (i.e. they do not reflect), it is possible to observe thermal radiation which is emitted by all the dust particles. Hence, the radiation intensity in these wavelength ranges can also be used to estimate the total masses of the dust disks.

Earlier investigations in the Ursae Majoris group had only yielded indications of circumstellar dust in the case of one star, Beta UMa. Using the ISOPHOT photometer on ISO, it is now possible for the first time to examine these stars in the far infrared range as well. The ISO observations took place between May 1996 and January 1998 at eight wavelengths in the range from 3.6 to 170 µm. In addition to this, observations at 10 and 20 µm were carried out in February 1997 with the MAX infrared camera (built at the MPIA) on the UKIRT 3.8 metre telescope in Hawaii.

In the case of eight stars, the infrared flux at 60 and 90 µm could be explained purely by emission from the stellar photosphere. This means that in these cases, there were no indications of circumstellar dust whatsoever (Figure II.2). It was only Beta UMa which showed a clear infrared excess at wavelengths above 60 µm. The measured fluxes can be represented very well by two components: the stellar component of the A1V star Beta UMa, and a dust component with a temperature of 50 to 80 K (Figure II.3). This value is below the figure of 150 K determined on the basis of the IRAS data, at the lower end of the range from 60 to 120 K determined for stars similar to Vega. The dust around Beta UMa therefore appears to be relatively cool.

This result is altogether surprising. IRAS observations had shown that ten out of 22 A-stars are surrounded by dust. This high proportion was not confirmed in the Ursae Majoris group (one star out of nine). This difference has not yet been explained. The stars in the Ursae Majoris group hardly differ from those in the IRAS sample. It is true that eight out of the nine stars in Ursae Majoris are double stars, whereas the IRAS group only contains 30 to 40% of double stars. However, there is nothing to argue against the existence of disks in double stars, particularly as Beta UMa itself is a double star.

It is possible that the high infrared values measured by IRAS are not actually attributable to circumstellar

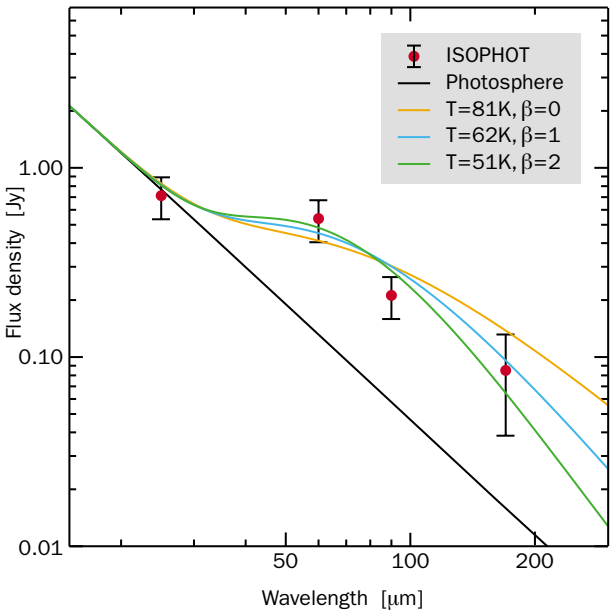

Figure II.3: The far infrared flux of Beta UMa can be explained by dust at a temperature of between 51 and 81 K; the actual temperature depends on the radiation properties of the dust (parameter β).

disks in every case, but rather to interstellar dust which was located in the measuring aperture of the IRAS telescope by chance. This would mean that the Vega phenomenon is by no means as widespread as had previously been assumed. This possibility is also favoured by an investigation dating from 1992, in which a search of 125 stars (many of which have an infrared excess according to the IRAS measurements) found no disks at visible wavelengths.

Assuming typical parameters for the dust particles, it was possible to deduce a dust mass of 0.22 lunar masses from the measurement data for β UMa. In the case of the eight other stars, upper limits of between 0.02 and 0.09 lunar masses were obtained. Together with the masses of dust disks around other A-stars which are already known, a trend appears, which suggests that the dust disks disperse over the course of several hundred million years (Figure II.4). While β Pictoris, one of the youngest stars at 10 to 100 million years, is still surrounded by a disk of about eight lunar masses, the disk around β UMa (300 million years) now has only one twentieth of this mass.

It is still too early to be able to speak of a general age evolution. In order to do so, more extensive data would be needed, especially for even younger stars as well. In order to obtain these data, a study is in progress at the MPIA on so-called Herbig-Ae/Be stars, the precursors of the main sequence A-stars. Investigations in the submillimetre range already suggest that these stars, aged only 100000 to one million years, are surrounded by disks with dust masses in the range of several tens of thousands of lunar masses.

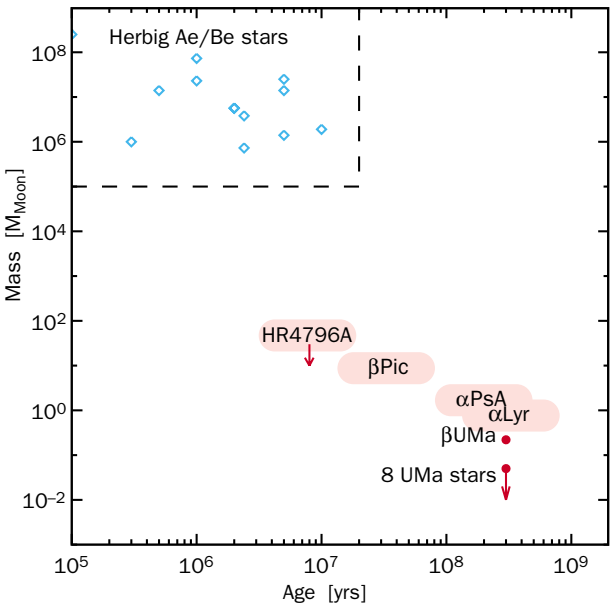

Figure II.4: The masses of the dust disks appear to decrease as the age of the star increases.

The precedence case of Beta Pictoris

The best-investigated dust disk around a main sequence star is the one around β Pictoris, an A5V-star with approximately two solar masses. In 1984, its large infrared excess was discovered in IRAS data, and shortly after this, american astronomers obtained direct evidence of the disk in the visible wavelength range. To do this, they used a telescope with a coronographic mask. This covers the bright star in the light ray, so that the dust disk (which emits weak light) is made visible. This image showed a disk which is viewed virtually edge-on. It could be detected up to an angular distance of about 40 seconds of arc from the star. Given that the distance from β Pictoris is 63 light years, this corresponds to a radius of 800 astronomical units (AU) – about twenty times the distance between the Sun and Pluto. Photographs with Hubble Space Telescope also became possible at a later stage. Surprisingly, these images – with a resolution in the range of one tenth of a second of arc – showed that the disk is not entirely symmetrical. It features a slight distortion in relation to the longitudinal axis beyond a radius of 150 AU, and its surface luminosity is also slightly asymmetric in relation to the star (Figure II.5).

The cause of this asymmetry has been – and still is – the source of a great deal of speculation. In all probability, a close fly-by of β Pictoris by another star could be ruled out. Some astronomers are considering the possibility of an invisible planet at a distance of 20 AU from the star. However, there are doubts about this hypothesis. Spectroscopic observations have suggested gas which is falling into the star. It is possible that what is visible here is matter from comets which vaporise in the vicinity of the star and then fall into the central star. As is also the case in the solar system, comets and bodies similar to planetoids could act as suppliers of dust. In 1997/98, the disks were also observed in the near infrared and in the submillimetre range. The latter observations provided an estimate for the mass of β Pictoris of eight lunar masses – considerably more than for Vega (0.7 lunar masses) and Fomalhaut (1.5 lunar masses). Interestingly, the disk evidently does not extend down to the star, but has a hole at its centre with a radius of about 70 AU. This finding has also contributed towards speculations that a large planet or several small planetoids have formed there, sweeping the space around them empty of dust. However, it is also possible that dust particles are vaporised in the vicinity of the star, or that they have been removed by the Poynting-Robertson effect.

It is now possible to close the data gap between the near infrared and the submillimetre range, since an opportunity has arisen for astronomers from the MPIA and colleagues from the Max Planck Institute for Nuclear Physics in Heidelberg and Great Britain to observe Beta Pictoris with ISOPHOT on ISO.

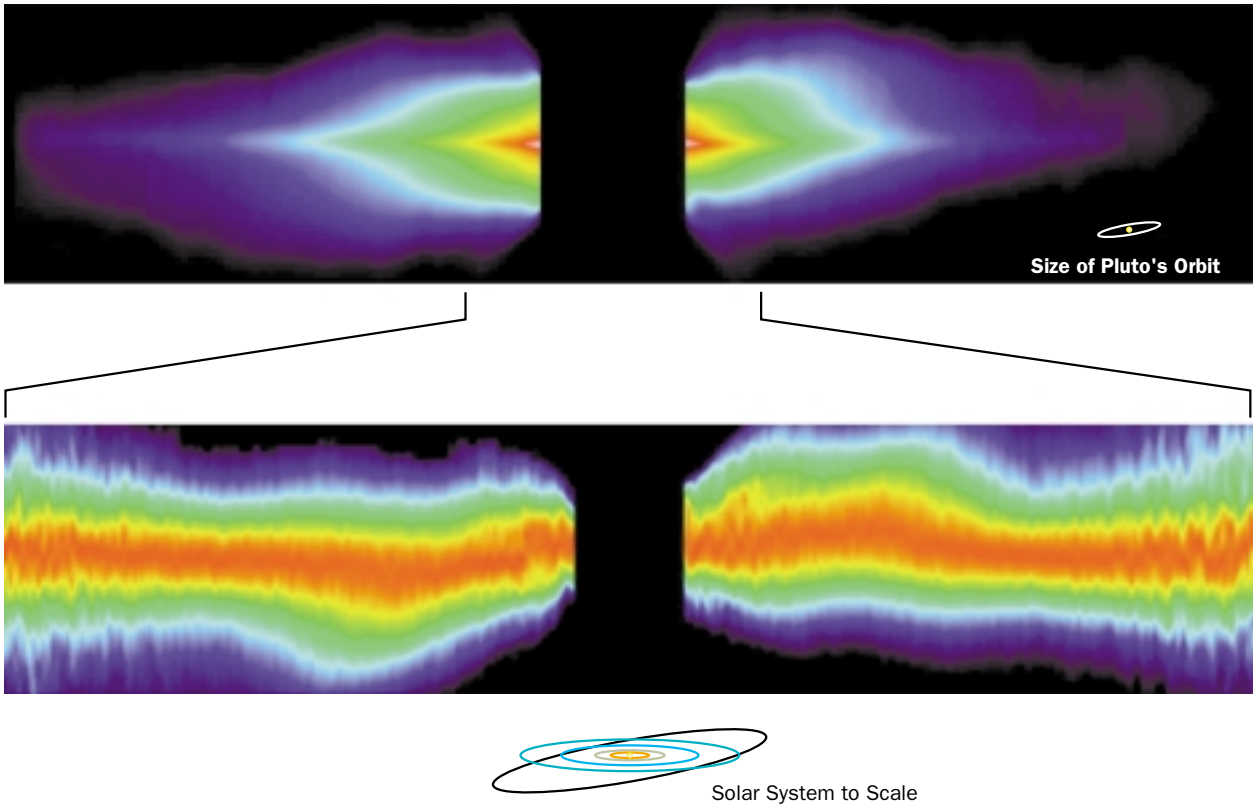

Figure II.5: On the high resolution images of the Hubble space telescope, the dust disk of Beta Pictoris shows slight asymmetries whose cause has not been clarified. (Photo: NASA/ESA)

The images were obtained by first scanning the object in fine stages with an aperture smaller than the diffraction image of the source. The image was then synthesized by interpolation between the points of a total of eight overlapping scans (Figure II.6). A comparison of the image which was obtained in this way with the star Gamma Draconis, which has a pointlike appearence, shows that the disk around Beta Pictoris was spatially resolved, and the longitudinal extent (at wavelength 60 µm) of 25 seconds of arc (Figure II.7) is substantially less than in the optical range (40 to 48 seconds of arc). The measured infrared flux showed a maximum at 60 µm in the range from 4.9 µm to 200 µm (Figure II.8). The measured curve can be explained by a thermal spectrum with a temperature of 85 K, if sizes of between 1 µm and 5 µm are assumed for the dust particles. Between wavelengths 8 µm and 24 µm, a second component is apparent with higher temperature of 300 to 500 K. Moreover, between 9 µm and 11.6 µm, an emission feature of silicate dust shows up. However, there were no indications whatsoever of polycyclic aromatic hydrocarbons, which are suspected to be a major component of the interstellar dust.

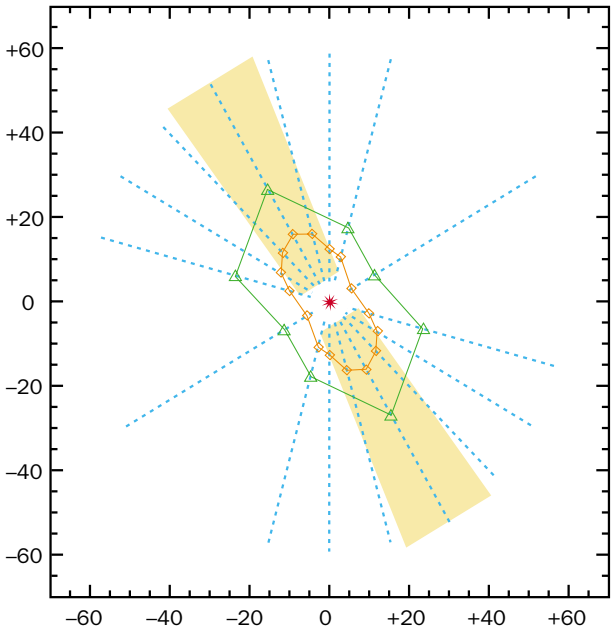

Figure II.6: The dust disk around Beta Pictoris was scanned in eight different directions by ISOPHOT.

Since the properties of the dust particles are not known, estimating their mass is also a uncertain. The total mass lies between 0.9 and 2.7 lunar masses, which is significantly smaller than the figure deduced from the submillimetre measurements. This can probably be attributed to the fact that there is very cold dust in the

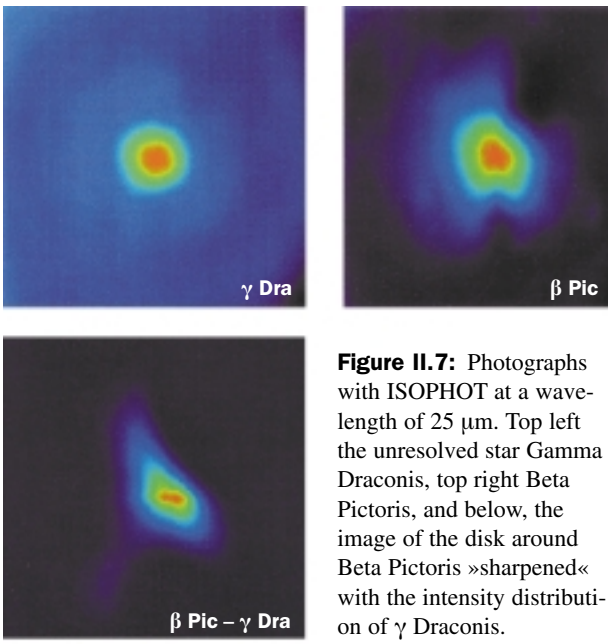

Figure II.7: Photographs with ISOPHOT at a wavelength of 25 μm. Top left the unresolved star Gamma Draconis, top right Beta Pictoris, and below, the image of the disk around Beta Pictoris »sharpened« with the intensity distribution of γ Draconis.

outer regions, which cannot be detected in the far infrared range.

Even the rather lower mass figure which has now been determined with ISO still corresponds to the total mass of at least one million comets. The data do not exclude the possibility that Beta Pictoris is surrounded by a cloud of comets, similar to the Sun.

Figure II.8: The infrared flux of Beta Pictoris shows a maximum at a wavelength of 60 μm.

Dust Disks in Double Stars

Speckle polarimetry in the infrared

The star Z Canis Majoris (Z CMa) has not yet reached the main sequence. It belongs to the Canis Majoris OB1 association which is some 3000 light years distant. It has a mass greater than the Sun, and is one of the group of young Ae/Be stars. It is also a member of the rare group of »FU Orionis« stars. These are young objects which feature large luminosity outbursts at irregular intervals. These outbursts are not due to the star itself, but rather to instabilities in an accretion disk.

Z CMa has a number of other interesting features as well. In 1989, astronomers at the MPIA discovered two jets which are emitted from near the star in opposite directions (Chapter IV.1). Their velocities, of up to 620 km/s, are among the highest known in jet systems. It has also been possible to detect an extensive bipolar molecular outflow.

In 1991, when emission was detected from Z CMa in the millimetre and submillimetre ranges, this was attributed to a circumstellar dust disk with 0.2 solar masses. Interestingly, it was established in the same year that Z CMa is actually a double star, whose components are at a distance of only 0.1 seconds of arc (corresponding to 100 AU) from one another. Z CMa therefore offers a good opportunity to approach the question of how disks behave in double star systems.

Moreover, the disks may also contain information about the birth of the double stars themselves. One possibility is in fact that two stars form separately, and bond together gravitationally when – by chance – they

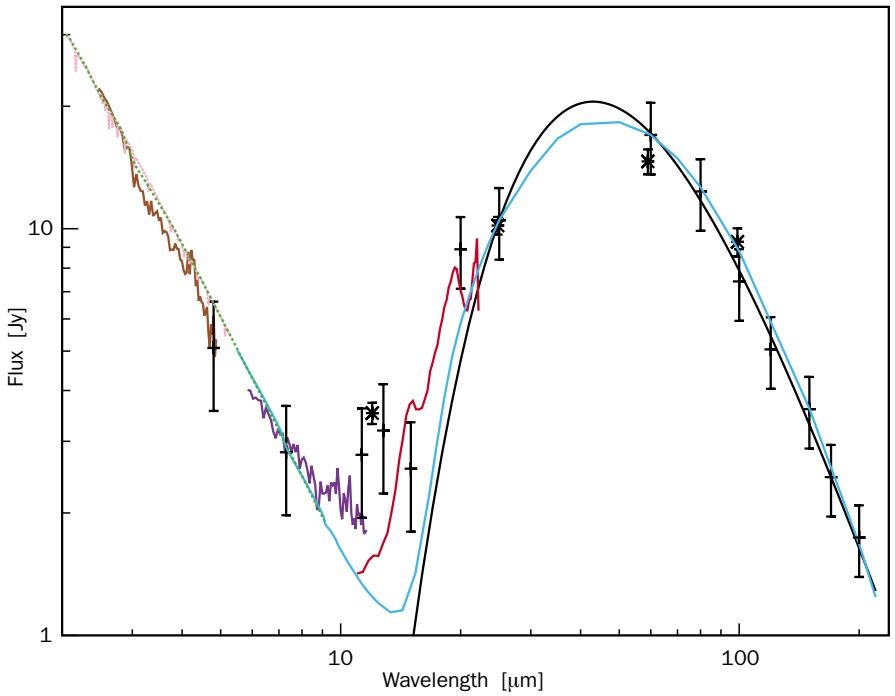

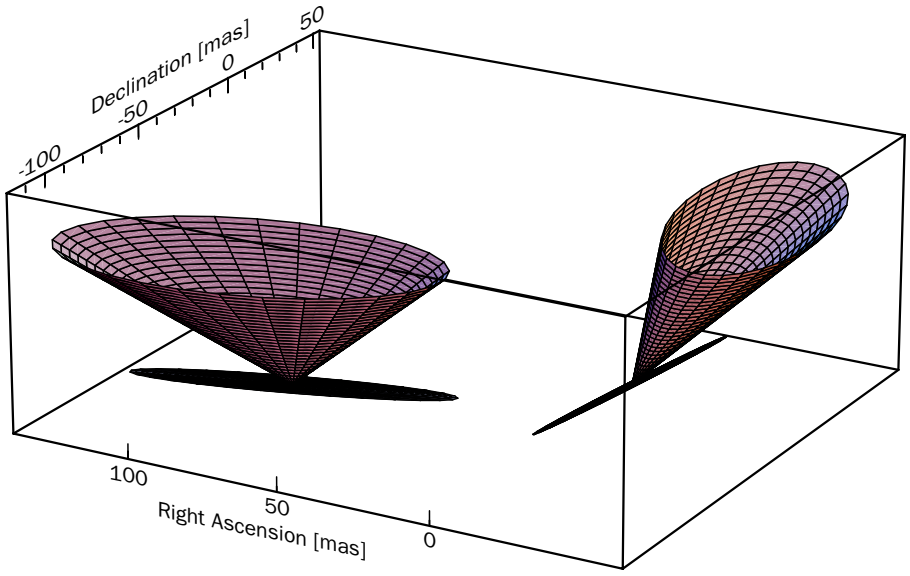

Figure II.9: The disk planes of the main star of Z CMa (right) and its companion, derived from Speckle polarimetry. The cones indicate the limits for the normal on the disk planes, which were derived from the observations.

fly past one another at close range, with some form of braking on one or both stars. In a case of this sort, one would expect that the axes of rotation of the stars – and therefore the equatorially positioned disks as well – would be inclined randomly in relation to one another. However, it is more probable that two stars are formed in the same molecular cloud core, which fragments in the course of its contraction (see Chapter IV.1). In this case, both disks should lie approximately in the same plane. Regarding Z CMa, it was suspected not only that the individual components are each surrounded by a disk, but also that a circumbinary disk surrounds both the stars. However, this question remains unanswered, due to the proximity of the two stars.

Thanks to a high-resolution astronomical method known as speckle polarimetry, astronomers at the MPIA, together with colleagues from the Thuringian State Astronomical Observatory, Tautenburg and the Jena University Astronomical Observatory, are now able to obtain further details about this interesting star system.

Polarimetry is a very effective tool for obtaining information about the distribution of the dust in the surroundings of a star, in cases where the structures under observation are too small to be resolved directly. This method has been used for many years at the MPIA to examine circumstellar nebulae, and has been constantly refined since then with great success. It operates on the basis of the following principle: normal stellar light is not polarized. In this case, the electrical vector of the electromagnetic radiation field oscillates in random directions. However, if the light is scattered or reflected by dust, the electrical vector will then oscillate in a preferred plane – and the light is polarized. The direction of polarization and the degree of polarization (the proportion of polarized light in the whole beam) yield information about the spatial arrangement of the dust cloud.

Polarimetry has now been combined with another modern observation technique which was perfected at the MPIA after many years of work: this is the speckle technique, which makes it possible to »outwit« the turbulence of the air. In normal cases, astronomical images are exposed for several minutes or even hours. During this time, the image constantly jumps around in the focal plane of the telescope due to turbulence in the air. The consequence of this is that the images become blurred, and the large telescopes never attain their theoretically possible resolution (limited by diffraction). One possibility of circumventing this is the speckle technique, in which a large number of images are exposed for such a short time that the air turbulence does not blur the picture during exposure. Then, the individual diffraction-limited images can be analyzed in a computer and added together to create a diffraction-limited image.

This technique has been used in the near infrared on the 3.5 metre telescope on Calar Alto, in order to examine the two components of Z CMa. About a thousand single images each with an exposure time of 200 milliseconds each formed the basis for the first separate polarization measurement of the two stars.

Surprisingly, both the stars show relatively high polarizations. The north-western component (regarded by many as a Herbig-Ae/Be star) was polarized at 4.2% (angle of polarization 173 ± 34 degrees), and the south-western component (probably the FU Orionis star) showed even stronger polarization, at 8.1% (angle of polarization 102 ± 45 degrees).

The data were analysed using a model in which the light from a star is reflected from the disk surrounding it in the direction of the observer. From this model, we infer that both the stars are each surrounded by a disk, with planes inclined at 40 to 60 degrees in relation to the celestial plane (Figure II.9). A circumbinary disk (one surrounding both the stars) is probably present as well, but this could not be confirmed directly on the basis of these measurements. In fact, the two polarization angles that were measured appeared not to correspond, which could allow the conclusion that the two disks do not lie in the same plane (the disk plane is parallel with the polarization plane). However, the observation error is very large, and on the basis of other arguments, the astronomers have arrived at the conclusion that the planes should be regarded as coplanar. This would argue in favour of the formation of the double star from one single cloud core, but it does not entirely rule out a separate formation.

The fact that both the stars have a disk is also very interesting in its own right. If both the components are only about 100 astronomical units away from one another, the disks must be relatively small because of their mutual gravitational influence. On the other hand, if this is merely a projected distance, then the true spatial distance and the disk radii could be substantially greater.

The young system Haro 6-37

The situation may well differ in the case of Haro 6-37. This star is located in the star forming region of Taurus-Auriga, about 500 light years distant. It is a double system, whose components are separated from one another by 2.6 seconds of arc (corresponding to 400 astronomical units). An age of just 600,000 years has been determined for both stars. In 1995, astronomers inferred a disk of 0.017 solar masses from measured fluxes at millimeter wavelengths.

At the end of 1997, astronomers at the MPIA, together with colleagues from Potsdam and Arcetri, observed Haro 6-37 at the 3.5 meter telescope at Calar Alto, using two different methods. Firstly, the system was briefly occulted by the moon on 16 November. This event offers a unique opportunity to detect extended structures with high spatial resolution in the range of one thousandth of a second of arc! The principle is simple: if a single star is occulted by the moon as it passes in front of the fixed stars in the sky, the star will disap-

Figure II.10: Observed decline of brightness when Haro 6-37 is occulted by the moon. The fluctuations allow us to conclude the existence of a third component, Haro 6-37/B.

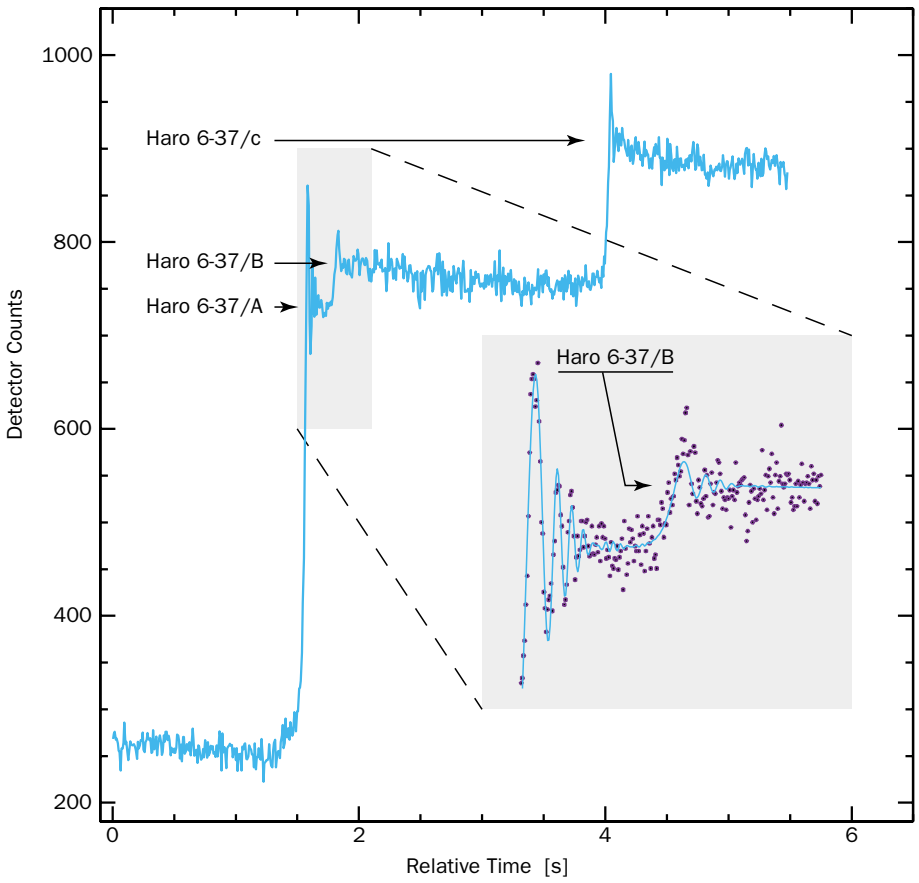

pear abruptly. However, if the star consists of several components, the measured intensity signal becomes weaker by stages, since first one and then the other component will disappear behind the moon. If there is also a compact luminous nebula, the intensity will decrease continuously.

An infrared photometer with a time resolution of 1.95 milliseconds was available on the 3.5 metre telescope. This made it possible to detect the two stars that were already known, the main component Haro 6-37 and its companion Haro 6-37c, without any difficulty (Figure II.10). Surprisingly, only 0.09 seconds of arc away from the main star, now called Haro 6-37A, a third component was observed, which was named Haro 6-37B. In the near infrared, this object is about ten times weaker than the primary star. Only one week later, this component (which had not been known until then) was confirmed with the help of speckle interferometry.

What do we know about the existence of circumstellar disks in this system? The data from the lunar occultation suggest an extended emission around the main component – this could involve the disk which was observed at millimetre wavelengths. These observations argued in favour of a compact disk with a radius of at least 15 AU, starting at a distance of 0.013 AU from the main star. The newly discovered stellar component is at least 46 AU away from the main star. It could exert gravitational influence on the disk. Whether this close companion is also surrounded by a disk, and whether there is perhaps a circumbinary disk as well, are matters which could not be resolved on the basis of these observations.

These observations supplied the first empirical approaches to dealing with the question of protoplanetary disks in double and multiple systems. Model calculations by the theoretical group at the MPIA have suggested that the question as to whether circumstellar or circumbinary disks form in a double star system is dependent on a variety of factors (cf. p. 59 in the 1997 Annual Report). In particular, these factors include the masses and distances between the components, and the angular momentum of the system. This problem will also need to be treated with high priority in the future, since latest observations show that virtually all stars are formed in multiple systems (cf. below, Chapter IV.1, and p. 49 in the 1997 Annual Report). How this affects the formation of planets remains largely unclear.

II.2 Quasars and Radio Galaxies

The unified scheme on the test bench

When the American radio engineer and amateur astronomer Grote Reber discovered a bright radio source in the constellation of Cygnus in 1944, using a home-made radio telescope in his own garden, he opened up the path to a type of celestial object which had until that time been unknown. The object discovered by Reber, Cygnus A (Figure II.11), belongs to the group of radio galaxies which are now numbered among the active galaxies. Active galaxies are stellar systems which release enormous quantities of energy that cannot be explained by normal stellar processes. Since this energy is generated in the central regions of the galaxies, the term »active galactic nuclei« is also used. They include objects such as radio and Seyfert galaxies, BL-Lac objects, blazars and quasars. Although these galaxy types show very different characteristics in their spectrums, they share an unusually high level of nuclear (core) activity as a common feature. For about ten years now, there has been discussion of a unified scheme, according to which these objects – which appear to be different – are actually all of one single type, whose members are merely seen from different angles.

At the MPIA, active galaxies – in particular quasars – are among the focal points of research. The ISOPHOT infrared photometer of the ISO space telescope opened up the possibility of observing active galaxies in the far infrared with high sensitivity, and also of examining them with polarimetry for the first time. The first results not only support the unified scheme, but also confirm that the prototype of all radio galaxies, Cygnus A, is actually a quasar hidden behind dense clouds of dust.

The unified scheme for active galaxies

For the purpose of the unified model, all active galaxies contain the following basic components (Figure II.11, centre): at the centre of the galaxy, there is a black hole of several hundred million solar masses, which attracts gas and dust from the surroundings. Initially due to its angular momentum, this matter gathers together to form a disk around the black hole. Friction or other processes cause the matter to lose kinetic energy, and it spirals slowly into the black hole, following helical paths. As this happens, high-energy radiation is emitted by the hot gas, and this radiation can escape into space. Supported by strong magnetic fields, two gas jets can shoot out into space simultaneously and almost perpendicularly to the disk plane in the direction of both poles, at virtually the speed of light. Strong jets end far beyond the galaxy in so-called »Hot Spots«, which are generally surrounded by extended bubbles of intensive radio radiation (cf. Figure II.11 and p. 64 in the 1997 Annual Report). In the interior of the jets, electrons are moving almost at the speed of light. As they do so, they move away from the black hole on corkscrew-like paths along the magnetic field lines, emitting synchrotron radiation primarily in their direction of movement. The synchrotron radiation thus forms a cone, similar to the one created by a car headlamp, with the jet as the central axis.

Now, in the unified model, the different appearances of active galaxies are interpreted as a purely geometrical effect. In fact, if one looks at these systems from different angles, different areas supply the major portions of the observed radiation.

If one of the jets is pointing directly at the observer, the synchrotron radiation emitted by the electrons will dominate the spectrum. Objects with these spectral characteristics are known as BL-Lacertae objects and blazars. Blazars – a word constructed from BL-Lacertae and quasars – are primarily typified by the quick variability of their radiation. This is attributed to fluctuations in the ejection of the jet particles.

If the jet axis is viewed from a greater angle, then the radiation of the hot spots and radio bubbles will dominate. This has been observed in the majority of quasars with radio emission and in radio galaxies.

However, a large portion of the quasars and other active galaxies only emit weak radio radiation, or none at all. These are referred to as radio quiet quasars. To explain their appearance within the unified model as well, one would have to postulate the existence of a further component: a thick ring of dust which surrounds the black hole and the central disk. If one looks directly onto the edge of this torus, it covers the black hole and the central region of the disk. In this case, moreover, we do not register the optical and UV radiation which is typical of quasars.

In expert circles, this unified model is deemed very attractive, since it reduces the majority of active galaxies to a simple basic scheme. However, it is by no means taken as guaranteed. For one thing, the central components – primarily the accretion disk and the dust ring which surrounds them – are so small that they cannot be detected directly even with instruments of the highest resolution. There are only indirect indications of the existence of an absorbing medium (probably dust) in the area surrounding the black hole. However, no reliable statement can be made about its spatial distribution. Furthermore, the model seems to over-simplify matters in the view of certain astronomers. More specifically, it fails

to take into account the fact that the central machinery in various objects may be in different physical states. Hence, for example, the dust disks can have different temperatures and can therefore emit radiation of differing intensities and wavelengths. Also the activity in the jet close to the black hole can fluctuate significantly, which has an effect on the emission of the jet particles.

Observations with ISOPHOT in the far infrared

The unified scheme can be verified using far infrared observations, among other methods. The dust ring in fact absorbs the optical and ultra-violet radiation from the central region, and heats up. As a result of this, the ring itself emits thermal radiation in the far infrared. Since the dust is transparent to radiation in this wavelength range, this happens uniformly in all directions. This means that while the proportions of synchrotron and optical radiation vary with the angle of vision, all objects should show the same far infrared characteristics for the dust torus.

The radiation emitted by the jet and the dust disk differ in their characteristics due to the different mechanisms by which they are caused. The dust emits thermal radiation. Its spectral distribution therefore corresponds to a Planck curve with a marked maximum whose position depends solely on the temperature of the dust. By contrast, the electrons in the jets that are accelerated in magnetic fields emit non-thermal synchrotron radiation. Their intensity rises monotonically as the wavelength increases.

The infrared range plays a crucially important role in the differentiation between thermal and non-thermal radiation: at dust temperatures of several hundred to several tens of Kelvin, the radiation maximum occurs at several tens to about two hundred micrometers, that is to say precisely in the range covered by ISO. Observations in this range allow a reliable statement as to whether the received infrared radiation comes from the dust disk or the jets. To investigate this question, astronomers from the MPIA, together with colleagues from the University of Bochum and the MPI of Radio Astronomy in Bonn have observed more than 70 selected quasars and radio galaxies in the range from 4.8 to 200 μm with ISO. The

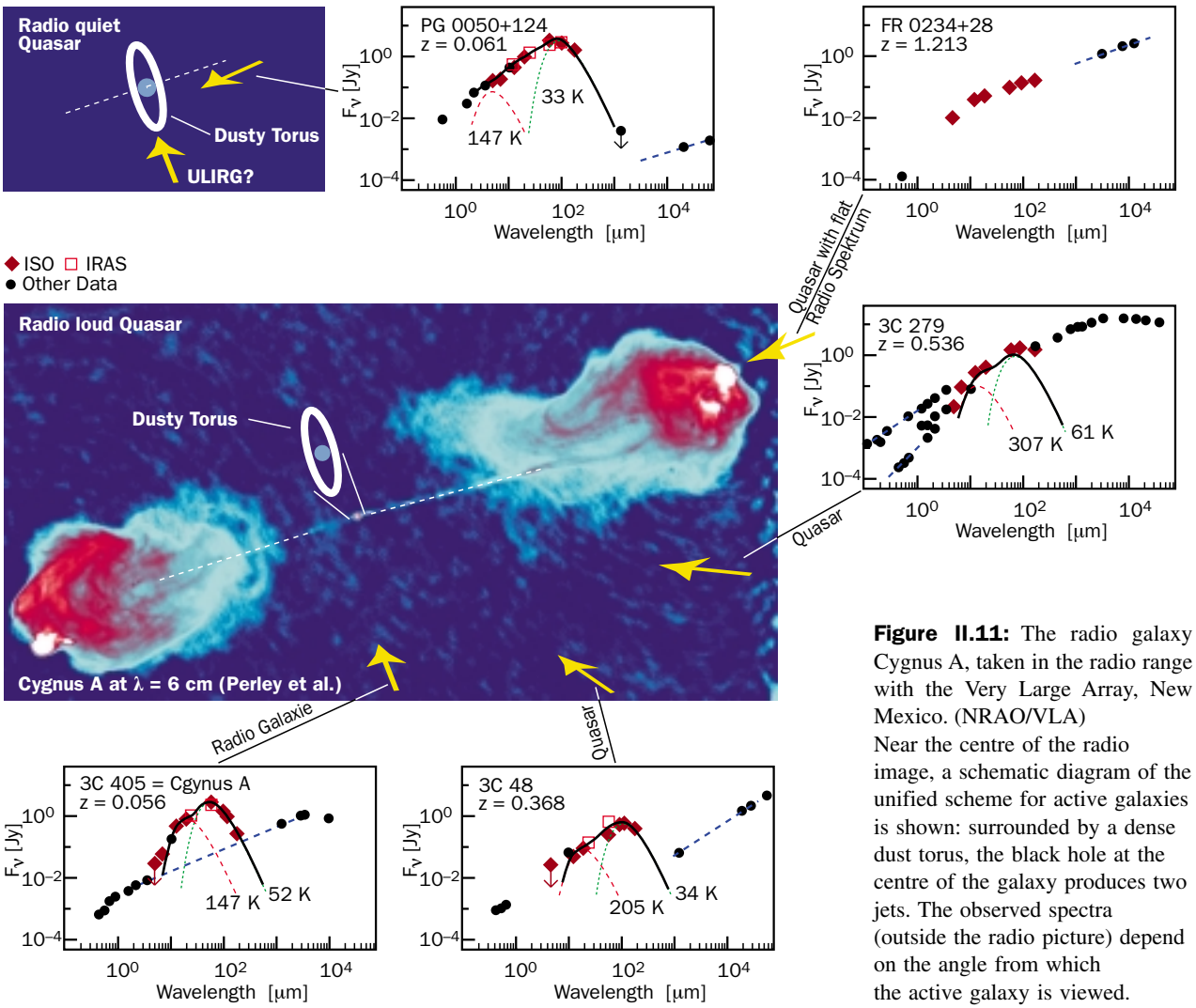

Figure II.11: The radio galaxy Cygnus A, taken in the radio range with the Very Large Array, New Mexico. (NRAO/VLA)
Near the centre of the radio image, a schematic diagram of the unified scheme for active galaxies is shown: surrounded by a dense dust torus, the black hole at the centre of the galaxy produces two jets. The observed spectra (outside the radio picture) depend on the angle from which the active galaxy is viewed.

first results based on ten representative objects support the unified scheme.

In the case of the three radio quiet quasars (PG 0050+124, PG 1206+459 and PG 1634+706) and radio quasar 3C 48, the spectral energy distribution unambiguously shows maxima in the range between 60 and 100 μm (spectral profiles in Figure II.11). In these cases, the whole spectral profile is best explained by thermal radiation from a dust torus. The derived temperatures are then between 30 K and 600 K, and the total infrared luminosities range from 7 10^{11} to 10^{14} solar luminosities. In terms of the unified scheme, this can be explained by saying that we are looking at the system along the axis of symmetry or at an oblique angle. The three radio quiet quasars have no jets, and accordingly they emit no synchrotron radiation, whereas in the case of 3C 48, we not only receive synchrotron radiation from the jet but also thermal radiation from the dust torus (Figure II.11, bottom right).

By contrast, no pronounced intensity maximum is apparent for the blazars. In this case, the intensity progression joins up seamlessly with the synchrotron emission in the radio range. It is quite evident that the non-thermal radiation from the jet dominates here, as would be expected if one is virtually looking onto the jet. The infrared flow of 10^{14} solar luminosities is very high – significantly higher than the typical luminosity of a dust ring, as has been found in the radio quiet quasars. This also means that in the case of the radio quiet quasars, it is altogether possible for a dust ring of about 10^{12} solar luminosities to exist, as would be expected according to the unified scheme. However, the jet emission is the dominating component.

Two objects also show surprisingly interesting details: quasar 3C 279 has an intensity maximum located between 20 and 60 μm, which is clearly recognizable as it towers above the smooth synchrotron spectrum of the jet. 3C 279 is known in the optical and radio ranges as an extremely variable source, and it shows extreme outbursts in the gamma range, which are ascribed to activities in the jet. Other long-term observations now suggest that this quasar was in a quiescent phase with low jet emission at the time of the ISO observations. The consequence of this was that the infrared radiation of the ring exceeded the radiation from the jet, which enabled it to be detected in the first place.

As expected on the basis of the unified model, the classical radio galaxy Cygnus A shows an infrared spectrum which is very similar to that of the radio quiet quasar 3C 48. The thermal dust radiation has maxima at temperatures of around 147 and 52 Kelvin, and it supplies a luminosity of 5 10^{11} solar luminosities. This suggests that Cygnus A is also a quasar whose nucleus is hidden by dense dust clouds.

Despite these first very attractive results, we must wait to see whether the unified scheme can also be applied in its simplest form to the other radio galaxies observed with ISOPHOT.

Polarimetry of quasar 3C 279

3C 279 is a frequently observed quasar whose spectrum is known from the gamma to the radio range. Thanks to the ISOPHOT measurements, it has now been possible to fill in a gap which still existed until recently in the far infrared. This object had already attracted attention at an earlier stage, because it showed major fluctuations of intensity within a few weeks or months: in the gamma range, up to a factor of 20, and in the range from UV to infrared up to a factor of 10. Interestingly, only one jet can be detected in it in the radio range. In actuality it very probably possesses two jets, but the second is not visible to us. This can easily be explained in terms of the present-day jet theory. When electrons move in a magnetic field at virtually the speed of light, they only emit synchrotron radiation in a narrow cone, in the same direction as their movement. The radiation therefore spreads out like a headlamp along the axis of the jet. The consequence of this is that we only see a jet when it is actually pointing more or less towards us.

With the help of polarimetry, it is now possible to verify this idea for the first time on a quasar in the far infrared. This is a valuable method for investigating the physical conditions in the jet. The basis for polarimetry is a characteristic property of synchrotron radiation. In a magnetic field, electrically charged particles move on corkscrew-like paths around the field lines. Since they are accelerated as they do so, they emit radiation – this is the synchrotron radiation. The energy is radiated in the current direction of movement, into a cone whose opening angle decreases as the speed increases. And as the energy of the particles increases, the wavelength decreases. The observation with ISOPHOT made use of the fact that the synchrotron radiation is heavily polarized, which is to say that the electromagnetic wave only oscillates in one plane and in such a way that the vector is perpendicular to the magnetic field. Polarization measurements therefore allow us to reach conclusions about the acting magnetic fields.

Investigations of this sort had already been undertaken in various wavelength ranges in the case of 3C 279. In the visible spectral range, for example, variations between 4 % and 19 % in the degree of polarization had been observed. Likewise, the angle of polarization changed with time. Simultaneous observations in the optical and radio ranges during an outburst of brightness showed that the polarization in both ranges quite clearly arises within the jet, and that the degree and angle of the polarization both vary. This is generally interpreted to mean that during an outburst, a gas cloud shoots into the jet from the central area, and the magnetic field is more heavily »collimated« at the same time. The degree of polarization increases as a result of this.

ISOPHOT now makes it possible to undertake polarization measurements in the far infrared for the first

time. Two measurements at an interval of about one year yielded the following values: on 26.7.1996, the degree of polarization was 23 % and the angle of polarization was 78°. On 20.6.1997, the polarization fell to 6.5 % and the angle rotated to 98°. The source had therefore changed its physical state. Now, the first measurement took place half a year after the outburst, and the intensity fell from July to December. By June 1997, it already rose again. Accordingly, the quasar completed a brightness change, but at the times of the two measurements, it showed comparable brightnesses in the far infrared.

The rapid variations measured with ISOPHOT suggest that the infrared radiation came from a very compact spatial area, probably from the »base point« of the jet. Astronomers at the MPIA and their colleagues from the ISO data centre in Villafranca, Spain, suspect that the blazar nucleus had ejected a new gas cloud half a year prior to the first measurement, which had led to the outburst. While the new hot gas bubble was moving outwards in the jet, it formed turbulence throughout the magnetic field, which then assumed a new orientation. This was revealed in the ISOPHOT measurements by changed polarization values. This interpretation is also supported by polarization measurements which were taken more or less simultaneously in the optical and radio ranges. In this way, the observers had quite evidently succeeded in witnessing how a hot gas bubble was generated in the vicinity of the central black hole and was shot into the jet.

II.3 Evolution of Dwarf Galaxies

One of the fundamental astronomical discoveries of this century concerns the hierarchical structure of the Universe. Stars often form clusters comprising several tens to several thousands of stars; these clusters are part of a galaxy, and the galaxies in turn are assembled into still larger accumulations. Following Edwin Hubble, the astronomers distinguish between three major classes of galaxies: elliptical, spiral, and irregular galaxies (Figure II.12). On wide-ranging photographs of the sky, a cluster is generally dominated by large elliptical and spiral galaxies with diameters of several hundreds of thousands of light years, which can contain up to 10^{12} stars.

Dwarf galaxies are not taken into account in the original Hubble classification. These systems, only a few thousand light years in size, contain 10^6 to 10^{10} stars and they can only be detected with difficulty due to their low surface brightness (Figure II.13). Some massive dwarf galaxies can nevertheless be observed in the Virgo cluster of galaxies. The best-known examples are the Magellanic Clouds and M 32, a companion of the Andromeda galaxy.

Dwarf galaxies are interesting research objects for a number of reasons. For example, it is now considered certain that there are substantially more dwarf galaxies than large galaxies. On the other hand, the fraction of the total mass in the universe contained in dwarf galaxies is not known. Some of their known properties are still far from being understood. For example, most dwarf galaxies feature unusually small quantities of heavy elements, and most elliptical dwarf galaxies appear to be more diffuse than the large elliptical galaxies.

Figure II.12: The classification scheme for the galaxies introduced by Edwin Hubble.

The »Cloud Liquid« model

The theoretical group at the MPIA has worked on a series of attempts to investigate some of the problems indicated above with the help of computer simulations. It emerged from this work that – as had already been suspected for a long time – supernova explosions play a very major part in shaping the appearance and the evolution of dwarf galaxies. Comparisons between the theoretical results and observations demonstrate that the basic characteristics of dwarf galaxies are reproduced correctly by these models, and that the researchers have evidently understood the fundamental physical processes behind them. Some essential points may already be developed on a qualitative basis.

The large, massive galaxies such as the Milky Way system have a deep gravitational potential, in which stars and gas move around the centre. Gravitational attraction and centrifugal force are in equilibrium almost everywhere. Supernovae only take effect locally here, in the range of a few hundred light years, but they cannot affect the overall structure of the galaxy on a significant scale.

Dwarf galaxies are considerably smaller, and the relatively few stars which they contain generate a much weaker gravitational potential. For this reason, energetic processes such as supernova explosions and intense stellar winds have a much stronger effect on the overall picture of the stellar system. The hot expanding gas bubbles of the supernovae violently agitate the interstellar gas, and a dynamic imbalance prevails at many points. The consequence: the dwarf galaxy is dispersed and takes on a diffuse appearance.

A second important aspect is the Dark Matter. Since as long ago as the mid-1970s, observations suggested

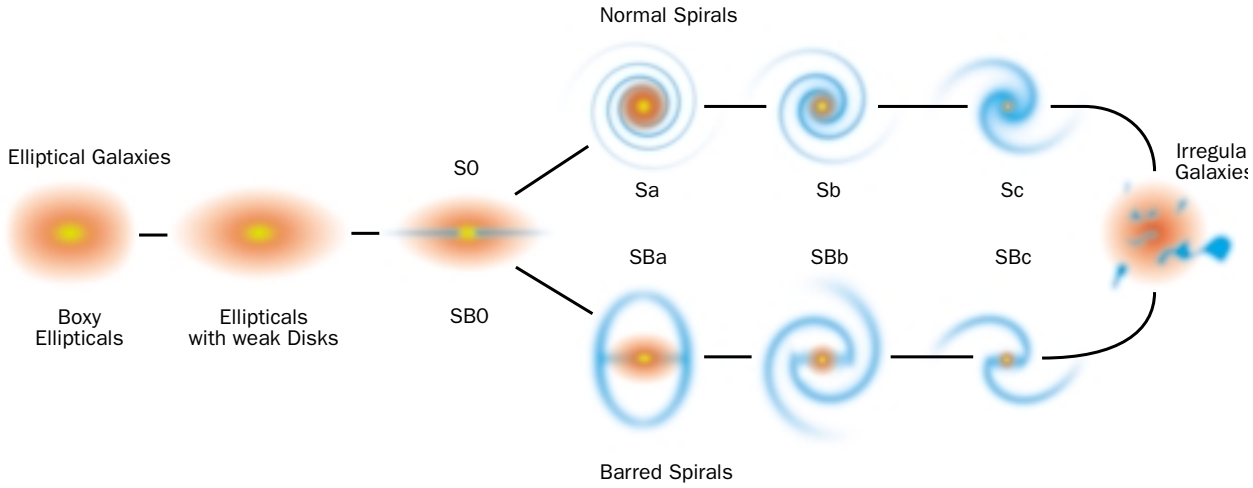

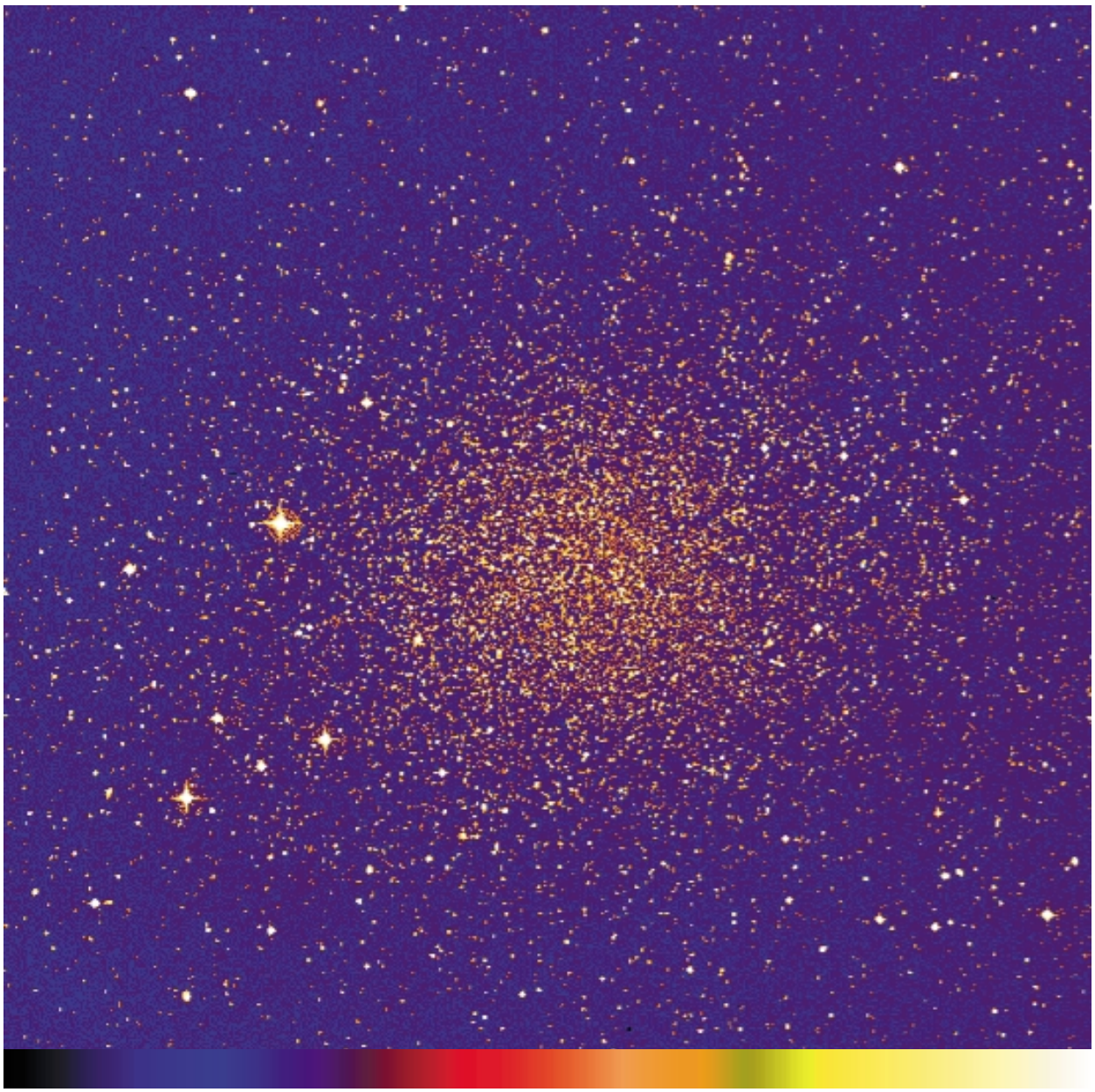

Figure II.13: The spherical dwarf galaxy in the constellation Sculptor.

that the galaxies are surrounded by extended shrouds of matter, or »halos« as they are called. However, so far it has been impossible to detect this matter directly and its nature is unknown. It only reveals its presence by means of its gravitational force: all the large spiral galaxies rotate considerably faster in the region of the disk than would be expected on the basis of the luminous matter, stars and gas. This is caused by the additional gravitational potential of the dark matter halos. Dwarf galaxies appear to be dominated even more heavily by the dark halos than the massive galaxies (cf. Annual Report 1997, p. 73).

Results from the simulations

The aspects which have been outlined, namely the effects of supernovae on the structure of the stellar and gaseous systems and the dominance of a dark halo, were incorporated into the model calculations undertaken at the MPIA as important boundary conditions. Now, even with the most powerful computers available at present, it would be impossible to simulate all astrophysical processes in detail. The interactions between gas, stars and dark matter are too numerous, on spatial scales of less than a light year up to several hundred light years. Instead, the theoreticians have concentrated on individual processes, in order to determine their effects on the morphology and evolution of dwarf galaxies.

In one of these calculations, the objective was to provide the most realistic possible simulation of the behaviour of the interstellar medium. The following plausible basic assumptions were incorporated into this model: the stars and the dark matter behave like an ideal gas; there are no collisions, and consequently no energy is transferred or converted. Interaction takes place solely through gravitational force. By contrast, the interstellar gas behaves in a totally different manner. In this case, electromagnetic forces are also acting; it expands and is compressed, heats up and cools down.

In a large number of earlier models, the interstellar medium was treated as a diffuse component without structures, on scales of less than a few hundred light years; this was done for reasons of simplification. This assumption proves to be unjustified. Observations of dwarf galaxies, and also of our own Milky Way, have shown that the gas is heavily aggregated and that it exists in different states. Accordingly, the theoreticians at the MPIA assumed a two-component model in which dense, cool clouds (particle density $n < 10\ \mathrm{cm}^{-3}$, temperature $T < 100$ K) are embedded in a thin, hot gas ($n = 10^{-3}\ \mathrm{cm}^{-3}$, $T = 10^6$ K).

In reality, stars are formed in the denser regions; the massive ones explode as supernovae over the course of several tens of millions of years. These supernovae increase the kinetic energy of the surrounding medium, heat it up and make it turbulent. This matter, then, is the hot component. In addition, the clouds move about in the galaxy and they can collide with one another. In this case, they condense and heat up over short periods. The hot gas quickly radiates its kinetic energy and cools off again as a result.

In the model, these processes were simulated by suitable parameterization. To do this, each cloud had to be considered individually. From the physical viewpoint, however, the system can be treated as a »liquid« in which the clouds act as dissipative (energy-transforming) particles. Observations of large spiral galaxies have shown that if these clouds have masses of between 10^3 and 10^6 solar masses, their radii will be from 10 to 250 light years. In dwarf galaxies, the clouds do in fact have quite a similar morphology, but their diameters are

Figure II.14: Snapshot of a dwarf galaxy after three billion years of evolution. a) The surface density of the gas features an aggregated structure; b) at the same stage of evolution the stars are uniformly distributed.

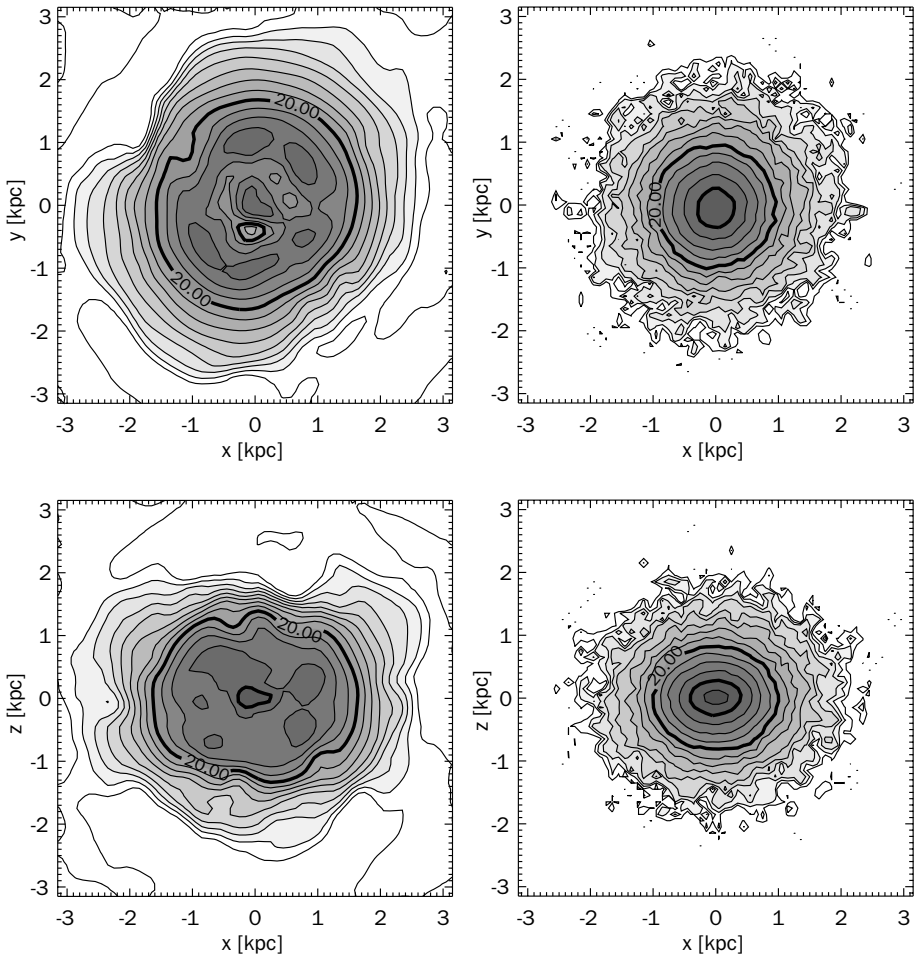

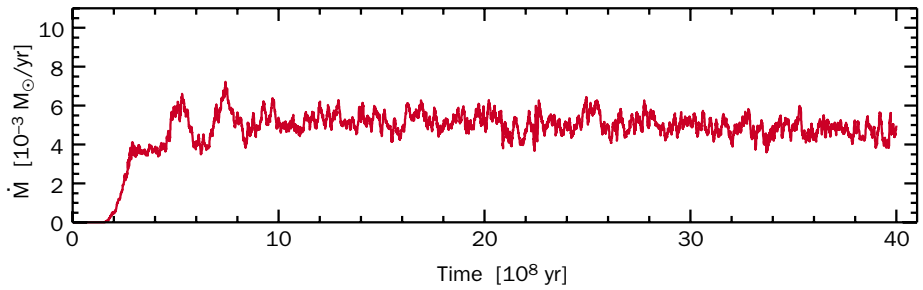

Figure II.15: The star formation rate rises sharply in the first 100 million years, and then it remains at a more or less constant level of about 0.003 solar masses per year.

approximately twice as large, and the theoreticians at the MPIA took account of this in their simulation. The density of the clouds typically amounts to one particle per cubic centimetre. At an average speed of the clouds relative to each other (velocity dispersion) of 10 km/s, this means that on average every ten million years two clouds collide.

A decisively important factor for the simulations was the calculation of the heating and cooling of the clouds. For this purpose, the following factors were taken into account, in some cases empirically and in others on the basis of theoretical considerations:

- in a collision of two clouds, shock fronts are formed in which about 10% of the kinetic energy is converted into thermal energy, that is to say heat.
- supernovae also heat up the gas. About 10% of the total kinetic energy of a supernova is transferred into the kinetic energy of the surrounding gas. Particle winds of massive stars contribute just as much kinetic energy.
- the heated cloud radiates and cools off again. This energy loss depends on the density and size of the cloud, as well as on its relative speed at the time of the collision.

The goal of the simulations was to determine the effects of local processes, in the range of a few hundred light years, on the global characteristics of the dwarf galaxies (in the range of several thousand light years). It became apparent that the time scales on which the heating and cooling mechanisms act are comparable. This means that a global dynamic equilibrium begins to be established in the galaxy after a certain time.

The three-dimensional calculations were undertaken with a resolution of 300 and 600 light years within a volume of 20,000 light years edge length. It was assumed that the dwarf galaxies are embedded in a halo made of dark matter, whose extent and density distribution was deduced from the observed rotation curves of dwarf galaxies. This yielded the gravitational potential that was assumed to be constant in time and to dominate, as opposed to the dark matter potential of our galaxy. When two clouds collided, momentum conservation was assumed and a part of the kinetic energy was transferred into new stars, which consequently obtain a specific velocity distribution. It was also assumed that stars with more than 8 solar masses explode at regular intervals within 1 to 8 million years of their formation.

In two standard simulations, it was assumed that initially, the cool clouds (with a total mass of 10^8 solar masses) are uniformly distributed in the spherical dwarf galaxy with a radius of 6500 light years. The two simulated cases only differ in the choice of the average relative speed of the clouds, namely 15 km/s and 24 km/s. However, it became apparent that the precise value does not have any great influence on the result of the simulation. The cloud system contracts, and the first stars are formed (Figure II.14)

An interesting result emerged regarding the formation of the stars. In the model galaxy, which consists entirely of gas at the outset, the star formation rate increases over the course of several hundred million years, after which it attains a virtually constant level (Figure II.15). The average star formation rate of 0.0024 solar masses corresponds fully to the observations – an important point which suggests that this model takes account of the major aspects. By comparison: in our Milky Way system, the star formation rate of 2 to 3 solar masses per year is about one thousand times higher. In the dwarf galaxy model, the star formation rate shows very heavy local variations on a time scale of less than ten million years, and there are also global fluctuations of about 10%.

After ten billion years, only 25% of the gas has been converted into stars. This means that dwarf galaxies with 10^8 solar masses (such as those under consideration here) still have the equilibrium today which was established several hundred millions of years after their birth, and the formation of stars is continuing with undiminished intensity. These are the dwarf irregulars, a category which also includes the Magellanic Clouds. However, this only applies to undisturbed evolution. It may also happen that the largest part of the interstellar

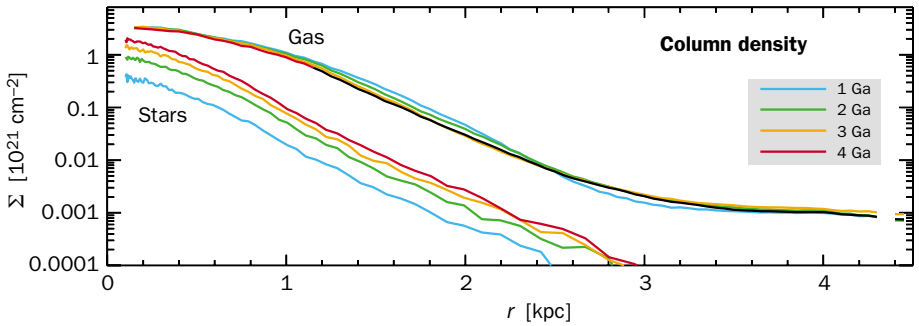

Figure II.16: Results of the numerical simulation. The surface density of the gas (top curves) and of the stars, with increasing distance from the centre of the galaxy. The gas component dominates because the star formation rate is very low. Both components show a more or less exponential decline, as is also observed. The continuous lines show the corresponding solutions obtained by purely analytical methods.

gas is swept out of the interior of a dwarf galaxy (ram pressure stripping, as it is known) if it crosses a large galaxy. No more stars are then formed in these systems, and they evolve into very faint and diffuse dwarf ellipses. The surface density of the clouds and stars which was derived from the simulations showed an exponential decline in the outer two thirds of their extent after four million years, when the system had been in dynamic equilibrium for a long time; this phenomenon is also observed in nature. (Figure II.16)

The principle of this model of the dwarf galaxies is very simple, and it reproduces the observed circumstances very well indeed in some cases, especially as regards the irregular dwarf systems. Even after ten million years, however, the model galaxies still contained a great deal of gas, unlike the elliptical dwarf galaxies which no longer have any significant reservoirs of gas. Observations have now shown that elliptical and irregular dwarf galaxies hardly differ from one another as regards their distribution of stars. For this reason, it may be surmised that dwarf ellipticals are formed by original dwarf irregulars losing their gas. Future simulations should clarify the manner in which this can happen.

Hot supernova bubbles

As described above, star formation and supernovae play a central part in the evolution of dwarf galaxies. However, the violent processes entailed in a stellar explosion have not been simulated in detail in the model described; rather, account was only taken of the kinetic energy released into the surroundings. A second comprehensive project dealt with the question of what happens to the matter which is blown into the interstellar medium by the supernovae.

The background to this problem consists of several surprising observational pointers. One relates to the frequency of heavy elements in dwarf galaxies. Cosmologists now assume that the Big Bang gave rise almost exclusively to the two lightest elements, hydrogen and helium; very small amounts of lithium and beryllium were also formed. The present theory totally rules out the possibility that such heavy elements as carbon, nitrogen or oxygen resulted from the original fireball. They were only formed during nuclear fusion reactions in the interior of stars, and they returned to the interstellar medium in the final stages, via particle winds or supernova remnants. In this way, the universe has constantly been enriched with heavy elements ever since it was created, up to a level which occurs nowadays in the area surrounding the sun.

It is noticeable that dwarf galaxies mostly have only one tenth of the solar abundances of heavy elements, although adequate numbers of supernovae must have exploded within them to produce more heavy elements. Have heavy elements not formed on the usual scale here for some reason, or have they disappeared somewhere?

One possible answer is suggested by observations over recent years, according to which gas appears to be escaping at high speed from certain dwarf galaxies. So would it be possible for the supernova winds enriched with heavy elements to break out of the galaxy and escape into intergalactic space? This does actually appear to be possible in certain cases.

Until now, model calculations have not been able to provide an unambiguous explanation of the conditions under which gas can break out and escape from a dwarf galaxy. Most simulations have not followed the development of the gas bubbles over sufficiently long periods.

At the MPIA, the theoreticians have gone into this problem in detail with the help of computer simulations. For this purpose, they represented the dwarf galaxy as a thin gas disk in hydrostatic and centrifugal equilibrium, as occurs in the gravitational potential of a halo made of dark matter. (The halo was assumed to be an isothermal sphere, which corresponds accurately enough to previous observations.) If a supernova explodes in the interior of the galaxy, a hot bubble of expanding gas is formed with a shock front which pushes the surrounding

gas away in front of it like a snowplough. If the interstellar matter is homogeneously distributed, the bubble expands spherically. However, in a dwarf galaxy, there is a steep decrease in density of the matter perpendicular to the disk plane. As a consequence, the gas moves faster perpendicularly to the disk plane than it does in the plane. A sort of nozzle is created through which the gas can break out from the disk. If this matter fails to attain the speed required to escape, it falls back into the disk, rather like the water in a fountain. But if it is fast enough, it escapes into intergalactic space. So the question as to whether a supernova's gas can escape from the galaxy – and if so, how much – depends crucially on two conditions:

- the gravitational potential of the galaxy, and
- the conditions in the interstellar medium, which dictate how quickly the gas can expand.

To deal with these questions, several galaxies with masses between 10^6 and 10^9 solar masses were considered. In the case of the three-dimensional simulations over a volume of 100000 × 100000× 65000 ly^3 with a spatial resolution of 80 ly, axial symmetry was assumed. In addition, all the stars were assumed to be formed in a single phase within a circumference located at a distance of 300 ly from the centre. The subsequent supernovae were assumed to explode within 50 million years at constant intervals. These intervals were from 30,000 to 3 million years, which could considered in the model as a kinetic energy input of between 10^{37} erg/s and 10^{39} erg/s. This energy range corresponded to 15 to 150 supernovae. Moreover, account was taken of the cooling of the expanding gas bubble over the course of time.

Figure II.17: Simulations of the gas of hot supernova bubbles escaping from dwarf galaxies. The state of evolution after 100 million years is shown for galaxies with masses of between 10^6 and 10^9 solar masses and mechanical luminosities of the supernova winds between 10^{37} and 10^{39} erg/s.

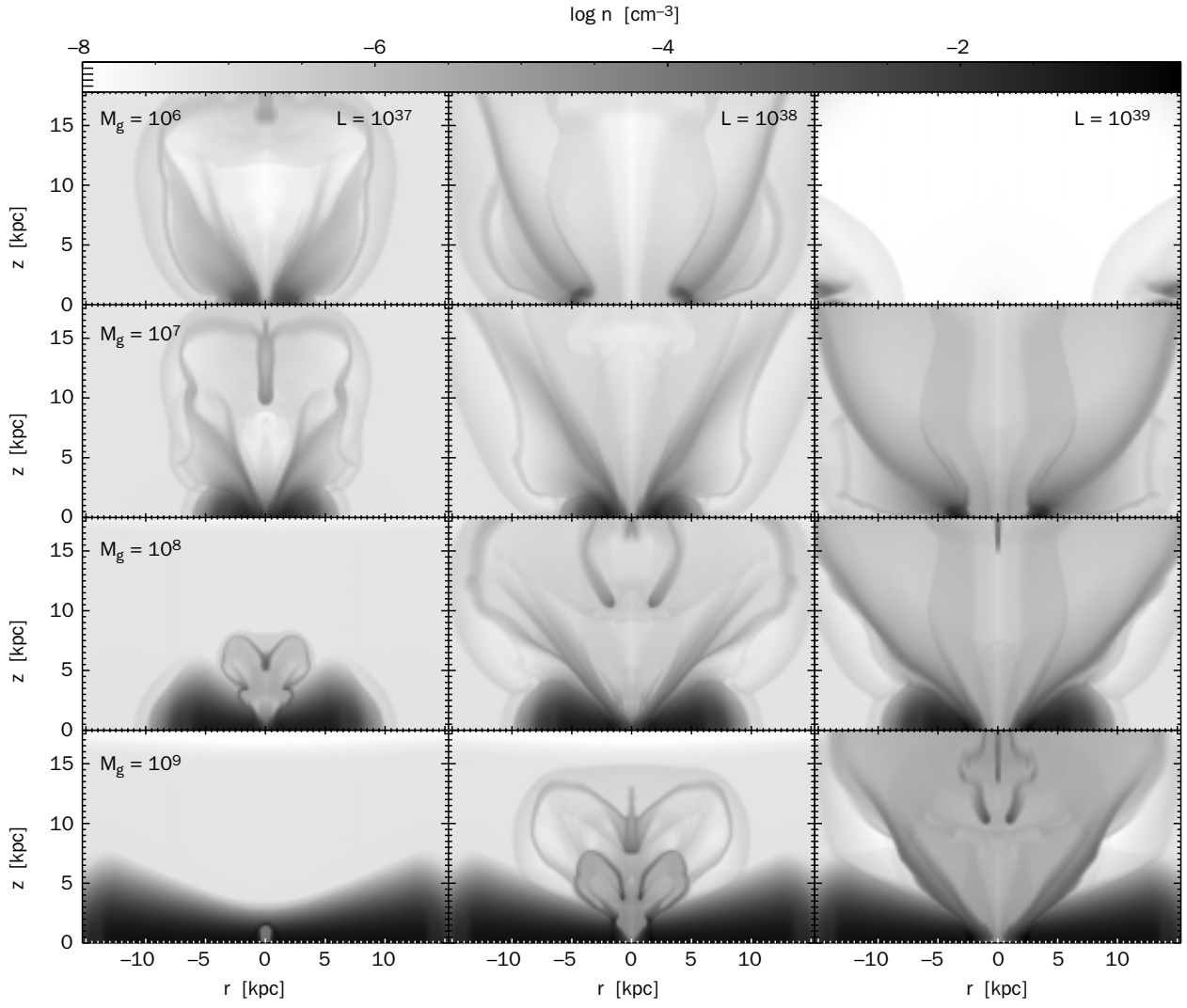

The simulations covering a period of 200 million years clearly showed that the supernovae gas enriched with heavy elements can escape from the galaxies in large quantities. In the low-mass galaxies of up to a million solar masses, interstellar gas is also carried along and hurled out of the galaxy by the shock waves (Figure II.17). But the more massive a system is, the more interstellar matter remains in the galaxy – and this is predominantly the cool gas containing only small quantities of heavy elements. New stars are then formed from this with equally low fractions of heavy elements.

The simulations have also shown that the characteristics of the dark matter halo are decisively important for the output obtained from the simulations. The dark matter therefore plays a central part in the development of dwarf galaxies. Its total mass and spatial density distribution must therefore be considered as carefully as possible when carrying out calculations of this sort.

The comparison with observations is interesting. According to the simulations described, at least some dwarf galaxies should be surrounded by very extended halos of matter with a high fraction of heavy elements. How could these be detected? Two further computer runs attempted to calculate the radiation behaviour of these suspected halos. In this case, it emerged that this gas should shine in the optical wavelength range in the light of certain emission lines of heavy elements, and also of hydrogen (Hα). In particular, elongated filaments should be visible close to the galaxy. They are cooler fragments of the bubble edges (Figure II.18). The hottest gas component should also emit X-ray radiation. If the gas were to carry magnetic fields with it as it flowed outwards, then radio radiation would also be expected. This is created if electrons are accelerated along the field lines.

In actuality, gigantic bubbles and filaments were found in the visible range in certain dwarf galaxies.

Figure II.18: Optical luminosity of the gas escaping from the galaxies after 100 million years, for galaxies with masses between 10^6 and 10^9 solar masses and mechanical luminosities of the supernova winds between 10^{37} and 10^{39} erg/s.

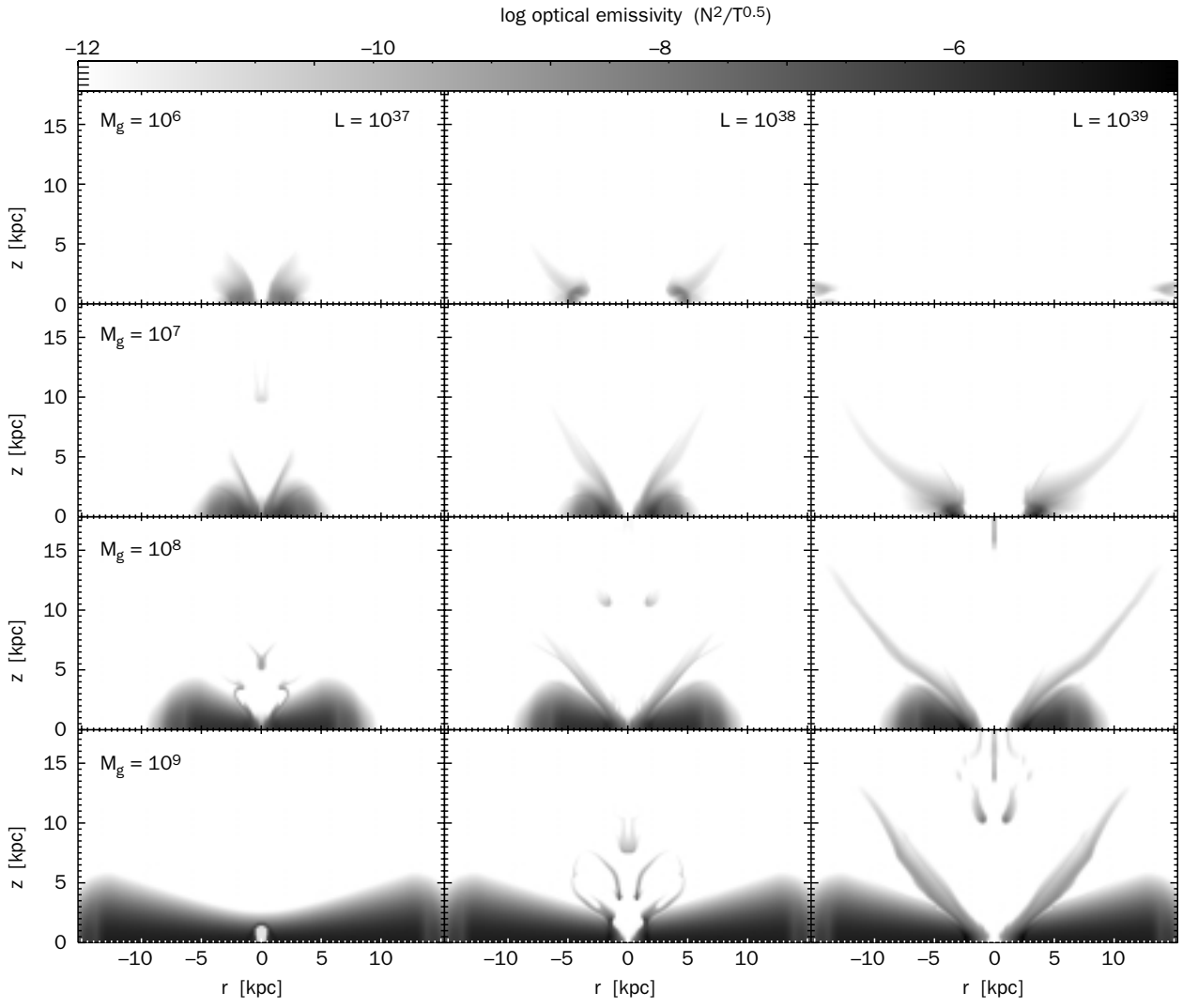

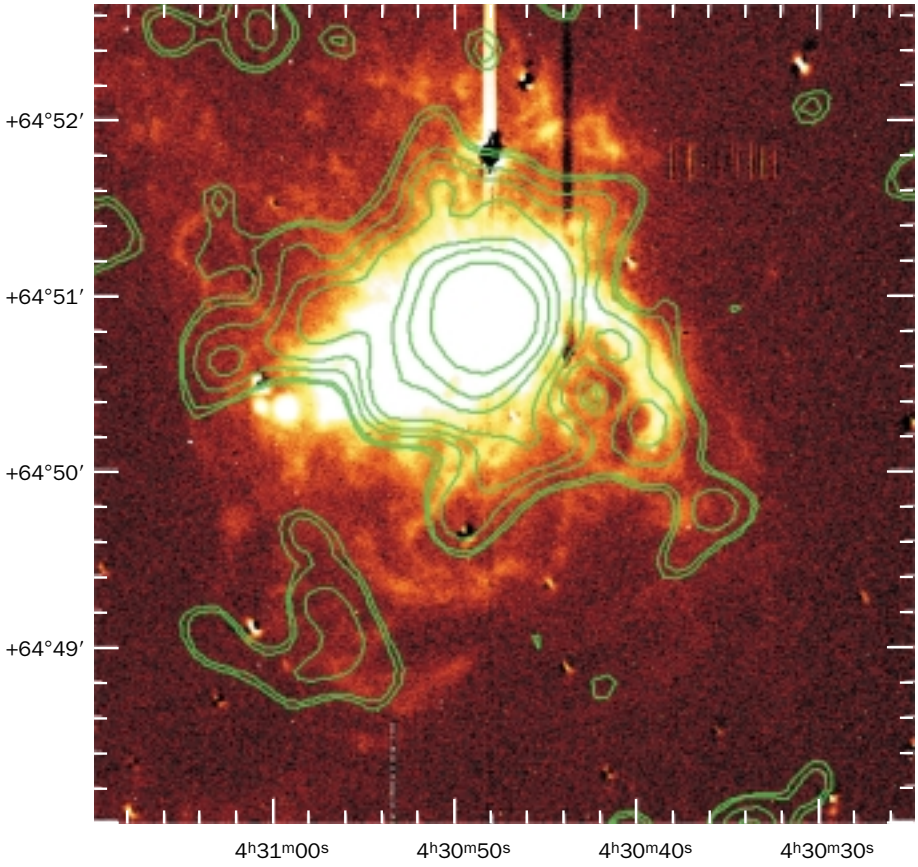

Figure II.19: The dwarf galaxy NGC 1569 (optical image) shows an extended X-ray emission of hot gas (contour lines), as would be expected from supernova winds flowing outwards. (Picture: Della Ceca)

Observations with the Japanese-American ASCA satellite telescope provided indications of X-ray halos, for example on galaxy NGC 1569 (Figure II.19), and in the radio range, there are indications that blue compact dwarf galaxies are surrounded by a radio halo that is some ten times more luminous than that surrounding massive spiral galaxies.

Hence there is much to suggest that dwarf galaxies greatly enrich the intergalactic medium with heavy elements. Detailed studies are still needed to pursue this theory. The results are extremely important for cosmological models of the chemical evolution of the universe.

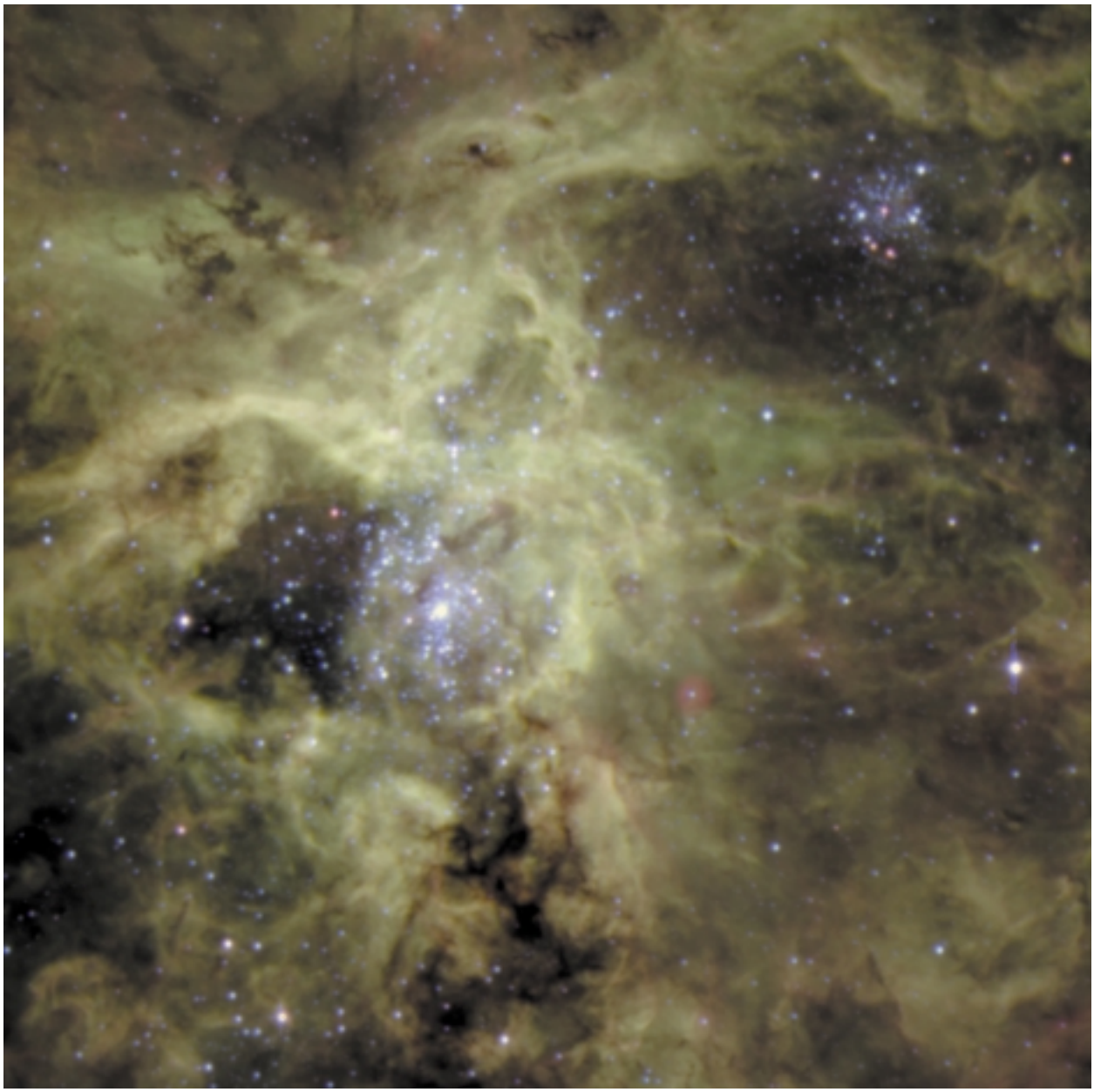

Enlargement of the central region of the 30 Doradus complex including the star cluster NGC 2070 and the Tarantula nebula (from Figure III.3). The scale of 1.″8/mm shows the full spatial resolution of the image. The dynamical range of the colour scale is expanded, so that also the details of the brightest structures can be seen.

III Development of Instruments

One of the essential criteria governing the performance of a telescope is the size of its main mirror. But an equally decisive factor is the choice of the detector which registers an image or a spectrum of the targeted section of the sky in the focal plane. For about one hundred years, astronomers used photographic plates as the means of recording the image; their emulsions had a so-called quantum efficiency of less than one per cent, which means that the emulsion had to be impacted by more than one hundred light particles before it would register one of them.

Since the start of the 1980's, astronomers have had so-called Charge Coupled Devices (CCDs) at their disposal. These are light-sensitive semiconductors which attain quantum yields ranging from 60 to almost 100 per cent, depending on the wavelength. By using these devices, a 50- to 100-fold increase is made possible in the sensitivity of the detectors, and hence in the efficiency of the telescopes. These miniature plates, just a few square centimetres in size, consist of a large number of light-sensitive pixels (picture elements). The largest CCDs have several million pixels. The light arriving generates an electrical charge in each individual pixel, which is stored in the first instance. At the end of the exposure, a special electronic system reads out the CCD chip, and a suitable computer program converts the charge distribution that has been registered into an optical image. A decisive advantage is that the number of charge carriers generated is strictly proportional to the intensity of the incoming light.

Nowadays, CCDs are used in commercially available video recorders and even in cameras, but the normal commercial CCDs cannot be used on telescopes. Only chips of the very highest quality are suitable for astronomy. These are produced by companies such as Philips or Rockwell, but detailed tests on their suitability have to be carried out at the MPIA's laboratories before they can be put to use on one of our telescopes.

The instruments themselves – that is, the cameras and the spectral equipment – are not available through commercial channels: instead, they have to be designed and built individually. In general, the scientist in charge of the project specifies the desired properties of the instrument, which then is produced in the MPIA's workshops. In a large number of cases, cooperation also takes place with companies, who are not infrequently confronted with entirely new tasks in connection with special orders of this type. The know-how which they acquire in this process strengthens their competitive edge on the world market.

There now follows an overview of the MPIA's more recent instruments and the current status in the reporting year.

The Wide Field Imager on the 2.2 m telescope on La Silla

In December 1998, astronomers from the MPIA and the ESO succeeded in starting operation of a jointly-developed Wide Field Imager (WFI) on the 2.2 metre telescope on La Silla (Figure III.1). This instrument has an exceptionally large field of view, with an edge length of 33 minutes of arc, corresponding to rather more than the surface area of the full moon. The CCD array is sen-

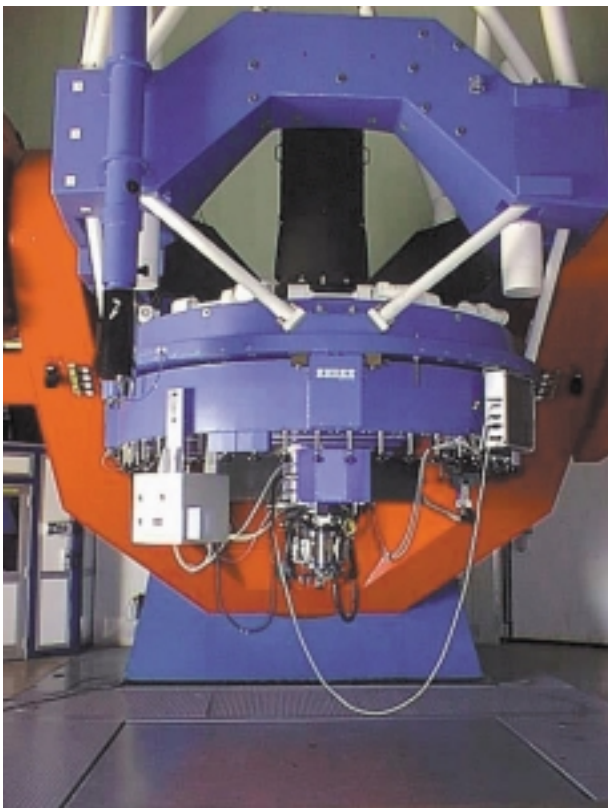

Figure III.1: The wide-field imager on the 2.2 metre MPIA/ESO telescope.

sitive over a very broad wavelength range from the UV (380 nm) to the near infrared (930 nm). Only four cameras with a comparable field of view and resolution are operational in the world. But when it comes to imaging quality and uniformity of illumination, the WFI is probably unparalleled (Figures III.2 and III.3).

The extensive filter set is also unrivalled: more than 30 narrow and medium band filters make it possible to scan the spectral intensity distribution of every object with a spectral resolution of about 3%, and to detect the emission of prominent nebula lines. For example, a meaningful spectrum can be derived for each of the 100000 or more stars, galaxies and quasars which are located in the field of view down to a visual brightness of 24 mag. The WFI has been available to all visiting researchers on La Silla since January 1999.

Around 1930, the German optician Bernhard Schmidt developed a type of telescope which was suitable for photographing large celestial fields, and this type of telescope was later named after him. It is a reflector telescope which has a corrective optical system on the telescope aperture. It creates a large image field which is free of coma. Present-day Schmidt telescopes have large image fields with diameters of between 5 and 15 degrees. However, they have relatively small apertures (Mount Palomar Observatory: 1.0 metres, Calar Alto: 0.8 metres) and they operate with photographic plates whose light yield is just a few per cent. These drawbacks are now obviated by the wide field imager on the ESO/MPG's 2.2 metre telescope on La Silla: it operates with a sensitive CCD array, 12 cm by 12 cm in size, on a telescope with a relatively high light transmitting capacity. The imaging scale of 0.24″ per pixel is selected so that no loss of resolution occurs even with very good seeing.

The new wide field imager makes ideal use of the optical qualities of the 2.2 metre telescope. Like its twin on Calar Alto, the telescope has an unusually large image field with excellent optical quality. Astronomers from the MPIA developed the WFI concept at the end of 1996 and proposed it to ESO. Just a short while later, the decision was taken to build the instrument as a joint project between the MPIA and ESO. The major part of the work was completed by the middle of 1997 in the record time of a year and a half. The entire opto-mechanical section was built at the MPIA, comprising the optical correction unit, the filters and the shutter. Our colleagues at ESO created the CCD mosaic with the cooling unit and the read-out electronics.

The optical corrector consists of two cemented lens triplets which create an absolutely flat image field in the focal plane. Moreover, it reduces the aperture ratio (ratio between focal length and mirror diameter) from 1/8 to 1/5.9. This enlarges the useful field and reduces the exposure times that are needed.

To avoid time-consuming and risky filter changes between exposures, a filter wheel with a diameter of 1.1 metres has been built; it can accommodate up to 50 filters. A micro-computer-controlled robot arm ensures smooth and speedy changes from one filter to another.

The shutter also proved to be technically demanding. The task was to open and close the camera aperture so rapidly that even in short exposure times, each pixel is exposed for the same period – by no means a simple problem on a detector which has diagonals measuring 175 mm. Exposure times of as little as 0.1 seconds are possible. For the range below 1 second, the exposure time for each image element is precise to less than 1/1000 second, and for longer times the precision is about 0.1%.

The CCD array was produced by the ESO. It was assembled from eight individual chips, each with 2046 × 4096 pixels, so that a mosaic totalling 67 million pixels was created. One single image comprises 140 Mbytes of data. To read out this massive quantity, the computer currently only needs 27 seconds. In terms of reading a book, this would correspond to a speed of 1000 pages per second!

Thanks to these technical characteristics, the new wide field imager on the 2.2 metre telescope closes a gap between the Schmidt telescopes and the large ones. This also determines the future area of application: the search for rare and faint celestial objects, such as supernovae in remote galaxies, very distant quasars or brown dwarfs, in large areas of the sky. Researchers at the MPIA have already made a start on two very promising projects to search for quasars and remote galaxies. Both these projects are based on the experience gathered in the CADIS project at the Calar Alto Observatory, and the search for protogalaxies is designed so that a large number of other interesting objects can also be discovered at the same time (cf. 1997 Annual Report, p. 18).

In connection with sampling for quasars, a celestial area of about one square degree (corresponding to the area of about five full moons) is scanned for quasars with redshifts of up to $z = 6$. The most distant quasars are then seen at a time when the universe was not even a tenth of its present age. The astronomers hope to find an estimated 1000 to 2000 quasars in this way. This is made possible by photographing the fields through a series of filters. Since the typical spectral characteristics of the quasars are known, these celestial objects can be identified with great certainty in the various filter shots because of their brightness. If it is also remembered that the spectra shift to ever higher wavelengths as the distance of the quasars increases (redshift), it is also possible to determine the distance of the individual quasars from the whole set of photographs.

The goal of this sampling is to obtain a homogeneously selected and virtually complete random sample of quasars, down to a brightness in the red of 23 mag, with red shifts and therefore distances which – just on the basis of the WFI observations – can be determined so accurately that it is possible to establish how the

Figure III.2 (above): The moon, taken with the new wide field imager.

Figure III.3 (next pages): This photograph of 30 Doradus in the Great Magellanic Cloud demonstrates the image field size and the outstanding imaging quality of the wide field imager.

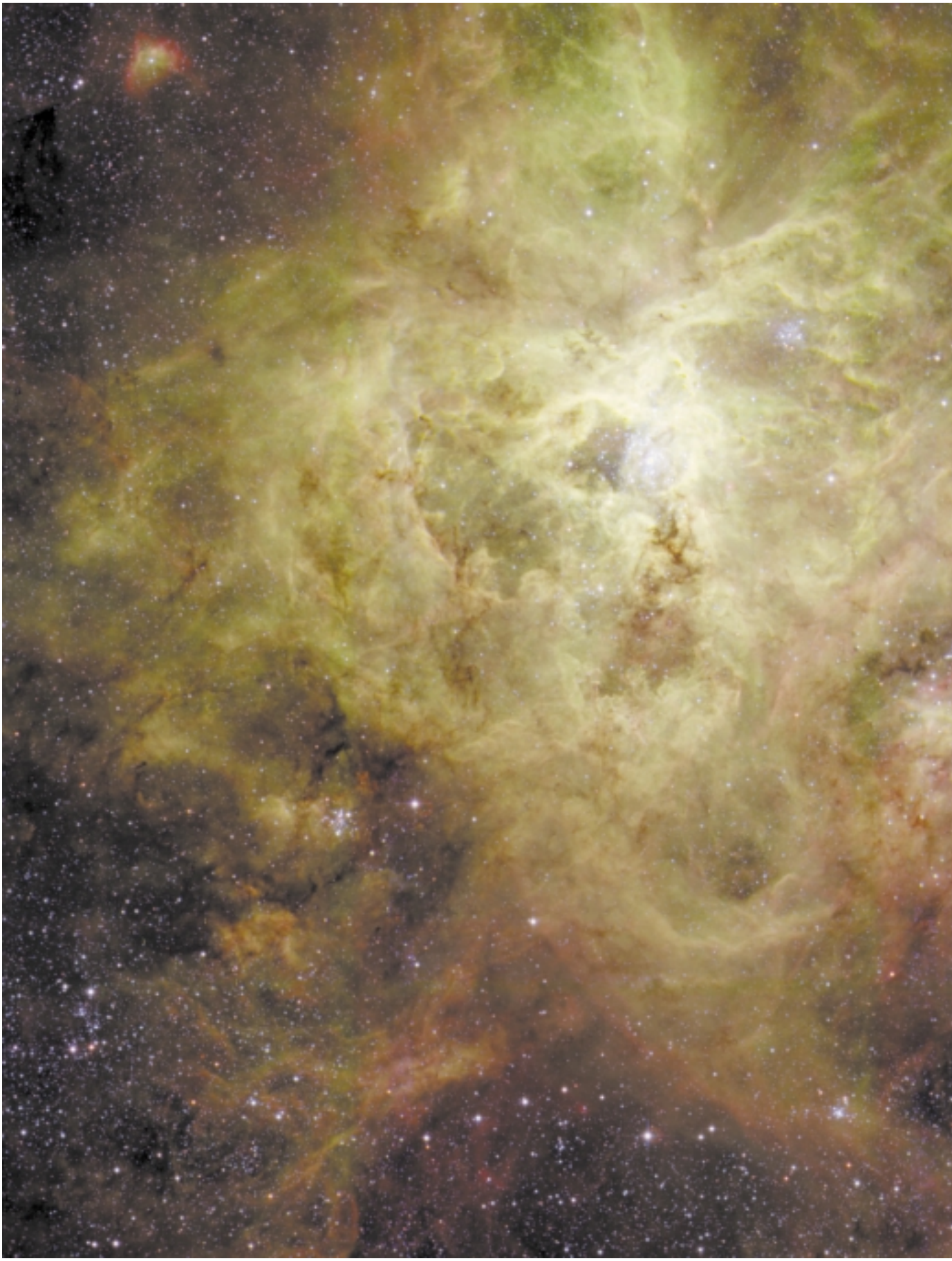

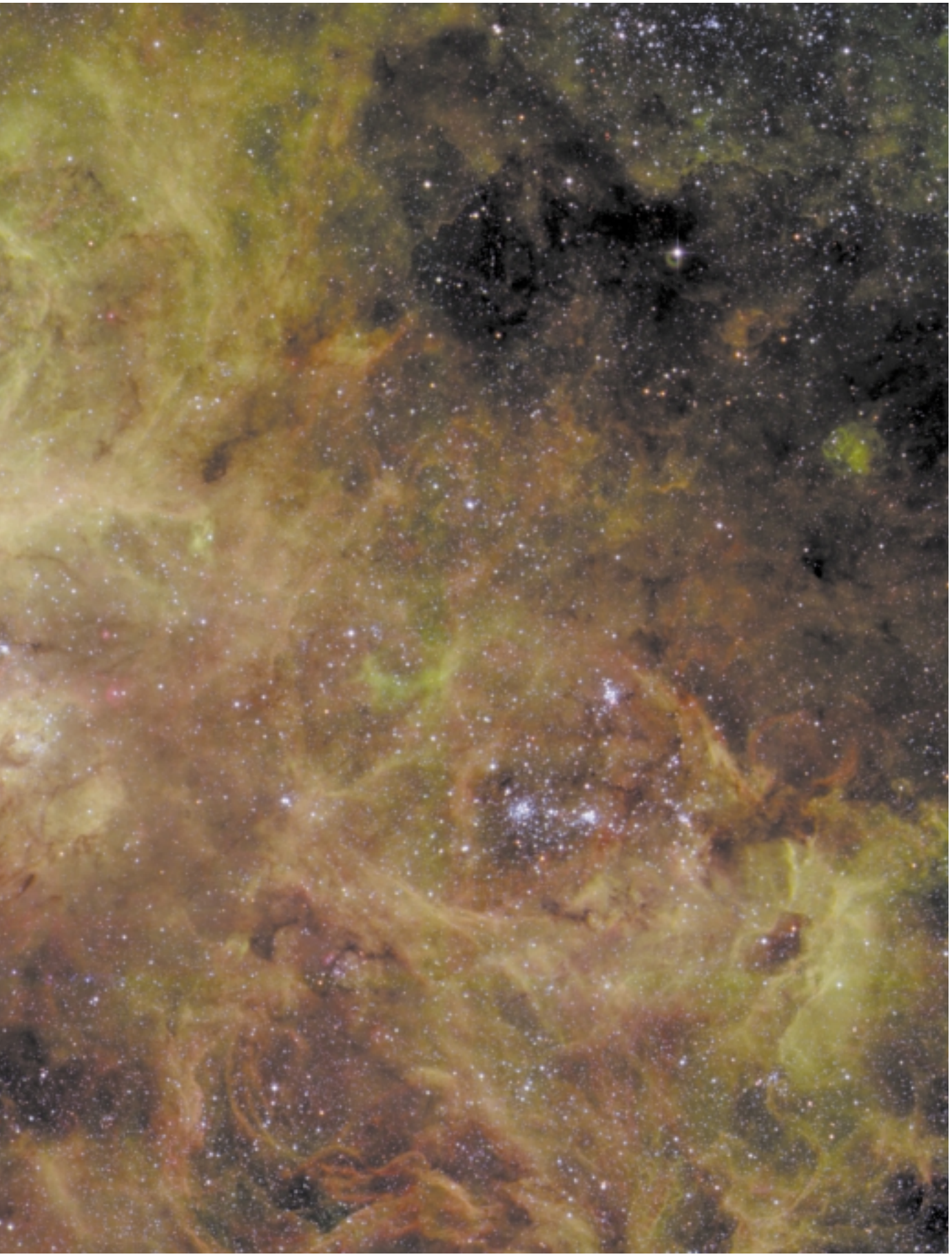

number and brilliance of the quasars has developed over the course of the universe's history. Thanks to this unique quasar sampling method, it should be possible to give answers to the controversial questions based on different search strategies: when did the majority of quasars light up, how much energy have they given off, and what connection is there between quasars and early stages of the creation of the galaxies?

The same photographs can also be used for a second project, which is already under way at the MPIA: the identification of about 10000 galaxies with red shifts of about $z = 1$. These systems can also be identified in the numerous colour filter photographs on account of characteristic brightnesses. They are all located in a distance range of 7 to 8 billion light years. We are therefore seeing these objects in a state when the universe was about half as old as it is today. In this way, the astronomers hope to discover the large-scale arrangement of the galaxies in clusters and super-clusters, and to compare it with the present situation in the environment of our Milky Way system. The WFI will only be undertaking the preliminary work on this project, while the next generation of instruments on the VLT are needed to determine precise distances for all galaxies within the selected volume of $1.3 \times 1.3 \times 0.1$ billion cubic light years. Using the large number of galaxies around $z = 1$, it will also be possible to establish the development of the galaxy population during the last eight billion years with a precision that has never been attained before.

The first photographs with the WFI (Figure III.2 and III.3) have already demonstrated its unique image quality. It therefore comes as no surprise that many astronomers from the ESO countries and elsewhere would like to exploit the potential of the WFI. At the moment, about half of all the good projects for which applications are received have to be refused due to the limited observing time. The awards committee has nevertheless decided to concentrate about 15% of the time on the WFI to a major European sky survey project, the results of which will be made available to all astronomers in the ESO countries within a few months.

This guarantees that the WFI will accomplish its main mission: to put European astronomy in a position where it can make optimal use of the unique possibilities opened up by the VLT over the next five years. In this way, within the scope of their limited finances, the researchers at the MPIA are contributing substantially towards the scientific success of the major European VLT project.

ALFA, adaptive optics with an artificial star

In principle, the resolution of a telescope (that is to say, its ability to show separate images of two objects that are located close to one another) depends exclusively on the diameter of the main mirror and the wavelength of the light. In the visible range (wavelength of about 550 nm), a 3.5 meter telescope has a theoretical resolution capacity – also known as the diffraction limit – of 0.03 seconds of arc; at 2.2 μm, the figure is 0.″13, or four times less. In practice, however, the turbulence of the air blurs images with longer exposures so heavily that the typical resolution is only one second of arc. This means that no large telescope will achieve better resolution than a 15 centimetre one!

In collaboration with colleagues at the MPI for Extraterrestrial Physics in Garching, astronomers and technical experts at the MPIA have built a so-called adaptive optics system for the near infrared range, which makes it possible to correct image fluctuations during the exposure (cf. 1997 Annual Report, p. 11). This system was tested successfully for the first time in October 1996 on the 3.5 metre telescope on Calar Alto, and it was possible to place it at the disposal of all astronomers two years later.

In practice, an adaptive optics system works more or less as follows (Figure III.4): a plane wave of light reaches the earth's atmosphere and is constantly distorted in it, like a cloth in the wind. When it arrives at the telescope, it shows »hills and valleys« with a height of several micrometers. Inside the telescope, the wave is split into two sub-beams by a beam splitter. While one sub-beam falls on a small adaptive mirror and enters the camera from there, the other reaches a wave front sensor. This device analyses the form of the wave, and sends this information to a computer. The computer uses the data to calculate how the surface of the flexible adaptive mirror must be deformed in order to correct the form of the other sub-beam. (In the case of ALFA, the wave initially falls on the deformable mirror and only reaches the beam splitter afterwards.)

In order for this process to function, it must be possible for the mirror to be adapted so quickly that the incoming wave trains are not already being deformed in a different way to the wave train which has just been analysed. Theory shows that about 200 correction steps per second are needed in the visible range, while only about ten are required at a wavelength of 10 μm.

Even in the test phase, ALFA was able to furnish evidence of its efficiency. During 1998, the system was optimised still further, making it possible (for example) to improve the optical quality of the images – expressed by the Strehl factor – by a factor of 15. The Strehl ratio describes the ratio of the light intensity in the centre of a star image to the intensity which the ideal, diffraction-limited image would have. With normal seeing of one second of arc, the Strehl ratio is about 3%, and in an ideal case it is 100%.

On photographs of the famous Trapezium star in Orion, astronomers using ALFA at a wavelength of 2.2 μm achieved a Strehl ratio of 62%; at 1.2 μm the value was 12 %. The photographs had a resolution (full width half maximum of the miniature star images) of 0.″14

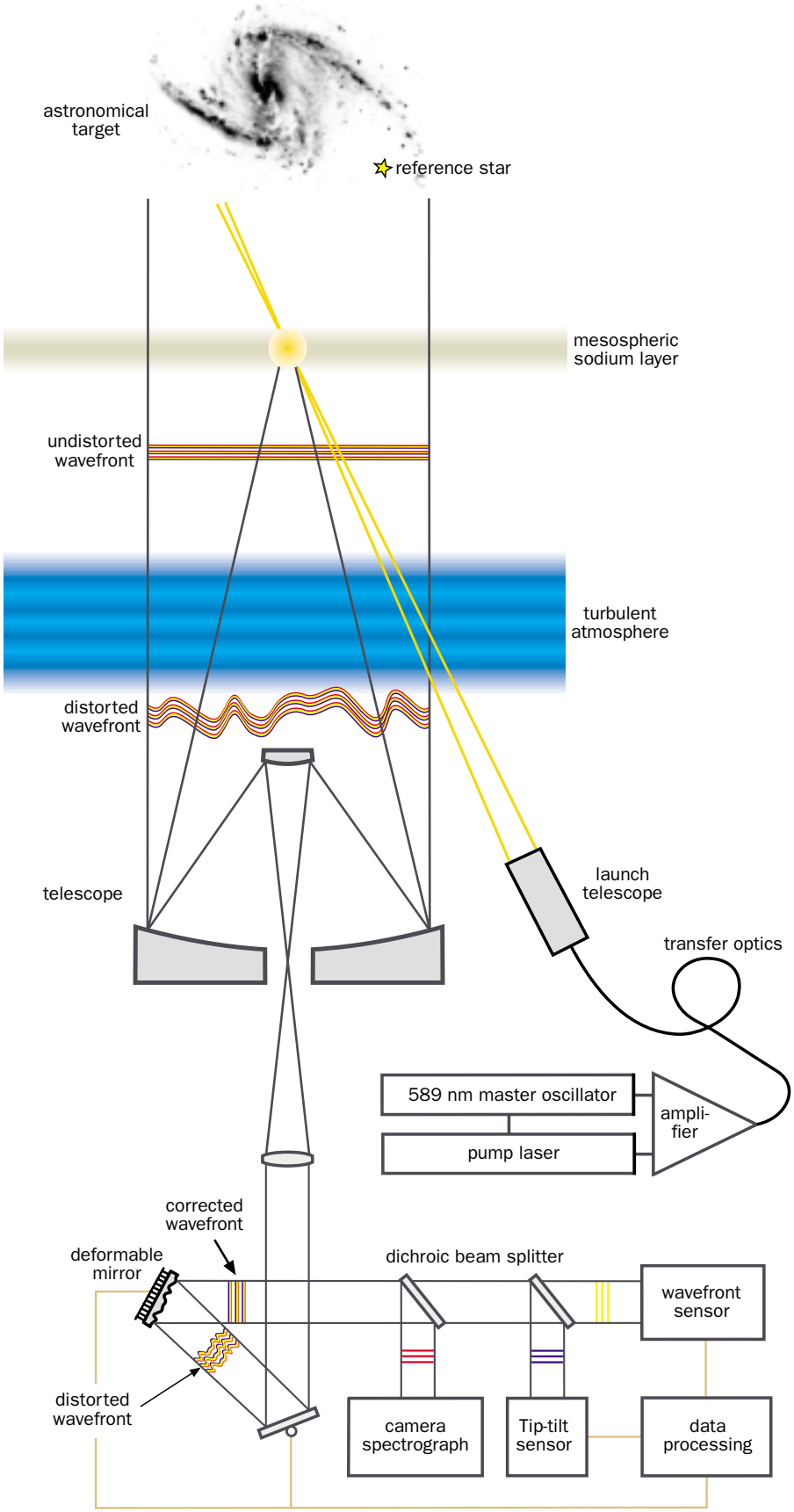

Figure III.4: The principle of adaptive optics on ALFA with the laser guide star.

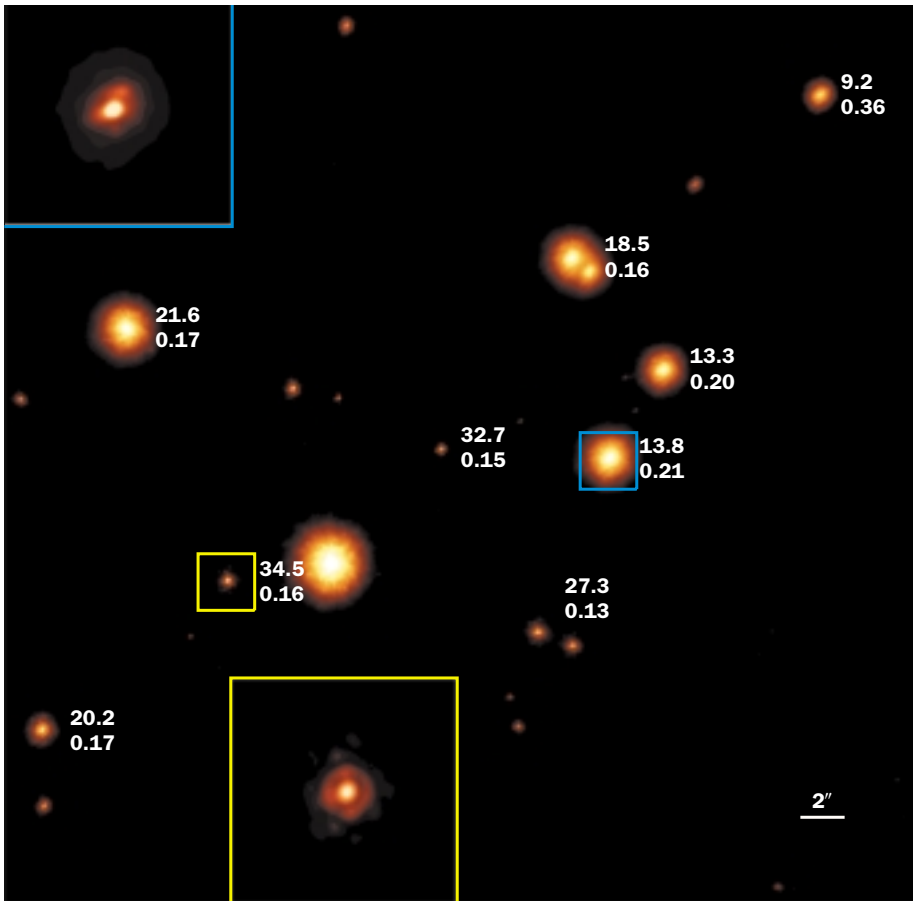

Figure III.5: ALFA photograph of the region of the Trapezium stars in Orion at 2.2 µm. The figures indicate the Strehl number (top) and the full width half maximum of the respective star image.

and 0.″1 respectively (Figure III.5). This means that they almost attained the theoretical limit of diffraction of 0.″13 and 0.″07 respectively.

In ALFA, a central part is played by the wave front sensor which analyses the light wave. So that it can work quickly enough, it requires a star of at least 14th magnitude. If the celestial body that is to be imaged is itself too faint for this purpose, another must be found, although it must be no further than 30″ from the object of interest. If this condition cannot be met, the astronomers have recourse to a trick: they send a laser beam along the telescope axis towards the sky. At a height of about 90 kilometres, this encounters a layer that is enriched with sodium atoms (Figure III.6). The wavelength of the laser is adjusted so that it excites the sodium atoms to shine. In this way a spot of light or »artificial star« is created above the telescope, corresponding to a star of 11th magnitude in an ideal case. The adaptive optics uses it as a bright comparative star during the image correction.

This system was tested successfully for the first time at the end of 1997, and it places the MPIA at the very forefront of research: in the astronomical sector, there are currently only two other comparable instruments of this sort anywhere in the world. In August 1998, it was even possible to image an extragalactic object for the first time using ALFA and the laser guide star: this was the active galaxy UGC 1347 (Figure III.7).

Despite major technical progress, it has only been possible to use the laser guide star on 15% of possible observing nights. Several factors are responsible for this.

- The laser can only generate a star of maximum brightness if it is pointing directly at the zenith. At a zenith distance of 50 degrees, the sodium layer is further away from the telescope, and so the artificial star appears more faint. Moreover, the laser beam is more heavily dispersed by scattering as it travels further, which reduces the brightness even more.
- The wave front sensor is sensitive to a broad wavelength range of about 400 nm to 900 nm. On the other hand, the laser only radiates at one wavelength (monochromatic), so it appears fainter to the sensor than a star which has the same brightness at the laser wavelength as the artificial spot of light.

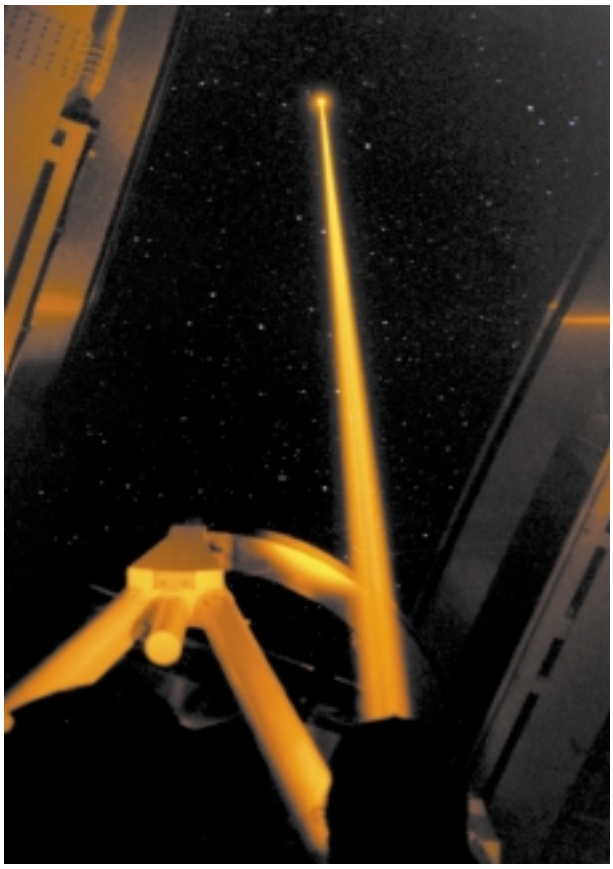

Figure III.6: The laser beam shoots into the sky parallel with the telescope axis, and it creates an »artificial star« there.

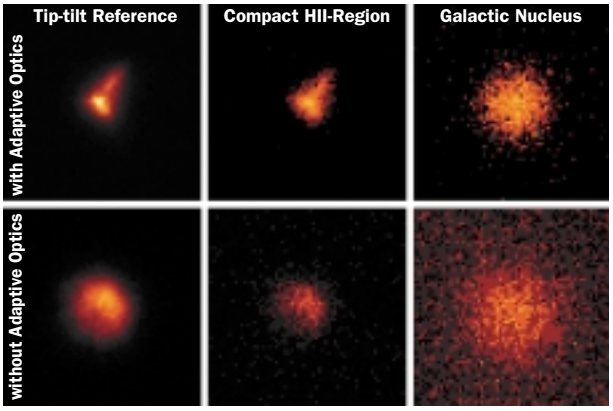

Figure III.7: Photographs of galaxy UGC 1347 (middle and right). Top, with ALFA and laser guide star, below without adaptive optics. The two pictures on the left show the reference star. The middle picture shows a compact HII region in UGC 1347, and on the right the galaxy's nucleus is visible.

- The laser beam has to be focused optimally on the wave front sensor. This requirement is particularly critical. Aberrations in the optical laser guidance system and air turbulence in the telescope dome degrade the focusing.

Intensive research is currently under way at the MPIA on this last point. It is possible to increase the brightness of the artificial star further by circular polarisation of the laser beam. This increases the proportion of sodium atoms which are excited to shine.

MOSCA – Multi-Object Spectrograph for Calar Alto

MOSCA is a multi-purpose instrument which can be used for direct images as well as for spectrographic investigations. This instrument, which went into operation at the end of 1996, is used on the 3.5 metre telescope behind the main mirror bore in the Ritchey-Chrétien focus (Figure III.3 and III.4). MOSCA is a focal reducer which lowers the actual focal distance by a factor of 3.7, resulting in an effective aperture ratio of *f*/2.7. This means that it enlarges the image field to 11 × 11 square minutes of arc, allowing complete imaging of relatively close and large galaxies. The detector currently in use is a CCD with 2048 × 2048 pixels, which is sensitive through a large wavelength range from 330 nm to 1 μm.

MOSCA is equipped with two filter wheels for direct imaging which can accommodate 17 filters together. A Fabry-Pérot interferometer is also built into the instrument: this can be set as a narrow-band filter (pass width 1.5 to 2 nm) throughout a range from 550 to 950 nm. Six different grating prisms (grisms) with various spectral resolutions are available for spectroscopic investigations.

During 1998, MOSCA was mainly used as a multi-object spectrograph. In this configuration, simultaneous records can be made of the spectra from several celestial bodies, such as the galaxies in one cluster. For this purpose, a metal plate is inserted in the focal plane of the telescope, with slits milled into the plate at precisely measured positions. This pattern of slits corresponds to the distribution of galaxies in the focal plane, so that spectra from all the celestial objects are obtained simultaneously with one single imaging operation (Figure III.9).

The masks can be produced in the MPIA's workshops, to a precision of one micrometer. All users of the instrument, including visiting observers, can have the masks they require produced at the MPIA. Finally, a semi-automatic procedure makes it possible to align the telescope and the mask within 10 to 15 minutes. One example of MOSCA's use was in the search for the remotest galaxies in the Calar Alto Deep Imaging Survey, CADIS.

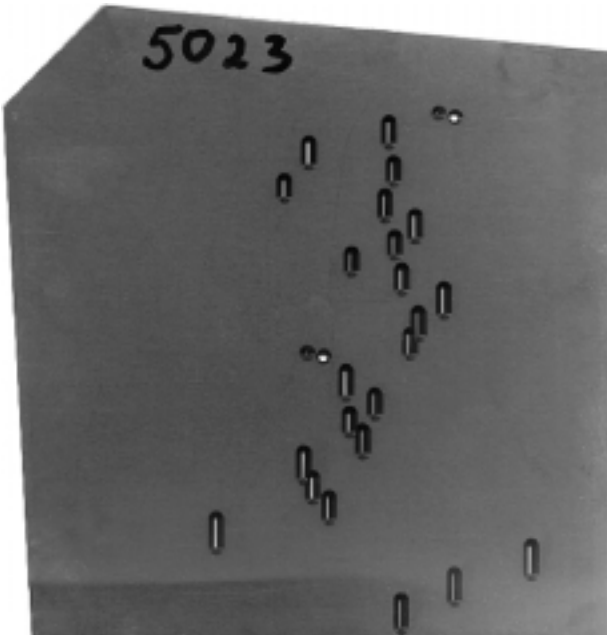

Figure III.8: A perforated mask produced for MOSCA.

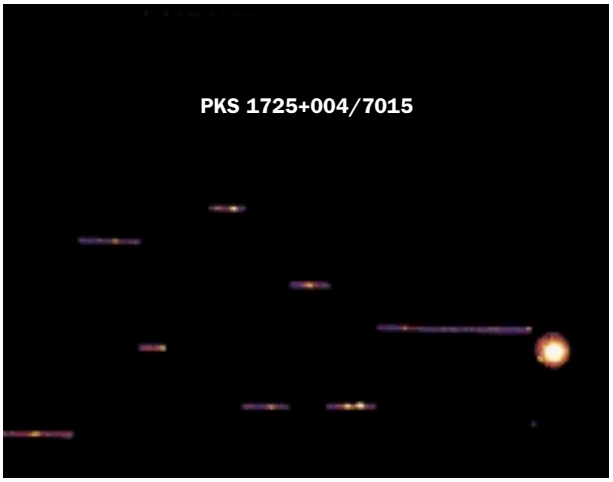

Figure III.9: Multi-spectral photograph obtained with MOSCA.

OMEGA-Prime – a near infrared camera for Calar Alto

OMEGA-Prime is the first camera of a new generation of infrared detectors on Calar Alto. It began operation in the spring of 1996 on the 3.5 metre telescope. At the heart of the instrument is a chip which was developed in the Rockwell Science Center and at the University of Hawaii, made from a mercury-cadmium-tellurium compound (HdCdTe) with 1024 × 1024 pixels. This chip is 16 times larger than its predecessor in the Magic camera. Its sensitivity range extends from 1 to 2.5 μm, so that it encompasses the near infrared. OMEGA-Prime was designed at the MPIA and built in the Infrared Laboratories at Tucson, Arizona.

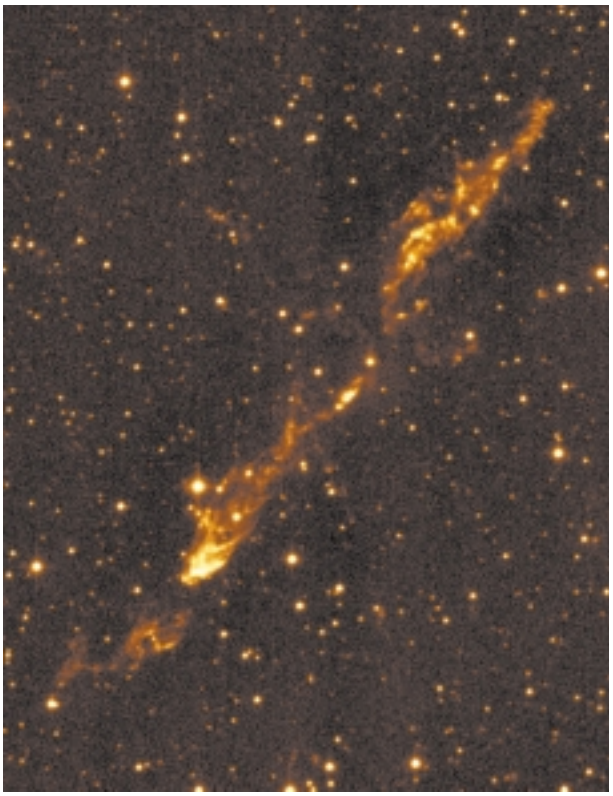

Figure III.10: Photograph of jet HH288 with OMEGA-Prime.

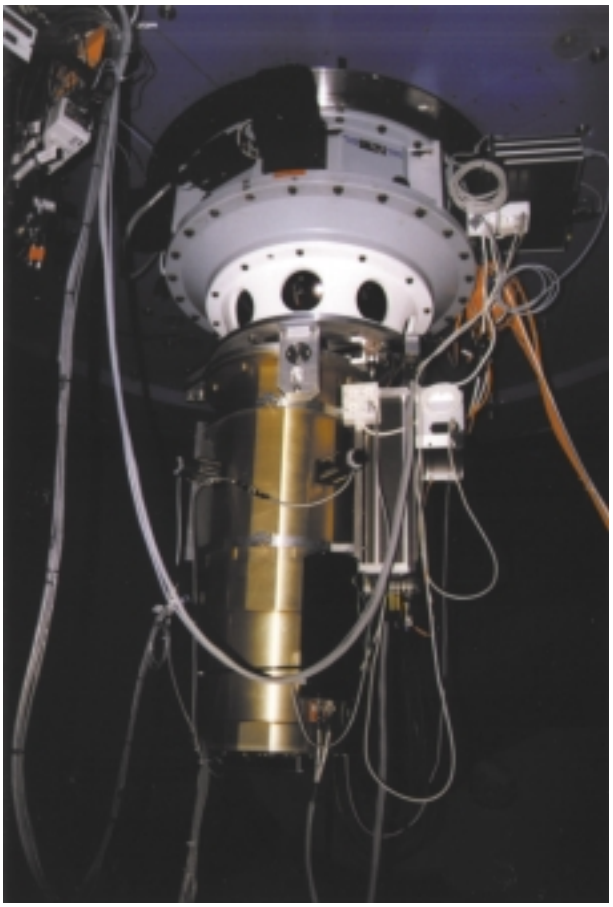

Figure III.11: OMEGA-Cass on the 3.5 metre telescope.

Filter wheels with 15 positions enable investigations to be made in various wavelength ranges, and excellent image quality throughout the entire field is supplied by a corrector consisting of three optical elements (Figure III.10).

OMEGA-Prime is mounted in the prime focus of the 3.5 metre telescope, where a large image field of 6.8 × 6.8 square minutes of arc is obtained. This makes the instrument outstandingly suitable for sampling the sky to locate weak infrared sources such as protogalaxies or brown dwarfs, and also for detailed study of star formation regions. OMEGA-Prime was released for general observing operation in the autumn of 1996, and it immediately became the instrument in greatest demand.

OMEGA-Cass – Spectrometer and camera for the near infrared for Calar Alto

OMEGA-Cass is a further development of Omega-Prime. This instrument is designed for use in the Cassegrain focus of both the 3.5 and the 2.2 metre telescopes (Figure III.11). The instrument operates on three imaging scales, and it offers possibilities for spectral and polarisation investigations as well as direct imaging.

The design and construction of OMEGA-Cass was started at the MPIA in the summer of 1996. As in OMEGA-Prime, an HdCdTe-Array with 1024 × 1024 pixels operates as the detector, with sensitivity in the wavelength range from 1 to 2.5 μm. The imaging scale can be changed by choosing between three different camera optics. In the *f*/10 beam of the 3.5 metre telescope, the scales are 0.1, 0.2 and 0.3 seconds of arc per pixel (Figure III.12). Last year, the instrument was frequently used on the 3.5 metre telescope on Calar Alto, often in conjunction with ALFA, the adaptive optics system (see above).

Two filter wheels can accommodate a total of 18 filters which allow imaging in various wavelength ranges. Moreover, OMEGA-Cass offers two possible methods of polarisation analysis. Four filters which can be rotated in stages of 45 degrees, as well as two Wollaston prisms, provide the linear degree of polarisation for extended sources. Three grisms give OMEGA-Cass its spectroscopic capabilities. The spectral resolution $\lambda/\Delta\lambda$ is between 500 and 1000.

Figure III.12: Galaxy M 82, taken with OMEGA-Cass.

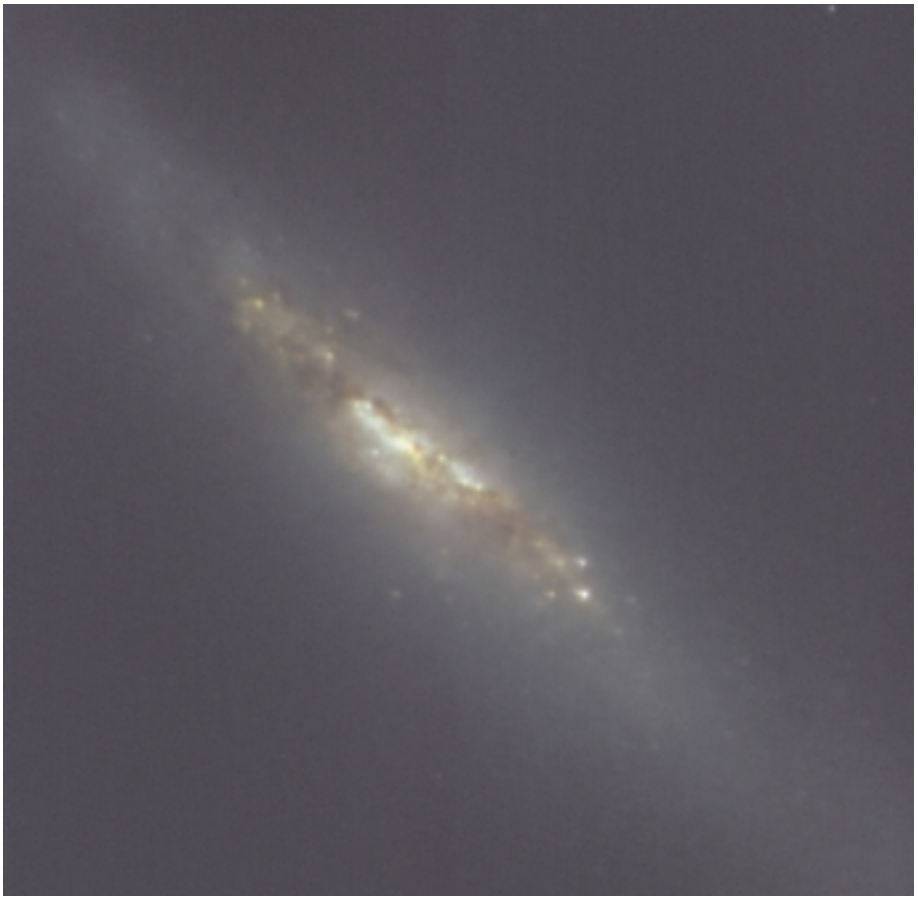

CONICA – High resolution near-infrared camera for the VLT

The European Southern Observatory, ESO, is currently setting up the Very Large Telescope, VLT, on the 2630-metre-high peak of Cerro Paranal in Chile's Atacama Desert. When fully completed, this facility will consist of four large telescopes, each with a mirror of 8.2 metres in diameter, and three smaller auxiliary telescopes with 1.8 metre mirrors. The VLT will then be the observatory with the largest total mirror area anywhere in the world. Each of the four large telescopes has three foci which will be equipped with extremely powerful cameras and spectral equipment. CONICA will operate on the Nasmyth focus of the first of the four telescopes, named Antu (Sun) and it will supply diffraction-limited images with a resolution as low as 0.026 seconds of arc in the near infrared from 1 to 5 μm, in conjunction with the NAOS adaptive optical system.

CONICA is currently being built under the coordinating leadership of the MPIA in collaboration with the MPI for Extraterrestrial Physics in Garching. This instrument (Figure III.13) is due to start operation in the year 2000. In return for their services, the astronomers at these institutes will receive 45 nights observation time with CONICA.

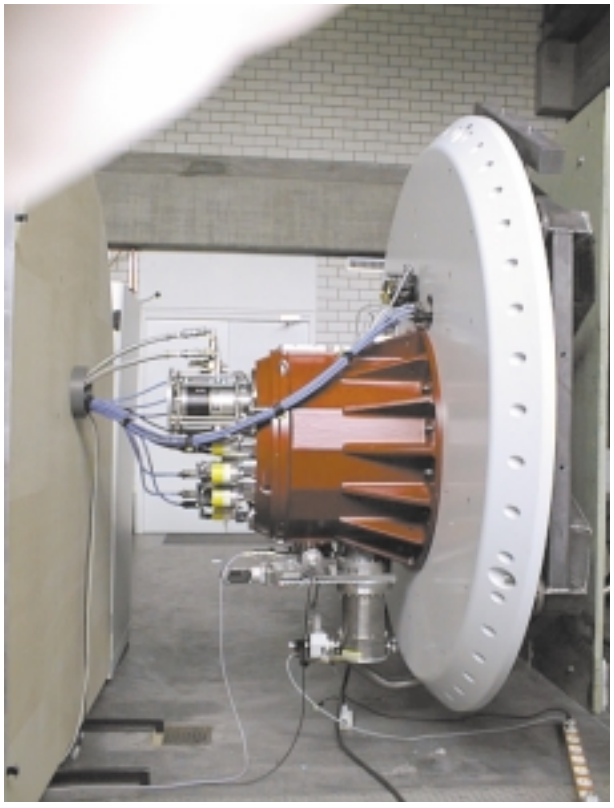

Figure III.13: CONICA on a test bench in the MPIA's laboratory.

The detector is an infrared array with 1024 × 1024 pixels, and the imaging scale can be adapted between 0.014 and 0.11 seconds of arc per pixel. For each of these scales, two camera systems are available, operating in the wavelength ranges from 1 to 2.5 μm and from 2 to 5 μm. Depending on the selected variant, the image field has an extent of between 14″ × 14″ and 56″ × 56″, and a diameter of 73″ at the lowest resolution.

CONICA is a multi-functional instrument with a Fabry-Pérot interferometer (2 to 2.5 μm), a set of 20 standard filters and 15 narrow-band filters, as well as Wollaston prisms and polarisation filters to measure the polarisation of extended objects. Furthermore, three grisms provide the possibility of two-dimensional spectral investigations with an intermediale spectral resolution.

In the 1998, the infrared camera for the adaptive optical system was largely completed, and it is currently being tested in the laboratory. The focusing device has been redesigned and has also been completed.

It will be possible to use CONICA for all current areas of research. Pride of place goes to investigations of areas where stars are being created and to protoplanetary dust disks, the Galactic Centre, the gaseous envelopes around Red Giants, and the search for extrasolar planets. In the extragalactic field, high priority will be given to observations of the central regions of active galaxies and the study of remote infrared galaxies.

MIDI – Infrared interferometer for the VLT

From the year 2000, the VLT will also operate as an interferometer. For this purpose, the beam paths of two or more telescopes will be combined and coherently superimposed in one common image plane. An interferometer of this sort has the spatial resolution of one single telescope with a mirror whose diameter would be equivalent to the basic length of the two telescopes linked by the interferometric coupling. Two of the VLT's telescopes, separated by a distance of 130 metres, will then be capable of achieving a resolution of a few thousandths of a second of arc in the near infrared range.

One of three interferometers, named MIDI, is being developed and built under the coordination of the MPIA. The project also involves colleagues from the Netherlands and France, and from the Kiepenheuer Institute of Solar Physics in Freiburg and the Thuringian State Observatory, Tautenburg. MIDI is intended to enable interferometry with two telescopes at 10 μm as from 2001.

The path lengths of the beams arriving from the two telescopes must be equal to within fractions of a wavelength, equivalent to about one micrometer, in the common image plane. Most of the difference in path lengths, which is principally due to geometry, will already have been compensated for, before the beams enter the instrument. Inside MIDI, the diameter of the beam will

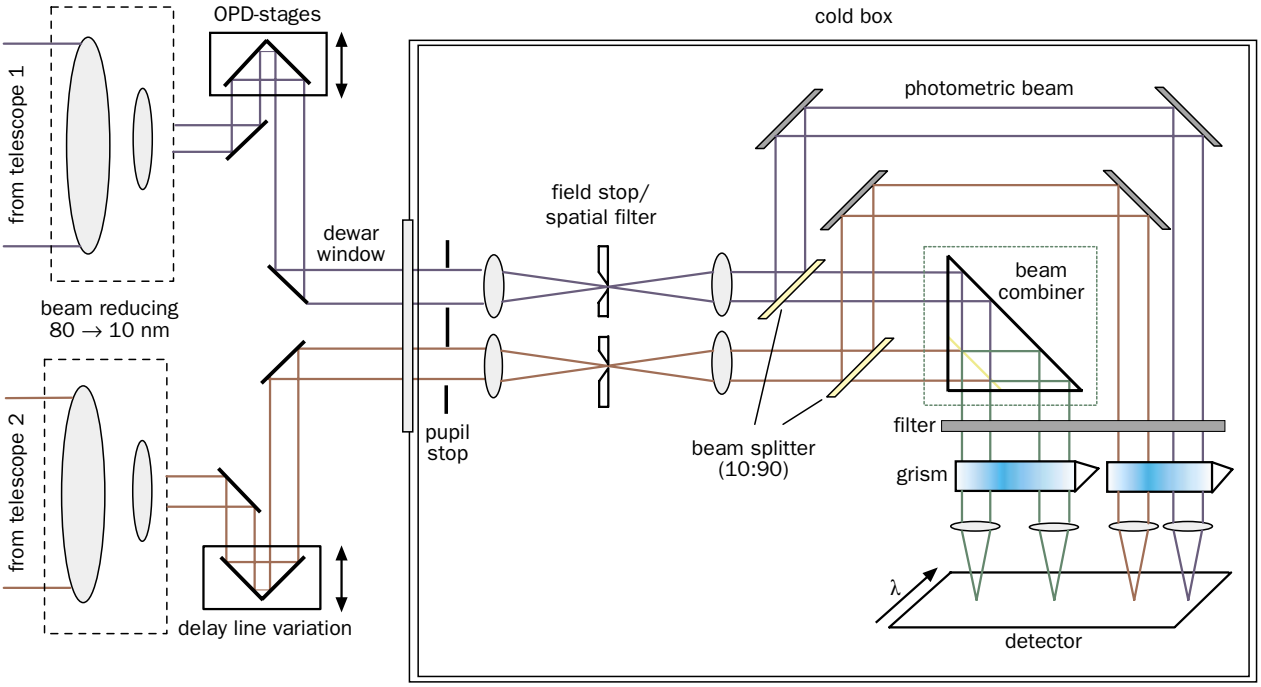

Figure III.14: Schematic diagram of the ray trace in MIDI.

be reduced from 80 mm to 10 mm, and the remaining difference in path lengths will be compensated for by means of movable piezo-electrically driven mirrors. A beam splitter combines the beams to create the interference image (Figure III.14).

At the same time, however, it must also be possible to measure variations in the brightness of the observed celestial object due to air turbulence or clouds. For this purpose, part of the two beams will be diverted out of the interferometric beam path so that continuous separate measurements of the brightness can be taken.

This project made great progress during 1998. At the end of the year, ESO accepted the proposed concept. The detector will probably be a 320 × 320 pixel Si:As-IBC array (IBC = impurity band conduction). Development of the read-out electronics was started in the autumn. Extensive model calculations have shown that the atmospherically induced fluctuations in the optical path distances for the VLT telescopes amount to no more than 1 μm in the course of the measurement period of 0.1 seconds. This makes them very much smaller than the observation wavelength of 10 μm, as is required for the measurements. Large parts of the cooling and vacuum concept developed for CONICA (see above) could also be transferred to MIDI.

The main areas in which MIDI is to work will probably be the observation of double stars, protoplanetary disks, brown dwarfs, extrasolar planets and active galaxies.

PACS – IR Camera for FIRST (Far Infrared Space Telescope)

In the year 2007, the European Space Agency (ESA) intends to launch FIRST, the Far-Infrared and Submillimeter Space Telescope. This is the ESA's fourth major cornerstone mission. FIRST will consist of a 3.5 metre mirror and three scientific instruments which are intended to cover a wavelength range from 85 to 900 μm. These are being built by international consortia of scientists. It will therefore link up to the field of radio astronomy at long wavelengths. One focal point of the research programme will be the observation of protostellar gas and dust clouds and protoplanetary dust disks. It will also be possible to detect the infrared radiation from very remote young galaxies in the submillimetre range.

The MPIA will be participating in the construction of PACS, one of the instruments. This project is being led by the MPI for Extraterrestrial Physics in Garching (MPE). PACS should make it possible to carry out photometric and spectrometric investigations in the wavelength range between 80 and 210 μm (Figure III.15). The MPIA will make major contributions towards the development of the cameras, the pre-amplifiers, the focal plane choppers and the optomechanics, and also towards the data centre.

The initial stages of work focused on an examination of the various read-out electronic systems. They have to meet special requirements, since they must operate reliably at a temperature of only 4 K. It emerged that none of the electronic systems could meet the requirements. In conjunction with the MPE, specifications and

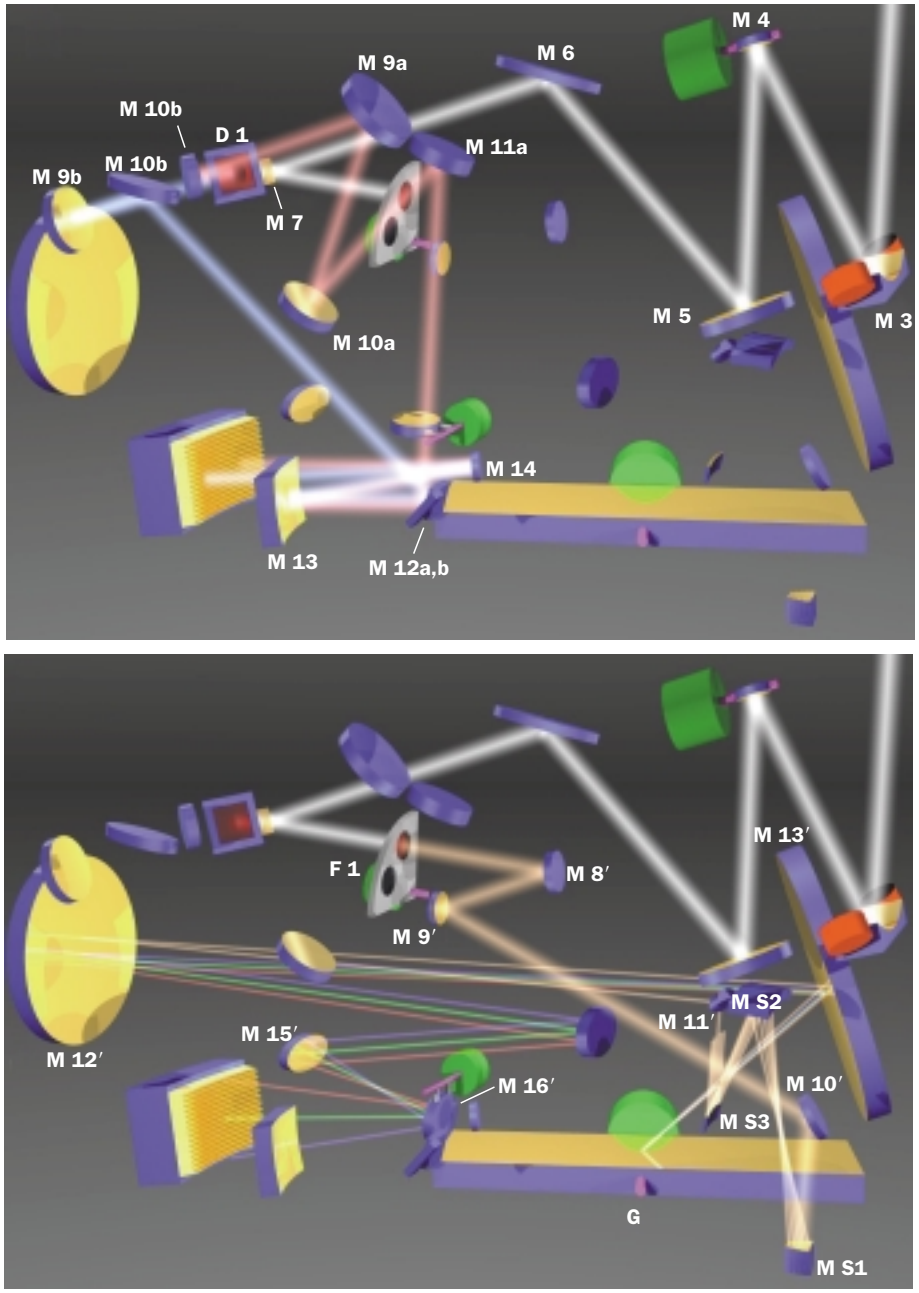

Figure III.15: Computer drawing of the ray trace in PACS: above in photometry mode, below in spectroscopy mode.

test procedures were devised which will determine the future development of the cold read-out electronics. A test device was prepared which will allow future examinations of larger number of detector lines in the detector array with 16×25 pixels each.

Initial work also began on the chopper, which has to satisfy unusual requirements for the articulated suspension, in order to operate in the cryo-vacuum. As well as this, the interaction of the cosmic radiation with the screening and the detector was simulated on the computer. These programs were able to give good reproduction of the incident rates observed during the ISO mission on the printed Ge:Ga detectors. For similar detectors in FIRST, it became apparent that effective screening – especially against high-energy protons – will hardly be possible. The incident rate could only be reduced with screening made of a very dense metal, several centimetres thick.

IV Scientific Work

IV.1 Galactic astronomy

Young double and multiple stars

Two hundred years ago, when Friedrich Wilhelm Herschel discovered that some pairs of stars are linked to one another by the force of gravity, he unleashed a sensation. Today, astronomers know that most stars are members of double or multiple systems. Studies on main sequence stars in the neighbourhood of the sun have shown that the proportion of multiple systems is virtually independent of the star type, at least in the range of classes F7 to M. Accordingly, the ratio of single to double to triple to quadruple systems for G stars (which include the sun) is 57:38:4:1, and for M stars it is 58:33:7:1. In the case of the G double stars, a Gaussian distribution of the orbital periods was obtained, with a maximum at about 180 years. For the Sun, this would correspond to a companion at a distance of some 30 Astronomical Units (AU) where Neptune orbits.

Surprisingly, observations of young stars produced a different result. For example, the proportion of multiple systems with reciprocal distances of between 18 and 1800 AU in the star formation regions of Taurus-Auriga, Chamaeleon and Lupus is substantially higher. Astronomers at the MPIA have been able to prove that in Taurus-Auriga, about twice as many stars are linked to one or more partners than in the later stage of the main series (see the 1997 Annual Report, p. 49). The cause of this discrepancy has not been clarified. Discussion essentially focuses on two possibilities:

- Originally, the systems that are formed are almost exclusively multiple. However, some of them split up in the course of their evolution. This could happen because the systems move about in the gravitational field of the dark cloud. As this happens, they could come so close to one another that they reciprocally tear stars from one another by gravitational force.
- It is conceivable that the conditions in the dark clouds that have been observed could particularly favour the formation of multiple systems in some way, and that there are other clouds where multiple systems are formed in far lower numbers. The size and temperature of the cloud nuclei could be decisive parameters for this phenomenon, according to a surmise.

How is it possible to resolve this question, which is so important for the birth of stars? On the one hand, it is possible to observe young star clusters of differing ages. If the first hypothesis is correct, the proportion of multiple systems should reduce as the age increases. Moreover, star formation regions in clouds of differing sizes and temperatures should be examined in order to test the second hypothesis. On the other hand, an attempt can be made to simulate the formation of stars by numerical calculations (see MPIA Annual Report 97, p. 54). By varying the physical parameters, it would then be possible to discover how these variables affect the formation of multiple stars.

At the MPIA, where star formation has been one of the focal points of research since the outset, both paths have been followed. Last year, it was possible to achieve progress on both the theoretical and observational sides. The work described below also demonstrates that theoreticians and observers can complement one another's work in highly important ways

Speckle holography in the Orion nebula

Most stars probably come into being in dense clusters in the interior of huge dust and molecular clouds which contain matter amounting to as many as several million solar masses. The Taurus-Auriga region which was studied in detail is, however, relatively small. According to estimates, the stellar density in young clusters of giant molecular clouds, such as the Orion cloud, is hundreds to thousands of times greater than in smaller clouds of the Taurus type. It therefore appears altogether plausible that more initial multiple systems are destroyed prematurely by mutual interaction in giant clouds than in small ones, and that more single stars are formed there. Since the giant molecular clouds generate far more stars than the small ones, this would explain why the proportion of multiple systems is substantially lower for main sequence stars than for young stars in the Taurus region.

Above and beyond this, different conditions in large and small clouds could play a part. It is reasonable to suppose that in more massive clouds, where the density of stars in formation is higher than in small clouds, the temperatures of gas and dust rise higher. It is conceivable that high temperatures impede the formation of multiple systems.

Figure IV.1: The Trapezium stars in the Orion nebula, photographed with the Hubble Space Telescope. (Photo: NASA/ESA)

A typical star formation region with a high stellar density is the region around the Trapezium stars in the Orion nebula (Figure IV.1). The Trapezium cluster is part of the gigantic Orion A molecular cloud, 1500 light years away, in the central region of which the stellar density attains a value of 1.4 10^3 stars per cubic light year. This is the densest known star cluster in the Milky Way. About 80% of the stars are younger than one million years, and the average age is about 300000 years.

This makes the Trapezium cluster excellently suited as an investigative object for a star formation region of high density. Previous studies on double star frequency were restricted to the visible wavelength range. A study carried out with the Hubble Space Telescope in 1994 produced a comparably low double star frequency of 12%. However, this investigation was restricted to visual double stars with separations of between 26 and 440 AU. This corresponds fairly accurately to the double star frequency among older main series stars with this separation. A subsequent observing campaign using Hubble yielded a similar value of 14% in the separation range between 138 and 828 AU.

However, the drawback of these first studies is that they took place in the visible range, where low-mass stars (which are at their brightest in the infrared) can only be detected with difficulty. Stars which are concealed by dust can also escape observations in the optical range. Moreover, in both of these studies, technical observational reasons meant that the central region with the high stellar density was precisely the one which had to be left out.

A group at the MPIA has managed to study the Trapezium cluster for the first time in the infrared, with high resolution. In this case, the speckle holography method was used, and an angular resolution of 0.″13 was attained. This made it possible to detect double stars down to a separation of 57 AU.

For their observations, the astronomers used the MAGIC infrared camera on the 3.5 metre telescope of the Calar Alto observatory. With the camera's high resolution of 0.″071 per pixel, the rectangular image field has a longitudinal extent of just 18.″2. Since the fields under investigation were substantially larger, with extents of about 40″ × 40″ (corresponding to 0.3 × 0.3 light years), eight to ten photographs had to be added together like a mosaic in each case (Figure IV.2). The effective exposure times were 352 seconds at 1.65 μm and 432 seconds at 2.61 μm for the respective mosaics. In this way, they attained a

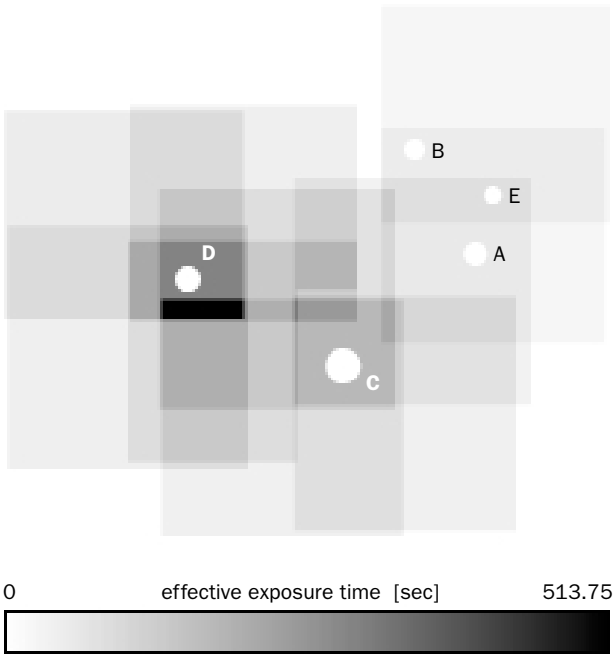

Figure IV.2: The entire exposure time for the individual images at a wavelength of 2.16 μm.

detection limit (with a confidence range of 5σ) between the 15th and 16th magnitude.

In this study, it proved particularly advantageous to use speckle holography. This is a further development of speckle interferometry, which functions according to the following principle.

In principle, the resolution of a telescope depends exclusively on the diameter of the main mirror and the wavelength of the light. In the visible range (wavelength of about 550 nm), a 3.5 meter telescope has a theoretical resolution capacity – also known as the limit of diffraction – of 0.″04, and at 2.2 μm the figure is about 0.″16. In practice, however, the turbulence of the air blurs the image so heavily that the typical resolution is only one second of arc. As the light wave coming from the stars passes through the various layers of the air, it traverses air cells with different temperatures and therefore different indices of refraction as well. The optical path length and the direction of dispersion of the light therefore change constantly as it passes through the turbulent atmosphere. The air cells act like optical lenses which float about.

As a consequence of this, the image of a star is split up into many small pictures, or so-called speckles (Figure IV.3). The number of speckles more or less corresponds to the total number of turbulence cells which the light has traversed. The speckles are distributed over a circular area with a diameter of about one second of arc, in which they dance to and fro in fractions of a second. In photographs with longer exposures, this blurs the star image.

The procedure for speckle interferometry is as follows. Photographs of the target area of the sky are taken in rapid sequence. The exposure time in this case must be selected so that the individual speckles are still recognisable in the image, not yet having become superimposed to form a fuzzy picture. To a certain extent, the speckles are »frozen« on the image. Then, a mathematical process (Fourier analysis) is used to analyse the diffraction-limited images on every photograph, from which a single image is reconstructed which – in an ideal case – has the diffraction-limited resolution. Speckle interferometry has been developed to such an extent that it ceased merely to be applicable to point sources (stars) a long time ago, and it can now supply images of extended objects as well.

One problem of speckle interferometry is the exposure times, which must necessarily be very short. This means that faint stars cannot be detected at all, or else they are only poorly defined on the individual images. The diffraction-limited intensity distribution of a stellar image is also known as the point spread function, which varies according to the time frequency of the photographs – about 0.1 seconds. In speckle holography, the photographs are set up so that a bright star is always located in the image field as well. This can then be used to determine the point spread function in all the photographs. On each photograph, it is also used as a reference for the other, fainter stars. Due to the optimal photographic quality which can be attained, this technique makes it possible to reach fainter objects than can be detected with conventional speckle interferometry.

A comparison with the largest telescope on earth at the moment, the 10 metre Keck telescope on Hawaii, shows how effective this technique is. Using the 3.5

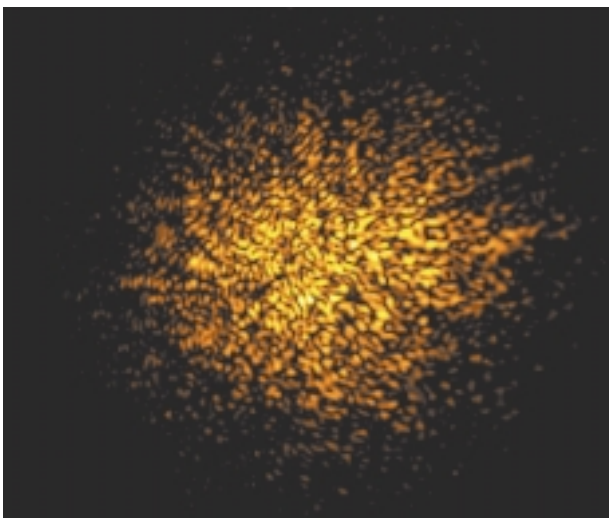

Figure IV.3: Turbulences in the atmosphere cause the image of a star to disintegrate into many random individual images. With speckle interferometry, a diffraction-limited image is constructed from these.

metre telescope of the Calar Alto observatory with speckle holography, the team led by the MPIA reached objects three times as faint as the Keck team could detect with normal speckle interferometry.

An example of star formation: the Trapezium Cluster

To study the Trapezium cluster, 9216 single photographs at a wavelength of 1.65 μm and 12800 at 2.16 μm were required, with exposure times of between 0.065 and 0.1 seconds. One of the bright Trapezium stars was always used as the reference for the point spread function. At these wavelengths, the theoretical resolution capacity of the 3.5 metre telescope is 0.″10 or 0.″13. In actual fact, values were attained between 0.″13 and 0.″17 (at 1.65 μm) or 0.13 and 0.″16 (at 2.16 μm) – an excellent result.

In the field, (Figure IV.4) the astronomers found a total of 35 (1.65 μm) and 44 (2.16 μm) stars, four of which proved to be double stars with separations between 63 AU and 225 AU. These included θ1 A Ori, itself one of the four bright Trapezium stars. It has a companion at a distance of 0.″2 (90 AU). It has already been known for some time that θ1 A Ori is an occulting variable. It is orbited by another star with a period of 65 days. These stars therefore form a triple system.

The technology used did not permit the discovery of any double systems with components less than 0.″14 to 0.″2 from one another. The precise figure depends on the brightness ratio of the two components: the higher the intensity ratio between the main star and the companion, the larger the interval required for detection has to be. Moreover, no faint companion stars below the detection limit of about 16 mag could be detected. With statistical methods, it was possible to estimate that only 0.28 companions could not be found for this reason. On the other hand, the stars may be a feigned pair in 0.21 cases. In a case of this sort, a star is only close to another one by chance in projection. The two effects therefore almost cancel one another out.

All in all, this yielded a double star rate of (9.5 ± 4.5) %. To be able to make a comparison with the statistics of main series stars close to the sun, the low mass stars with less than 1.5 solar masses would need to be counted separately. In this case, only two remain, yielding a frequency of (5.9 ± 4.0) %. In earlier studies which were also conducted at the MPIA, a frequency of (17.2 ± 2.9) % was obtained for young stars in the Taurus region at the same separation of between 63 and 225 astronomical units. For the evolved main sequence stars in the solar neighbourhood, the proportion is (8.1 ± 2.2) %.

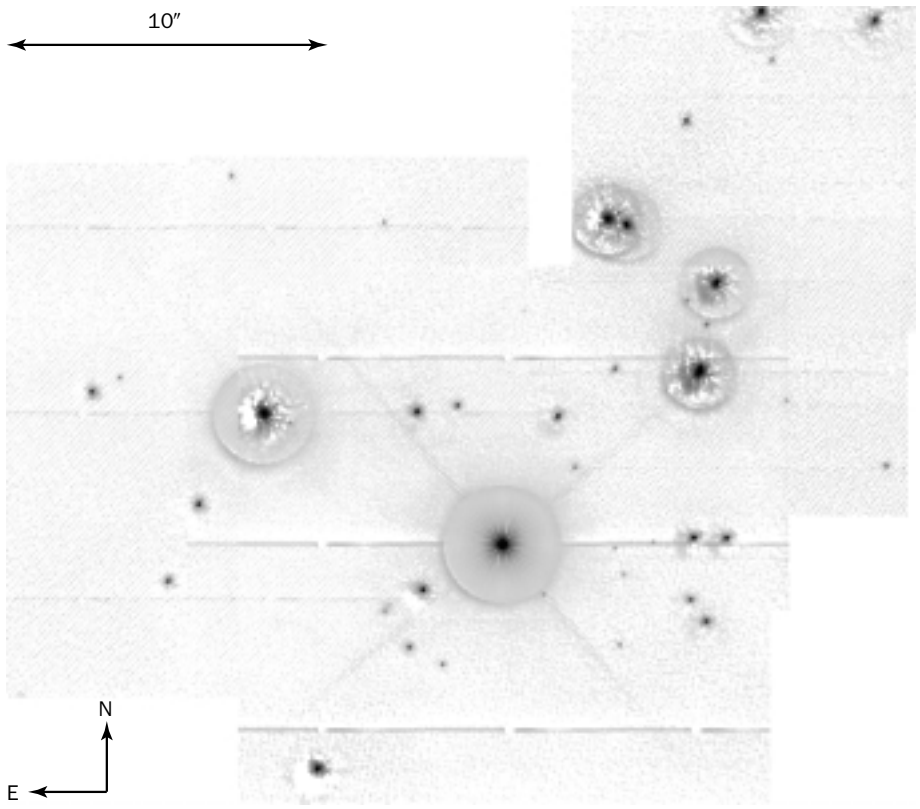

Figure IV.4: A photograph of the Trapezium region obtained with speckle holography at a wavelength of 2.16 μm.

The proportion of double stars in the centre of the Trapezium cluster is therefore comparable to the figure for the main sequence stars. This supports the hypothesis that most stars are formed in dense clusters like the Trapezium cluster. On the other hand, the smaller clouds, with their high numbers of double stars (as in Taurus), only make a minor contribution towards the total number of stars in the Milky Way. Model calculations show that in regions of high stellar density, double systems are destroyed if close fly-bys occur. It would therefore be interesting to study other star formation regions with high densities but differing ages. According to this hypothesis, the relative number of double systems should in fact reduce as the age increases.

Interestingly, the picture changes somewhat when only high mass stars are considered. In a total of six O and B stars, there is one double, one triple and one quadruple system. Due to the small number of stars, statistical statements should be treated with caution. Nevertheless, observations suggest that multiple systems may possibly occur more frequently in the case of high-mass stars than of low-mass ones.

Brown Dwarfs

It was also possible to use the observations to search for brown dwarfs. These celestial bodies are located in a transition area between stars and planets. If a celestial body has less than about 0.08 solar masses, the temperature and pressure in its interior no longer rise sufficiently high for the fusion of hydrogen to commence. It only triggers a deuterium-tritium fusion for a short time. Following this, a brown dwarf spends most of ist life cooling off slowly. Below 0.02 solar masses, deuterium-tritium fusion is no longer possible either. Because of their low brightness, brown dwarfs can only be detected with difficulty. Up to now, only about 5 are known. Nevertheless, the total proportion of them in the Milky Way may be very high. The question of their frequency is of great interest for many reasons, one being that they might constitute part of the dark matter in the universe.

On the speckle holographs, a brown dwarf with 0.08 solar masses would have an apparent brightness of about 13.5 mag at a wavelength of 2.16 μm, while one with 0.03 solar masses would have a brightness of 15.4 mag, still placing it above the detection limit. On the Trapezium mosaics, however, it was impossible to make out a single brown dwarf. So they would appear to be formed in smaller numbers than some astronomers believe.

From a molecular cloud to a star – calculations over 17 orders of magnitude

If it is intended to take a theoretical approach to the question of binary star frequency, various problems have to be combated. In broad outline, the birth of a star may be imagined as follows.

A large proportion of the interstellar matter is located in clouds which are mainly concentrated in the spiral arms of the Milky Way system. The diameters of the clouds vary between a few light years and 150 light years, and the masses they contain are between about one hundred and one million solar masses. In principle, all of these clouds are gravitationally unstable, which means that they ought to contract under the influence of their own gravitational force. However, this is prevented by turbulence, which counteracts the collapse with kinetic energy – but where local turbulence subsides, a region can contract. The term »cloud nucleus« is used in this case. Typically, this process ends after a million years, when one or more stars have formed in such a nucleus.

Last year, the theoretical group at the MPIA carried out detailed work on the physics of turbulent gas (1997 Annual Report, p. 55). In the year under report, it was possible for the first time to calculate the contraction of an interstellar cloud nucleus in three dimensions, over a range of 17 magnitudes in density, and seven magnitudes in spatial extent. According to these simulations, the formation of close binary star pairs is highly improbable. This suggests that important physical processes – especially in the last phases of the formation of a star – are not yet sufficiently understood.

Two theories are currently under discussion to explain the formation of binary stars. The capture theory assumes that two protostellar condensations meet one another and form a binary system. In physical terms, however, this is only possible if one of the two bodies loses kinetic energy during this process, for example due to the interaction of the protostellar disks in the cloud. This process is not favoured at present. Most astrophysicists now assume that a protostellar cloud flattens out into a disk during the collapse, initially due to the rotation. In this structure, individual areas become unstable and they break up into smaller fragments. These carry on condensing to form stars that move around a common centre of gravity. The theoretical group of the MPIA had already carried out extensive model simulations in 1997 to show how complex this process can be (see 1997 Annual Report, p. 59).

Nevertheless, these calculations could only be continued until the gas had attained a density of 10^{-13} g/cm^3. Up to that point, the gas is transparent. That means that all the radiation escapes from the interior, carrying energy away, so that the gas does not heat up during the contraction (isothermal phase). In these isothermal calculations, the protostellar disks under consideration fragmented, and multiple systems were formed.

However, if the gas exceeds a density of 10^{-13} g/cm^3, the infrared radiation which had previously carried energy away from the cloud is no longer able to escape. As a consequence, the temperature in the interior rises, making the simulations considerably more difficult. Earlier calculations had shown that as the density and temperature increase, a hydrostatic nucleus develops with an extent of about 4 AU, and this does not fragment any further. Accordingly, no close multiple stars with intervals of a few astronomical units were formed in these models.

Following the collapse further, an important new process starts at a density of about 10^{-8} g/cm^3 and a temperature of some 2000 K, and this cools the cloud down: the hydrogen molecules, of which the cloud is predominantly made up, disintegrate (dissociate) into hydrogen atoms (Figure IV.5). The energy required for this endothermic process is taken from the thermal energy of the cloud, causing it to cool off. A second collapse phase starts, in which the cloud contracts still further without heating up substantially. It is only when it has attained a density of 10^{-3} g/cm^3 that the temperature in the interior again rises more sharply with further contraction, until the fusion of hydrogen nuclei starts at several million degrees.

As earlier calculations have shown, the cloud could fragment in the second collapse phase (from a density of 10^{-8} g/cm^3 onwards), but only if it is rotating quickly enough. To put it more precisely, the ratio β of the rotation energy to the potential energy must be greater than 0.274. Otherwise, all that occurs is the formation of a star with a stable disk surrounding it. However, these results are based on computer simulations which are restricted to the innermost area of the protostellar nucleus. In these calculations, it was necessary to assume a plausible initial condition for the second collapse phase, since it was not possible to include the first collapse phase in the calculation on a self-consistent basis. Moreover, the ratio β has to be entered arbitrarily »by hand«. Models which comprise the entire collapse from the optically thin interstellar cloud with a density of 10^{-18} g/cm^3 as far as the protostar at 0.01 g/cm^3 must have spatial resolution on scales between 10^{17} and 10^{10} cm (7000 AU and 0.0007 AU). This was not possible in three dimensions until now.

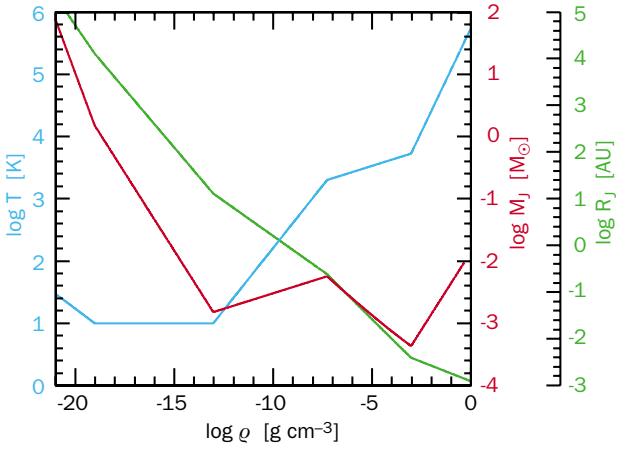

Figure IV.5: Evolution of the gas temperature (continuous line), the Jeans mass (dotted) and the Jeans radius (dashed) as a function of density in a collapsing gas cloud. The stepped temperature progression reflects the various phases of collapse.

For its calculations, the MPIA group used the so-called smoothed particle hydrodynamics (SPH) method. This program is especially well suited to the problem, because the computational resolution increases with the particle density. It was not possible in practice to take explicit account of radiation transport. However, this process could be taken into consideration by assuming a generally different physical behaviour for the gas (or to put it more precisely, the dependency of the gas pressure on the density) in the various phases of contraction.

The calculations started with a spherical interstellar cloud of constant density, of one solar mass and a radius of 7 10^{16} cm (4600 AU), which rotates at constant angular velocity. Initially, the ratio β = rotation energy / potential energy = 0.005. This cloud was represented by 300,000 particles of the same mass.

The collapse took place as follows: first of all, the cloud contracts isothermically, until – after 55 800 years – a density of 10^{-13} g/cm^3 is reached in the central region. This period is known as the free-fall time t_{ff}. The gas is now optically dense. It heats up, and the first hydrostatic nucleus with a mass of 0.01 solar masses and a radius of 7 AU has come into being. This nuclear area has flattened out and is rotating quickly, so that β has risen to 0.34. This means that the critical value for fragmentation has been exceeded. After as few as three full rotations (corresponding to 57 100 years), the disk becomes unstable and develops spiral-shaped arms. During this process, a substantial angular momentum is conducted from the central region to the outer regions over a short period, causing b to fall below the critical value of 0.273.

The nucleus goes on absorbing matter from the surrounding area, and it only goes on contracting slowly, due to the rising temperature. At a temperature of 2000 K, the hydrogen molecules then dissociate. This causes energy to be withdrawn from the gas, and it can contract further. It is only when the nuclear region has reached a density of 0.007 g/cm^3 that the contraction slows down again: a second hydrostatic nucleus has formed, with a mass of 0.0015 solar masses and a radius of 0.8 solar radii. It is surrounded by an inner disk. The calculation was discontinued when the inner nucleus had grown to 0.004 solar masses. The inner disk then had a radius of 0.1 AU and the outer disk (the remains of the first hydrostatic nucleus) extended to a distance of 70 AU from the star (Figure IV.6). In the further course of evo-

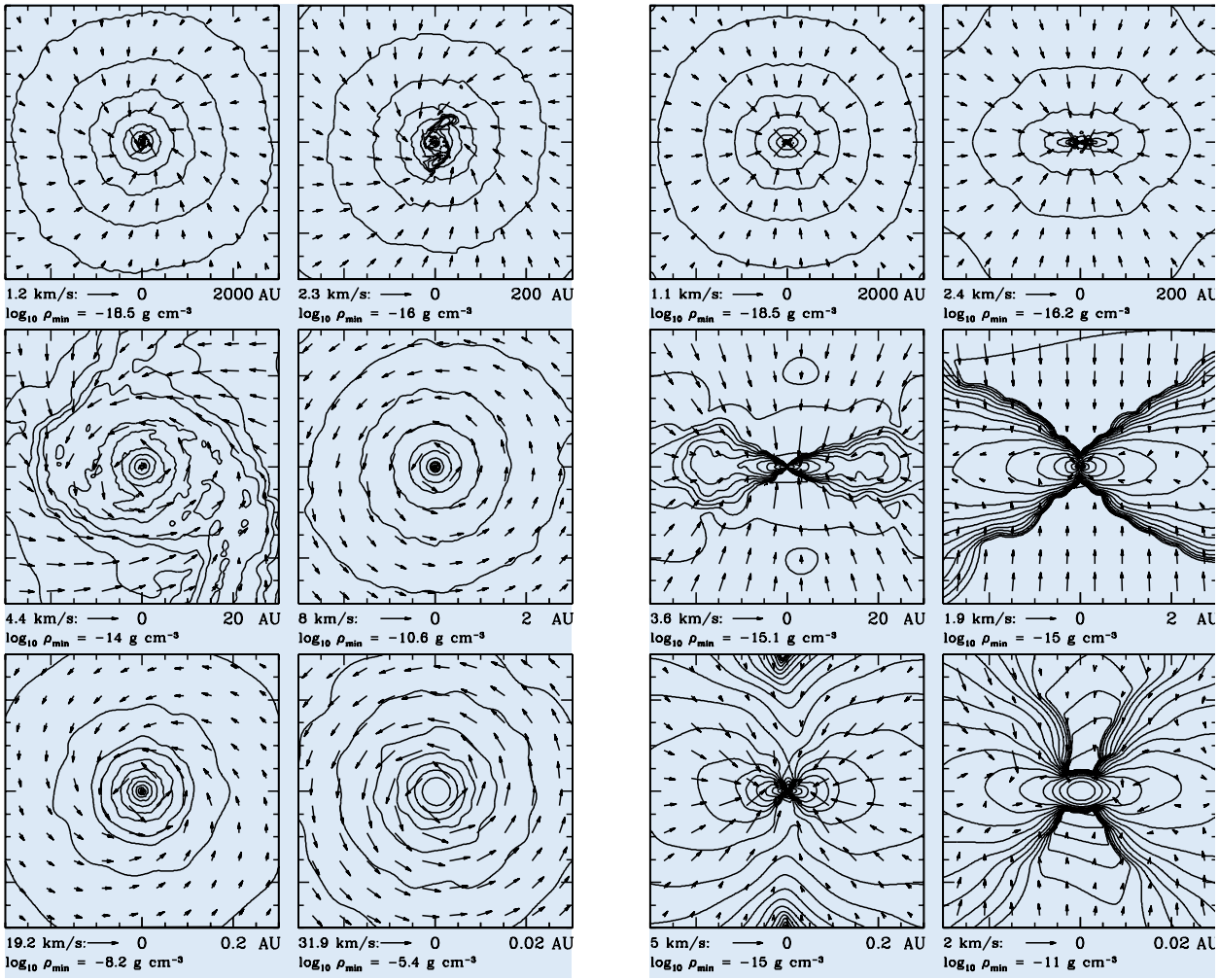

Figure IV.6: The condition of the gas cloud at the end of the simulations – left, top view onto the disk plane; right, perpendicular to it. The individual images reproduce the density and speed field on a scale reduced by one magnitude in each case. In this way, details with extents of 3000 AU to 0.2 solar radii can be detected.

lution, the inner disk will probably grow by absorbing matter from the outer disk.

A decisive point in this evolution was that β fell below the critical value after the first hydrostatic nucleus was formed, and it failed to exceed this value again during the second collapse phase. This means that the inner region, with a diameter of several astronomical units, cannot fragment in order to form a close binary star.

Since there are a very large number of double systems with separations of a few astronomical units. there must either be a different formation mechanism for them, or else the simulations do not adequately describe the real processes. In order to follow up the second of these questions, the MPIA researchers want to repeat their simulations with different physical starting parameters. For example the initial angular momentum of the cloud could have an influence on further evolution.

Beyond this, magnetic fields also play a part in the formation of stars. They were not taken into account in the simulations. However, it is improbable that magnetic fields promote the formation of double stars. Magnetic fields could form a link between the star and the disk. An analogy will illustrate how fields of this sort act. For this purpose, the magnetic fields should be thought of as rubber bands in a tough dough. If this dough is stirred, the bands are carried along with the movement and extended. Due to this, the disk matter loses kinetic energy and angular momentum, causing β to decrease. If β is too small, however, the disk condenses into a single star. Accordingly, magnetic fields should rather inhibit the formation of binary stars.

Kinematics of bipolar jets from young stars

At the end of the 1970s and the start of the 1980s, astronomers made an important discovery in star formation regions: particle winds were emanating from some young stars in two opposed directions. These flows were collimated to different degrees. For example, radio observations revealed molecular winds moving away from the star in two cones, typically with an angle of opening of 20 degrees and at speeds of 10 to 20 km/s. In the visible range, very tightly collimated particle »jets« were found, in which the particles were moving away from the central object at anything up to 400 km/s (cf. 1997 Annual Report, p. 43). In some cases, one object displays both types of bipolar wind.

Bipolar outflows and equatorial dust disks

Since the start of the 1980s, this phenomenon of bipolar outflows has been one of the focal points of research at the MPIA. Its discovery at the time came as a great surprise to theoreticians. According to their models, a star is born when a cloud made of gas and dust exceeds a specified mass. It then becomes unstable and starts to contract under the influence of its own gravitational force. Large clouds fragment into numerous smaller condensations during the contraction. In the process, these rotate and flatten out perpendicularly to the axis of rotation, on account of the centrifugal force. A gas and dust disk is formed and the star is formed in its centre. As theoretical investigations show, even two or more stars may form in a disk due to fragmentation (see this chapter, »From a cloud to a star« and the 1997 Annual Report, p. 59).

It was expected that the young star would continue to accrete matter from this disk. But it was surprising to find that it also shoots gas out into space. Further investigations, in which astronomers at the MPIA played a major part, ultimately proved that the particle winds flow away into space perpendicularly to the disk plane (Figure IV.7). So far, it has not been possible to clarify beyond doubt how these bipolar flows are accelerated, and at what distance from the star this happens.

The astronomers at the MPIA hoped that a series of observations of the closely collimated jets of matter over many years would provide further indications as to the precise processes which unfold in the course of the first million years of a star's formation. In this instance, it has been possible to track the movement of condensations in the interior of some jets and to measure their speeds. This new knowledge makes it possible to test various theoretical jet models.

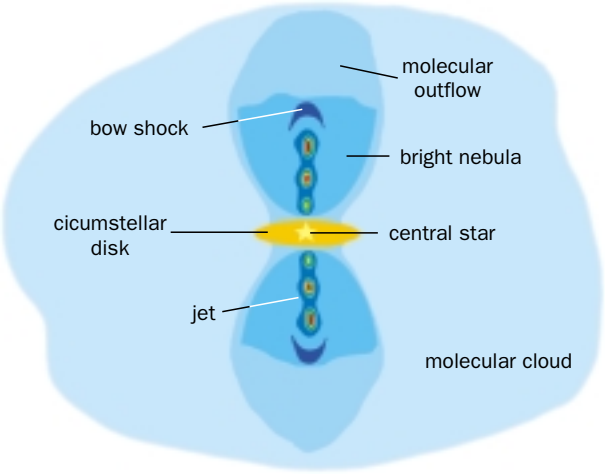

Figure IV.7: Schematic diagram of the surroundings of a young star during the bipolar phase. Two jets shoot out into the surrounding molecular cloud, perpendicularly to the circumstellar disk.

Movement of jet nodes

Many of these gas flows end up in arc-shaped clouds which are interpreted as the "bow waves" of the jets. They mark the end of the jet, where the flow meets the surrounding interstellar medium and bores on through it. In this regard, it may be compared with the pressure wave of a supersonic aeroplane or the bow wave of a ship.

Today about 50 stellar jets are known, 15 to 20 of which are credited to the MPIA. In extreme cases, these flows can be detected at distances of up to ten light years from the source. The dynamic ages are as much as 11000 years. The jet sources involved are T-Tauri and Herbig Ae/Be stars, which are often still deeply embedded in the cloud where they were formed. These stars constitute the transitional phase between the collapsing protostellar clouds and the main sequence stars; T-Tauri stars have about one solar mass and Herbig Ae/Be stars have more than two solar masses.

One striking feature consists of node-shaped compressions in the jets, whose origin has not yet been fully clarified. Spectroscopic examinations have enabled the unambiguous conclusion that the gas in the jet is largely ionised. It is evident that shock fronts develop in the interior of the jets, where the matter heats up to temperatures of about 10000 K. In the cool zones which adjoin »downstream« behind the impact fronts, electrons and ions recombine to give off the radiation that is observed. These shining compact clouds have already been known for a long time as Herbig-Haro objects. However, their connection with the jets was only discovered in the 1980s.

Since the gas in the stellar jets is moving at up to 30 times the speed of sound, it was initially suspected that

the bright nodes were static shocks, such as those which occur in the supersonic jets behind aeroplane engines, and which can also be formed in the laboratory. In this case, the nodes should virtually have no intrinsic movement, but should rather be almost stationary in the flow. Another theory assumes that the star ejects the gas at changeable speeds. In this case, it would happen that faster gas flows in the interior of the jet would catch up with slower ones proceeding ahead of them, and impact fronts would form when the »collision« occurred. These impact fronts should then take on a similar arc shape to the foremost bow waves from the jets. In fact, some of the nodes do show a form of this sort. A third theory assumes that impact fronts are triggered by instabilities which suddenly occur in the rapid flows.

One important variable in this question is the intrinsic movement of the nodes. While the radial speed of the gas flow is easily determined from spectra, we have to rely on a comparison of photographs from different years to determine changes when it comes to the intrinsic movement of the nodes. The measurements become all the more accurate as the intervals of time between the photographs become longer. As long ago as 1987, astronomers at the MPIA were able to determine an intrinsic movement of the jet nodes on object L1551 (see the cover illustration of the 1997 Annual Report). Further observations of sources HH 34 and DG Tauri followed in 1994. These already made it clear that not all of the nodes could be explained with the model of the bow waves created by speed variations.

In the reporting year, the intrinsic movements of five further jet systems have been described in the Taurus star formation region which is about 500 light years away. This work is also based on photographs of stars DG Tau, DG Tau B, FS Tau, T Tau and CoKu Tau 1, which were produced between 1983 and 1990 with the 3.5 metre and 2.2 metre telescopes on Calar Alto.

DG Tau is one of the first jet objects to have been discovered, although its outflow is rather inconspicuous. It only extends to a distance of ten seconds of arc from the star, which led to the early conclusion that the jet is virtually pointing at us (Figure IV.8, top). Relatively high radial velocities of the jet gas between –160 and –255 km/s (towards the observer) also argue in favour of this. DG Tau is also interesting because spectroscopic investigations have revealed major speed variations in the gas as it flows out close to the star. Within eight years, the speeds fluctuated between –167 and –300 km/s relative to the star.

Figure IV.8: The region around DG Tau and DG Tau B in the light of the sulphur line [SII].

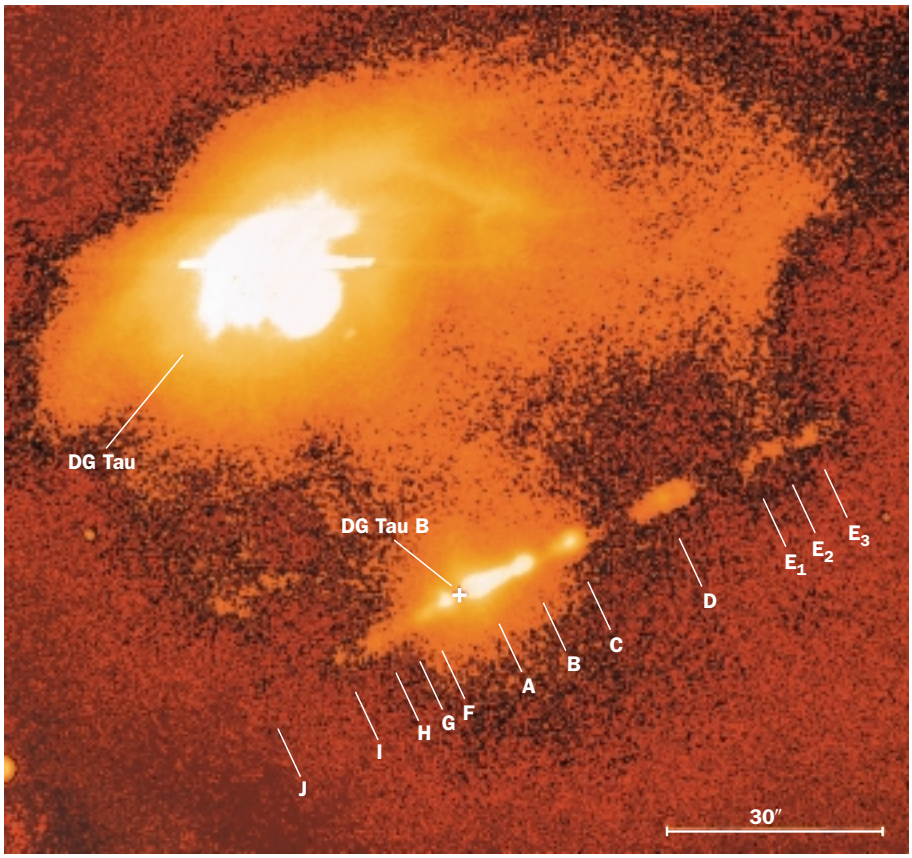

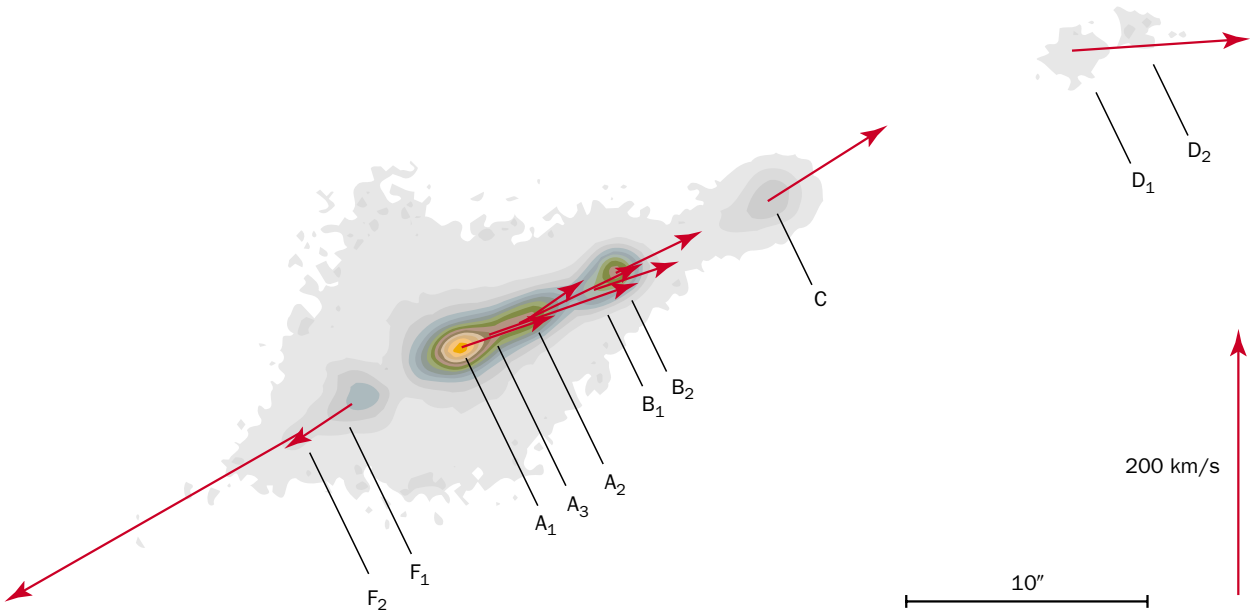

Figure IV.9: The intrinsic movements of the nodes in the jet of DG Tau B.

Now, a comparison of ten photographs obtained between 1983 and 1990 has also made it possible to detect intrinsic movements of four nodes with values of between 100 and 230 km/s. The astronomers at the MPIA now assume that the node furthest from the star is the bow wave. If this is so, the gas coming out of the jet should be braked there and should move on through the interstellar medium with the whole bow wave. This means that the speeds of the gas particles and the whole bow wave should match here. Given this assumption, the angle between the jet axis and the line of sight could be calculated. In the case of DG Tau it turns out to be 38 degrees, which confirms the above suspicion that the jet is pointing virtually towards us.

Using the angle of inclination, the observed intrinsic movements of the jet nodes and the radial speeds of the gas can also be converted into spatial speeds. In this instance, it emerges that ratio R of the node speed to the gas speed in the two innermost nodes is about 0.8. Moreover, assuming constant speed, it was possible to calculate that two nodes and the bow wave must have been sent out approximately in 1970, 1958 and 1936. Unfortunately the astronomers have not yet been able to find a complete photometric measuring series for DG Tau in which they could search for eruptions of brightness at these times.

Another of the first jet systems to be discovered is DG Tau B which is located just one minute of arc south of DG Tau. The star itself is concealed by dust and is therefore invisible – it can only be detected in the radio range. Near to it, there is a bright reflection nebula which it illuminates, and which was regarded as a star until recently. The radio source and the reflection nebula are located between two jets, one of which points towards us and the other away from us. The radial velocities are about 50 km/s and –100 km/s.

Here too, it was possible to measure the intrinsic movements on numerous nodes (Figure IV.9). Unfortunately, there is no evident bow wave in this system, so it is not so easy to convert the measured speeds into spatial movements. Instead, it was assumed that the

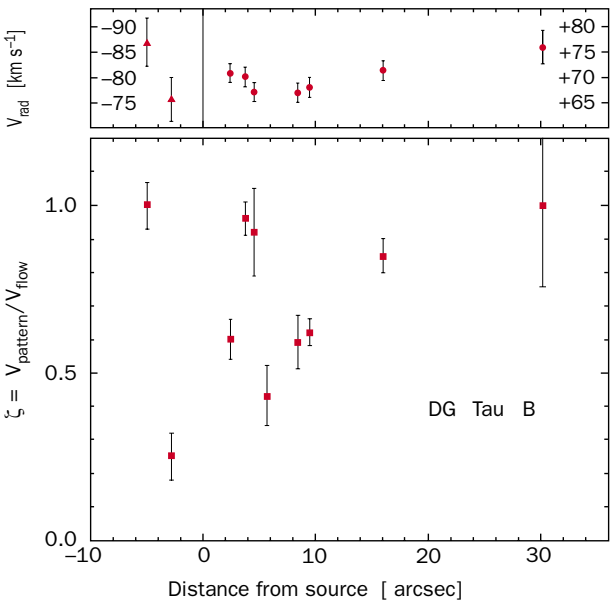

Figure IV.10: Radial speeds (top) and the ratio of node speed to gas speed in the jet of DG Tau B.

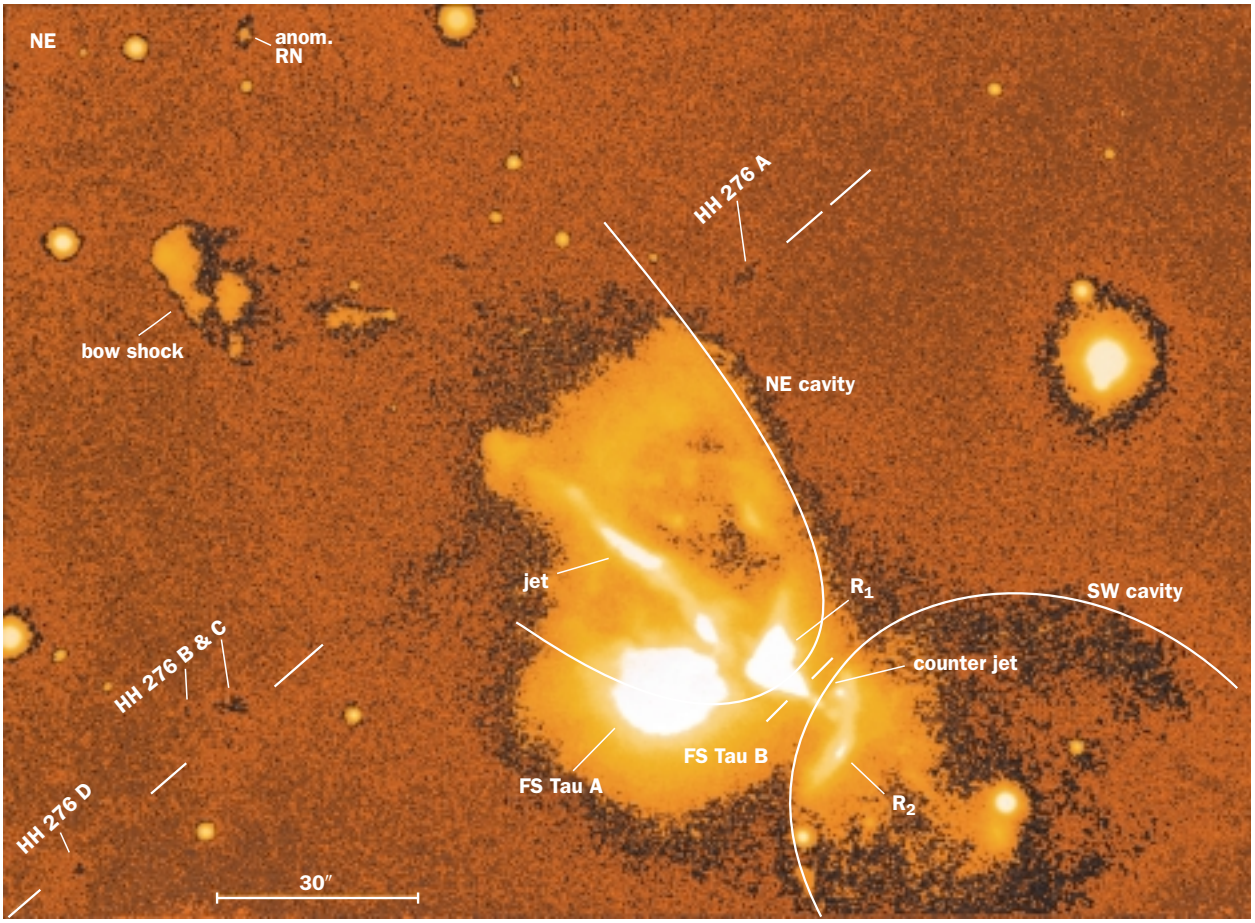

Figure IV.11: Region around FS Tau B with the bow wave of the jet and the conical reflection nebula.

maximum intrinsic movement of a node corresponds to the gas speed. In this way, an angle of inclination of the jet axis of at least 65 degrees is obtained. Surprisingly, the ratio R between node speed and radial speed fluctuated very substantially between 0.3 and 1, whereas the radial speed of the gas remains virtually constant (Figure IV.10).

The bipolar jet system FS Tau B, in which the source is also invisible in the optical range, is another system which has been known for a long time. A striking feature here is an arc-shaped reflection nebula, which possibly marks the marginal area of a cavity created by the stellar wind (Figure IV.11).

It was also possible to measure the intrinsic movements for a series of jet nodes on this source, (Figure IV.12) and given the assumption that one of the nodes represents a bow wave, to calculate the angle of inclination. With an inclination of 80 degrees, the system is virtually in the plane of the sky, which is why the observed radial speeds are very low and the measurement error of 5 km/s has a large effect here. In this case too, the spatial speeds of the node vary sharply between 20 and more than 400 km/s, and ratio *R* also varies between 0.06 and 1.

By way of example, DG Tau B was used to test the jet model which holds the speed variations in the flow responsible for the formation of the nodes. In extensive sections of the jet, very small radial speed differences of only 3 to 4 km/s were measured, and the maximum was about 15 km/s. At the same time, shock speeds can be deduced which are necessary to explain the intensity conditions of certain emission lines observed in the spectrums. Accordingly, impact waves occur with speeds of up to 40 km/s. The speed differences are consequently too small to explain the observed emission. Moreover, the model predicts a substantially lower variation width for ratio *R* between the node and the flow speed than is observed on DG Tau B. Since a similarly large fluctuation width had already been found on the jets from HH 34 and HH 46/47, this model would appear to give an incomplete reproduction of the processes in the jets. Whether instabilities or another process are responsible for the formation of the nodes is a question which still remains unclear.

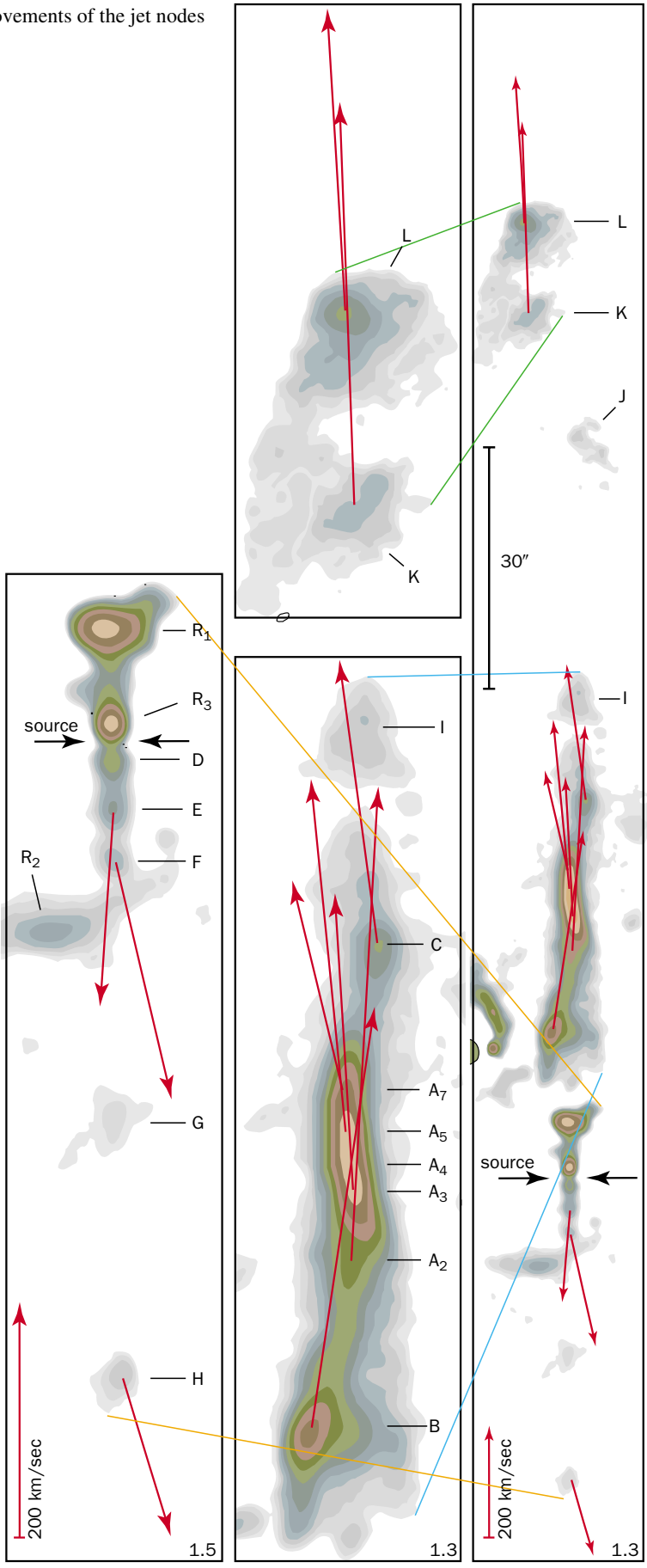

Figure IV.12: intrinsic movements of the jet nodes in FS Tau B.

Jets from »old« T-Tauri stars as well

The jet sources are primarily young stars which are called T-Tauri stars after their prototype. They are estimated to be between one hundred thousand and one million years old. We do not know precisely in which stage the jet phase ends. One feature of age is the surrounding matter. Whereas very young objects still reside deep in the cloud from which they have been formed, the more developed »classical« T-Tauri stars are already quite free, and they are surrounded by just a reflection nebula at most. The spectrum of these stars frequently shows indications of an outflow of high-speed gas. Ten years ago, it was already suspected that this gas is to be found in jets which perhaps cannot be detected because of their low brightness. Using the 3.5 metre telescope on Calar Alto, MPIA researchers set out to search for undiscovered jets on classical T-Tauri stars which had shown suspicious spectroscopic characteristics in earlier investigations.

All five observed cases revealed weak Herbig-Haro objects associated with the stars, or jets with extents of between a few tenths of a light year and several light years. Although the stars had been selected on account of their spectroscopic characteristics, the astronomers were surprised by the 100 per cent success rate. Another interesting point was that two of the stars, DP Tau and RW Aur, no longer appear to be embedded in a dust cloud and are not surrounded by reflection nebulae. The overwhelming majority of all known jet sources show dust nebulae of this sort. Does this mean that the jet phase lasts longer than has previously been suspected? RW Aur (Figure IV.13) is also of interest in that it is a hierarchical triple system: two members are only separated from each other by 0.12 seconds of arc, while the third star orbits the other two at a distance of 1.4 seconds of arc.

This first random sample taken from classical T-Tauri stars still does not allow any definite statements about the temporal evolution effects of the jet phenomenon, or the possible influence of star companions. However, it does suggest that these closely collimated flows are active over a substantially longer period than had hitherto been assumed, and in this respect they may have a major influence on the evolution of the circumstellar disk and the star.

Figure IV.13: The jet of RW Aurigae, taken in the light of the sulphur line [SII].

Eta Carinae and the Homunculus nebula

A star such as our Sun is in hydrostatic equilibrium over a period of ten billion years. In this phase, hydrogen nuclei fuse together in its interior to form helium. The energy released in this process builds up a pressure acting in all directions. The net effect is outwards, keeping the gravitation acting towards the centre in balance. The more massive a star is, the more extravagantly it behaves with its reserves of fuel, and the shorter its lifetime will be. Stars of 15 solar masses and more are in hydrostatic equilibrium for ten million years and less. After this, periodically varying combustion processes commence in their interiors, the star expands and perhaps explodes as a supernova.

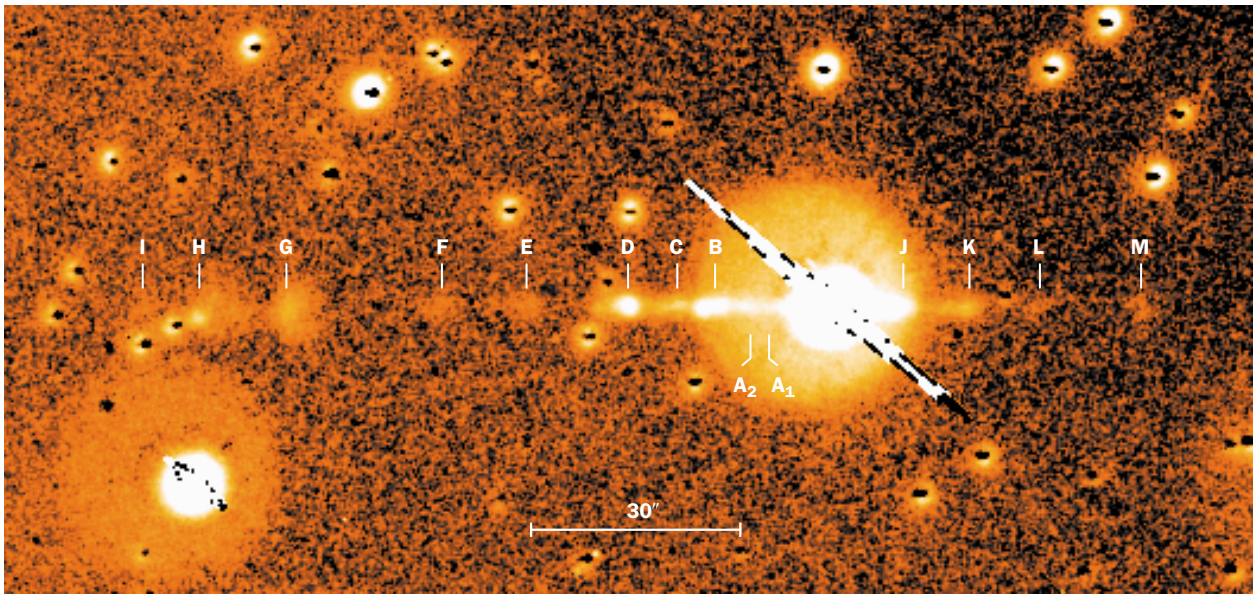

The eventful phase of Luminous Blue Variables

The last phase of a massive star is relatively short, which is why only a few stars in this phase are known. Moreover, the star loses quite a substantial part of its outer shroud, which makes a theoretical treatment of this problem considerably more difficult. Nevertheless, we do know of some massive stars in this stage. They are all surrounded by nebulae which consist of gas that the star has previously ejected. These gas shrouds reflect the varying activity of the star over the recent past. A study of these nebulae therefore opens up the possibility of obtaining important information about this final phase of massive stars. The theoretical group of the MPIA, in collaboration with colleagues from the MPI for Astrophysics in Garching and the Institute for Astronomy in Mexico City is attempting to simulate the observed nebulae with computer models. One of the most impressive examples is the star Eta Carinae with its surrounding nebula, also known as the Homunculus nebula. The models suggest that Eta Carinae is heading towards another outburst of brightness and that it will explode as a supernova in the not-too-distant future.

A star's late phase depends decisively on its mass, and in the case of massive stars, so-called »shell burning« develops in the following manner. Once the hydrogen in the central region has been used up, this part of the star contracts due to gravitation. As a result of this, it heats up again, on account of which helium nuclei now fuse to form carbon and oxygen there. In the surrounding spherically symmetric shell, the pressure and temperature also rise so that the still abundant supply of hydrogen fuses to form helium. When this happens, the outermost areas of the star expand: it blows up into a red giant or super-giant. Once the helium has been used up as well, the nuclear area contracts again. The pressure and temperature now increase until the carbon fuses. In the adjacent outer shells, the combustion continues with a shell burning helium and hydrogen. This cyclical change from contraction of the nuclear area and commencement of a new fusion sequence and an associated inflation of the outer layers ends when the atomic nuclei in the central area have fused to form iron. This area then collapses and the star can explode as a supernova.

Before this happens, the star loses large amounts of matter. This happens because the low gravitational force cannot hold the atoms of the blown-up outer layers, which are driven out into space by the pressure of the stellar light. Present-day star evolution models indicate that stars with 25 to 30 solar masses lose more than half of their original mass in this way, and stars with 30 to 35 solar masses lose as much as 80% of their initial mass. The major part of this mass loss probably happens in a phase known as »Luminous Blue Variable«. These are blue super-giants of spectral types O, B or A with more than 10^5 solar luminosities. Their hallmarks are major brightness variations of at least half an order of magnitude, and intensive stellar winds. Moreover, they are surrounded by nebulae, many of which feature a bipolar structure (cf. 1997 Annual Report, p. 52). Luminous Blue Variables possibly form the preliminary stage for the so-called Wolf-Rayet stars, which also show a major loss of mass. Some Wolf-Rayet stars have been found in the centre of planetary nebulae.

Three-phase model for Eta Carinae

The most impressive example of a Luminous Blue Variable is Eta Carinae (Figure IV.14). This star, some 8000 light years distant, has 80 solar masses, making it one of the most massive stars known in the Milky Way. As long ago as the last century, it attracted the attention of John Herschel when he was observing the southern skies at the Cape of Good Hope. From 1833 onwards, the star became constantly brighter, attaining its maximum brightness of –1 mag in 1843. This made it the second brightest star in the sky after Sirius. Its brightness subsequently fell to +7 mag.

During the outburst, which took place from about 1840 until 1860, the bipolar nebula surrounding Eta Carinae came into being (Figure IV.15). It was given the name of the Homunculus nebula. The star and the nebula have been observed in great detail, making Eta Carinae an excellent subject for a theoretical analysis.

There has been a great deal of discussion about the physical mechanism which might be responsible for the intensive particle winds during the Luminous Blue Variable phase. One attractive possibility is that these stars exceed the Eddington luminosity. This luminosity, named after the British astrophysicist Sir Arthur Eddington, is defined as follows: a star has the Eddington luminosity when the force transferred from the stellar light to a particle and directed away from the star is equal to the gravitation exerted by the star on the particle and directed towards the star. If a star exceeds this limit, the radiation pressure outweighs the gravitation and particles escape into space.

In the MPIA study, the theoreticians assumed that Eta Carinae had exceeded the Eddington luminosity in the past. In their simulation, they also took account of the rotation of the star. This has some major effects on the generation of the particle wind and the form of the nebula. As a result of the rotation, centrifugal force acts on the gas particles in addition to the radiation pressure, giving it an additional velocity component directed radially away from the star. This is at its greatest on the equator, and it reduces towards the poles. The astrophysicists therefore defined a new variable Ω, which represents an extension of the Eddington limit for rotating stars. If $\Omega = 1$, centrifugal and radiation forces are in equilibrium with the gravitational force at the equator. At higher latitudes, the gravitational force is increa-

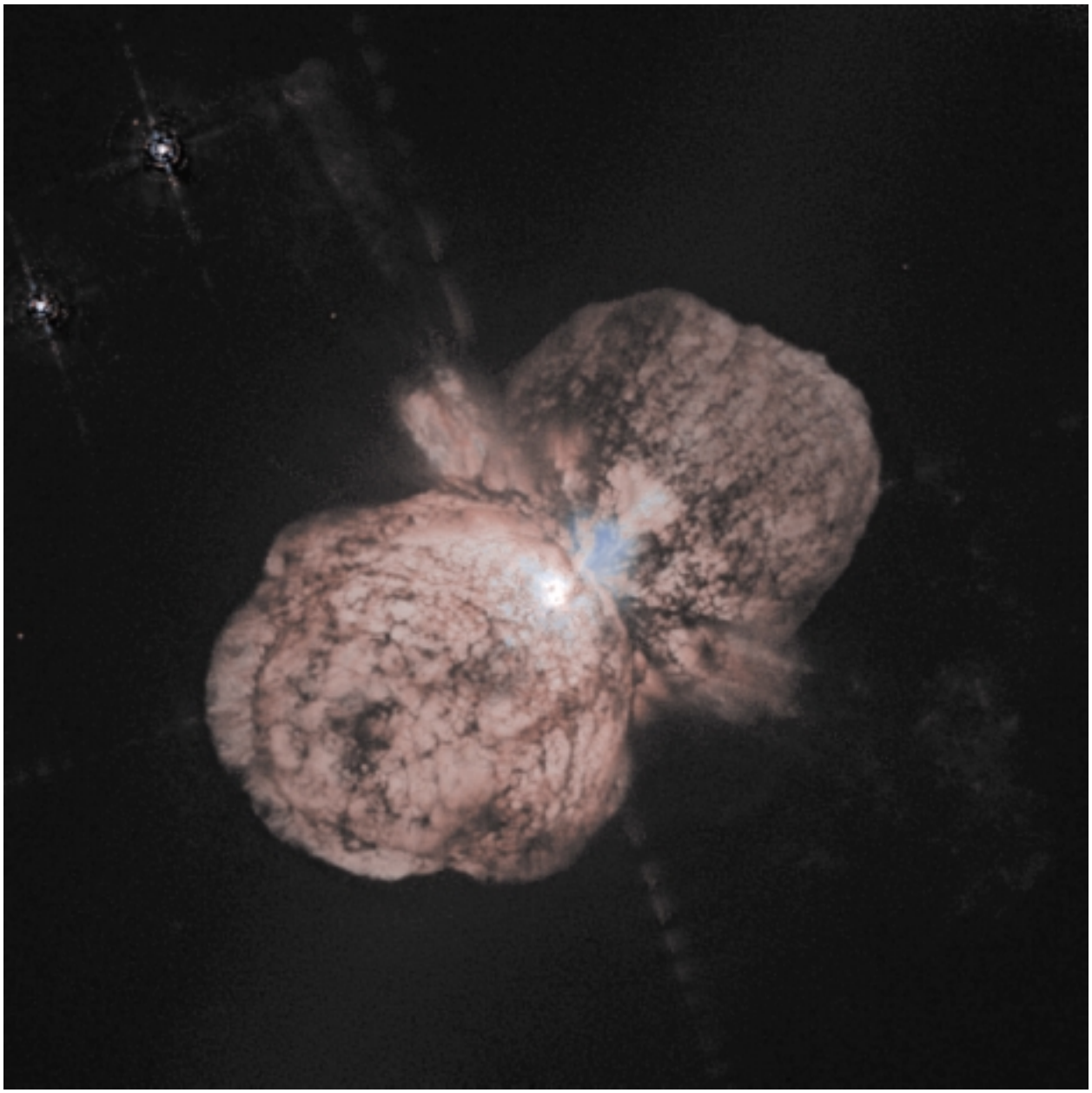

singly predominant. Stars which are close to this Ω limit generate a wind which is concentrated towards the equatorial plane.

The researchers differentiated three phases in the two-dimensional computer simulation. In the first phase, prior to an outburst of brightness, $\Omega < 1$. Then the star develops a fast wind with comparatively low density. During a brightness outburst, the star exceeds the Ω limit. In this second phase, it sheds a great deal of matter, although this cannot be accelerated so much due to its inertia. A slow, dense wind develops. In the third phase, after the outburst, conditions similar to those in the first phase prevail again. It was assumed that the wind speed and the particle density remain constant during the respective phases.

Figure IV.14: Photograph of Eta Carinae taken with the Hubble Space Telescope. (Photo: NASA/ESA)

For the model calculations, a wind with a mass loss rate of 10^{-3} solar masses per year ($M_{\odot}$) and a speed of 450 km/s were assumed for phase 1. The precise figures are not important here, since this wind only sweeps the surroundings of the star clear and creates a hot cavity. During the outburst (phase 2), the slower and denser wind then flows into this cavity, primarily in the equatorial plane. The form of the subsequent nebula essentially depends on the wind's physical variables. In accordance with estimates from observations, the following variables were assumed for Eta Carinae: a mass of 80 solar masses, a radius of 210 solar radii and a luminosi-

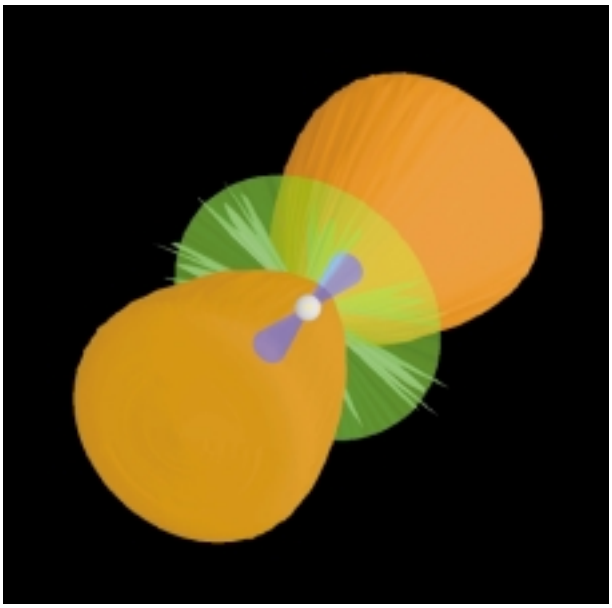

Figure IV.15: Model of the Homunculus nebula of Eta Carinae.

ty of 2.5 10^6 solar luminosities. During the outburst, according to the assumption, the star was close to the Ω limit. The wind speed hence depends on the star's speed of rotation. For this reason, six models were calculated in which the outward flow speed of the gas at the poles varied between 38 and 190 km/s. In addition, two mass loss rates were calculated: at a rate of 7 10^{-3} $M_\odot$/a, over the 20-year outburst phase, a total of 0.15 solar masses of matter flowed away from the star and formed the Homunculus nebula. At 5 10^{-2} $M_\odot$/a, the nebula now contains about one solar mass of matter.

The wind speed rose again after the outburst. The consequence of this was that the faster wind in this phase 3 caught up with the slower one, compressing it into a thin shell, similar to the way in which a plough pushes snow together. In this process, instabilities occur in this compressed gas and agglomerations of various sizes and shapes are formed. Moreover, the wind can now spread out considerably better towards the two poles than in the equatorial region, because the gas density of the wind from phase 2 is lower there. This creates the observed bipolar structure of the nebula (Figure IV.15).

Two models were considered for this phase 3 after the outburst: one with a mass loss rate of 3 10^{-3} $M_\odot$/a and a wind speed of 800 km/s. But the simulation, which describes the evolution of the nebula from 1840 until 1995, does not reproduce the present-day morphology well in that instabilities at the edge of the cavity

Figure IV.16: Model simulations of the Homunculus nebula. Due to the expansion, instabilities occur at the edge of the nebula. If the assumed wind speed is high (left), toothed instabilities occur, contrary to observations. Only a lower wind speed (right) leads to the observed form.

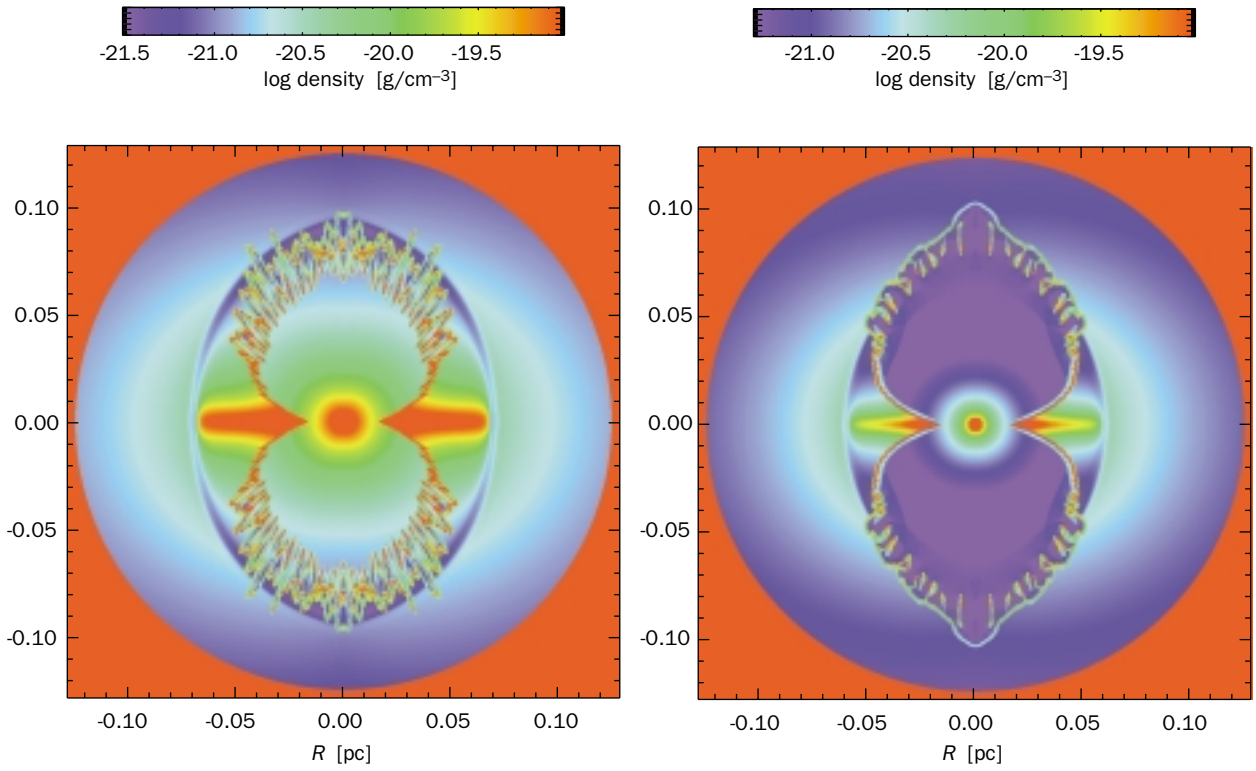

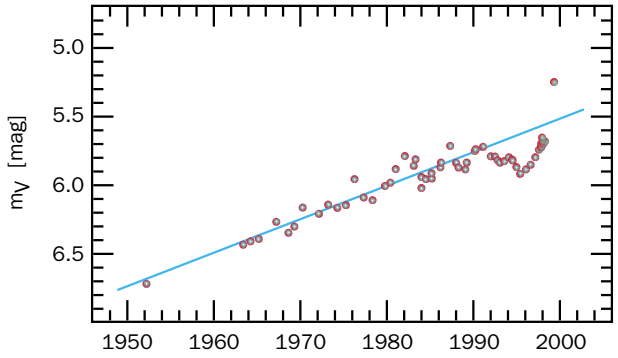

Figure IV.17: Brightness evolution of the star Eta Carinae. The sharp rise within the last year is clearly visible.

become too »sharp« (Figure IV.16a). When the mass loss rate was reduced to 1.7 10^{-4} $M_{\odot}$/a and the particle speed to 1800 km/s, the calculated morphology and size of the Homunculus nebulae corresponded strikingly well to the observations (Figure IV.16b).

Were these simulations to reproduce reality correctly, this would mean that the latest wind has not remained unchanged during the 140 years of phase 3 until today. Rather, it seems to have been thin and fast over the longest period (1.7 10^{-4} $MM_{\odot}$/a and 1800 km/s), only to become denser and slower more recently. This could mean that Eta Carinae is heading for another outburst. Another argument in favour of this is that the star has doubled its brightness in the red wavelength range over the last two years (Figure IV.17).

IV.2 Extragalactic Astronomy

Galaxies in the young universe

Virtually no other area of astronomy is currently developing at such a breathtaking speed as the search for galaxies in the early universe. Just a few years ago, it was barely possible to discover these faint stellar systems beyond a redshift of $z = 1$. At this redshift, we see such distant objects at a time when the universe had already attained two thirds of its current age. The galaxies, such as our Milky Way, were created substantially earlier than this, however. When and how this happened is still largely unclear. Likewise, astronomers do not know when the galaxies combined to form the galaxy clusters which can be observed today. Even so, well thought-out search strategies on the one hand, and the use of new detectors – especially in the infrared – on the other, have recently given considerable impetus to the search for protogalaxies.

Astronomers from the MPIA, in conjunction with colleagues from the Osservatorio Astrofisico di Arcetri, Florence, the NASA Goddard Space Flight Center in Greenbelt, Maryland, and the California Institute of Technology, Pasadena, have discovered several faint celestial objects which are in all probability young systems with a high rate of star birth. It would appear that these young stellar systems are already in the form of groups or clusters.

Star birth in young galaxies

The decisive problem as regards the search for remote galaxies is that they are extremely faint and that they do not stand out sufficiently from the celestial background on photographs taken through wide-band filters. One possibility of overcoming this problem is to use narrow-band filters. These must be selected so that they only permit passage of the wavelength range in which the galaxies have an emission line – that is to say, where they are especially bright. In this range, the brightness contrast between the galaxies and the celestial background is then at its greatest. In general, galaxies with a high rate of star birth shine particularly brightly in the hydrogen lines Hα, Hβ, and in the lines of doubly and singly ionised oxygen [OIII] and [OII].

Now, due to the expansion of the universe, these emission lines are shifted to higher wavelengths in the spectrum in the case of remote galaxies. The further away a galaxy is, the greater this redshift becomes. If we do not know the precise distance at which we must search for the galaxies, we are also unaware of the point in the spectrum at which the respective emission line will appear. This problem can be compared approximately to searching for a station with an unknown frequency on a radio set.

The team of astronomers at the MPIA actually suspected that young galaxies were present at redshifts where hydrogen absorption lines appear in the spectra of quasars. In the spectra of individual quasars, several hundred of these so-called Lyman-α-lines are found. They are caused by gas clouds which are located at various distances from the earth on the line of sight to the quasar. The Lyman-α-line always occurs in the laboratory at a wavelength of 121.6 nm. However, if a large number of absorption clouds are located in the universe at various distances on the line of sight between the earth and a quasar, they will have different redshifts. This is why as many as several hundred Lyman-α-absorption lines are to be found in the quasar spectra. In all probability, these clouds predominantly consist of gas inside galaxies or in their outer regions – the halos.

There is one class of hydrogen absorption lines which are extremely wide (speed equivalent up to 3000 km/s). These so-called damped Lyman-α-lines arise in gas with high column densities of up 10^{21} cm^{-2}, which is very probably located in the disks of spiral galaxies or their predecessors. Accordingly, this is gas in galaxies which we are seeing at a time when the universe

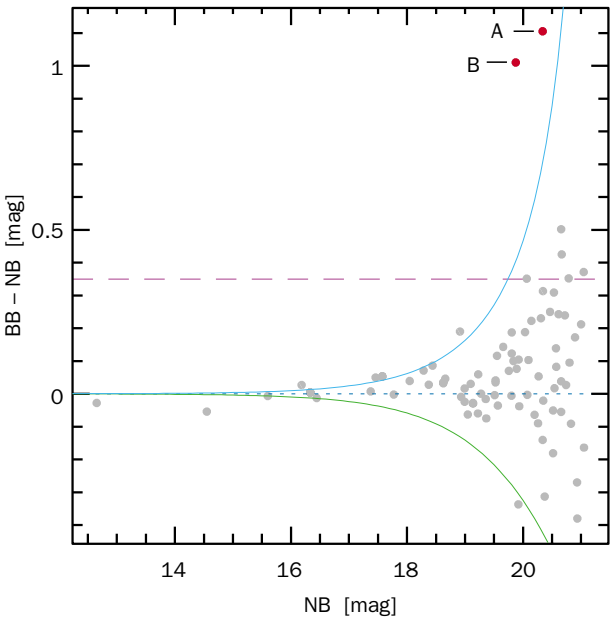

Abb. IV.18: Colour-brightness diagram in which the brightness difference of the wide-band minus narrow-band filter is plotted against the brightness in the narrow-band filter. The two candidates for remote galaxies A and B are immediately noticeable here.

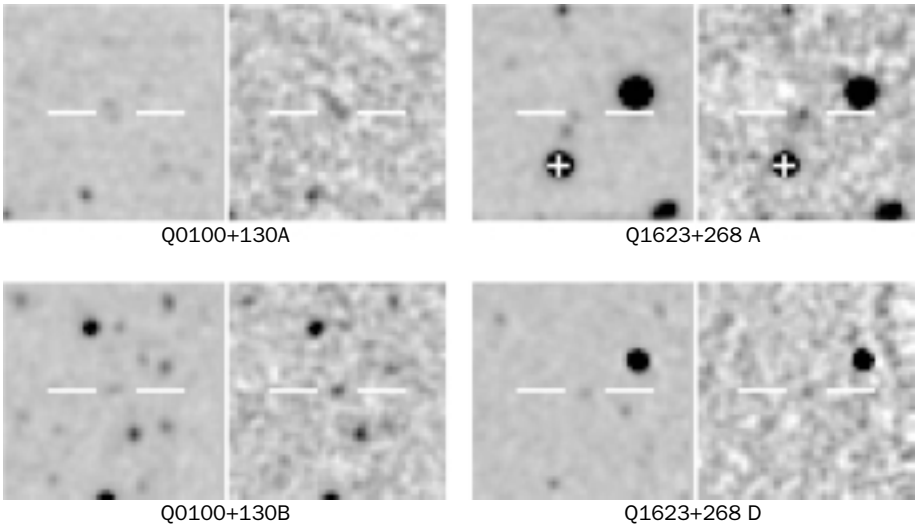

Figure IV.19: Photographs of the selected regions in the wide band and narrow band filters (left and right in each case).

was still considerably younger than it is today, and it had therefore not become so extensively enriched with heavy elements.

The idea, then, is this: the Lyman-α systems in the quasar spectra indicate the redshift at which young galaxies are located. Next, it was necessary to take photographs around the selected quasars, using narrow-band filters which are precisely matched to the suspected emission lines of young galaxies. In the case of the selected quasar spectra, the astronomers concentrate on the following redshift ranges z = 0.5 to 1.9, z = 2.1 to 2.5 and z = 3.1 to 3.8.

A total of 13 fields have been photographed with the 3.5 metre telescope on Calar Alto and the Magic and Omega Prime cameras, and five more have been photographed with the 2.2 metre ESO/MPIA telescope on La Silla. The total volume covered by the indicated redshift regions comprised 30 000 Giga-lightyears cubed. As potential candidates for young galaxies, those objects were selected which appeared definitely brighter on the narrow-band filter photographs than on the wide-band filter photographs. Candidates of this sought are immediately noticeable on a corresponding brightness diagram. (Figure IV.18).

In this way, the evaluation of five of the 19 celestial fields has so far revealed 18 candidates (Figure IV.19). If, as suspected, the emission involves Hα and/or [OII], then there would be six objects at z = 0.89, ten objects at z = 2.4 and two objects at z = 2.3. The small extent of the galaxies from one to two seconds of arc argues very much in favour of them really being as far away as this. However this could only be definitively ascertained by spectral images, for which observation time is needed on the large telescopes such as the Keck telescope or the VLT. By chance, two of the candidates from the

Figure IV.20: Two of the suspected remote galaxies, photographed with the Hubble Space Telescope (Photo: NASA/ESA).

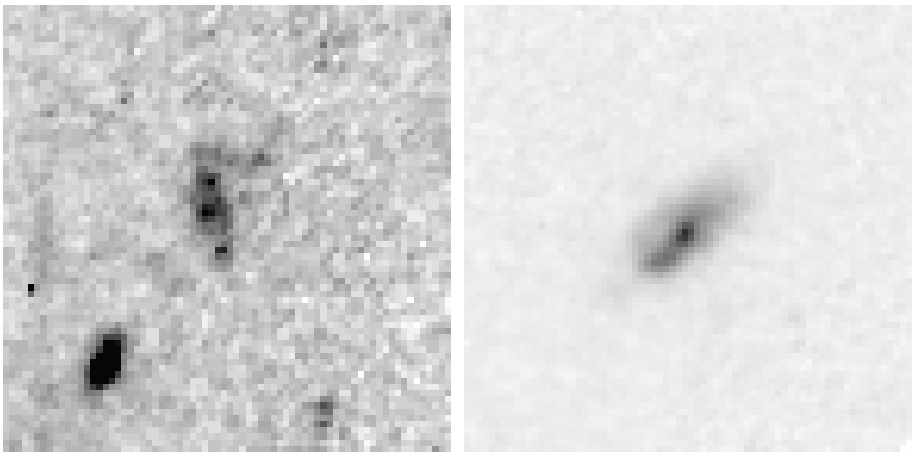

group with a suspected redshift 0.89 have already been observed in 1996 with the Hubble Space Telescope. The photographs with high spatial resolution (Figure IV.20) show irregular or spiral galaxies in both cases, with extents from 60 000 to 100 000 light years (Milky Way system: 100 000 ly). These are therefore galaxies which have evidently already developed to their full size. Likewise, the star formation rate of 5 to 10 solar masses per year is only slightly above that for the Milky Way. The fundamental evolution of the large galaxies had evidently already been completed in this phase, when the universe had reached two thirds of its present age.

Ultimate certainty about the nature of these celestial objects will not be obtained until we have spectra which can only be produced with the new large telescopes such as the VLT. If the present interpretation – that these really are remote galaxies – is correct, certain conclusions may already be drawn from the narrow-band filter photographs.

In this case, we are seeing the more remote systems in a phase when the universe was only about 15% of its present age. Based on the brightness in the filters, and assuming that the emission is Hα and/or [OII], the rough star formation rate can be deduced. While certain systems feature relatively low values of less than ten solar masses per year, the rate extends up to 200 solar masses. By way of comparison: in our Milky Way system, 1 to 3 solar masses of interstellar matter are transformed into stars every year. This means that at least some of the observed galaxies are in a phase of very violent star birth. Interestingly, it is the near galaxies which display the relatively low values, whereas the high star formation rates with values between 60 and 200 solar masses per year only occur in the remote galaxies. This indication of a high star formation rate in the young universe would have to be verified by spectroscopic studies.

Without spectral imaging, however, another interpretation for the emission line objects which have been observed cannot be ruled out. The radiation could originate from the central regions of active galaxies. In this case, the emission would not be an indication of star birth, but rather of an activity provoked by a central black hole. A mechanism of this sort is assumed for quasars and also for »Seyfert« galaxies. However, in this case, the density observed for these objects would be much higher than is known at present. The interpretation that these are primarily young galaxies with a very high star formation rate in some cases is therefore more probable.

EROs in the infrared sky

Another class of remote galaxies would also appear to consist of Extremely Red Objects (EROs). They were discovered at the end of the 1980s when it had become possible to use the first infrared arrays for astronomical research. EROs had attracted attention during observations of remote active galaxies and quasars. In the infrared range, at wavelengths of 2 µm, they featured unusually high intensity in comparison to the red (0.8 µm). However, in most cases it was impossible to establish the nature of these celestial objects unambiguously. All that was clear was that they were primarily remote galaxies, but how the infrared excess comes about and how strong this population is are questions which remain unclear.

To deal with the second question in particular, astronomers at the MPIA launched a search for more EROs. The decisive factors for success were: a large field of view, very high sensitivity so that even the weakest objects could be detected, and images throughnarrow-band filters so that EROs could be identified on the basis of their high infrared intensity. These conditions are met by images that are obtained as part of the Calar Alto Deep Imaging Survey, CADIS. CADIS is a programme set up for at least 5 years, with which astronomers from the MPIA search for the protogalaxies in the universe (see 1997 annual report P.18). For this purpose, they take images of several selected fields of the sky

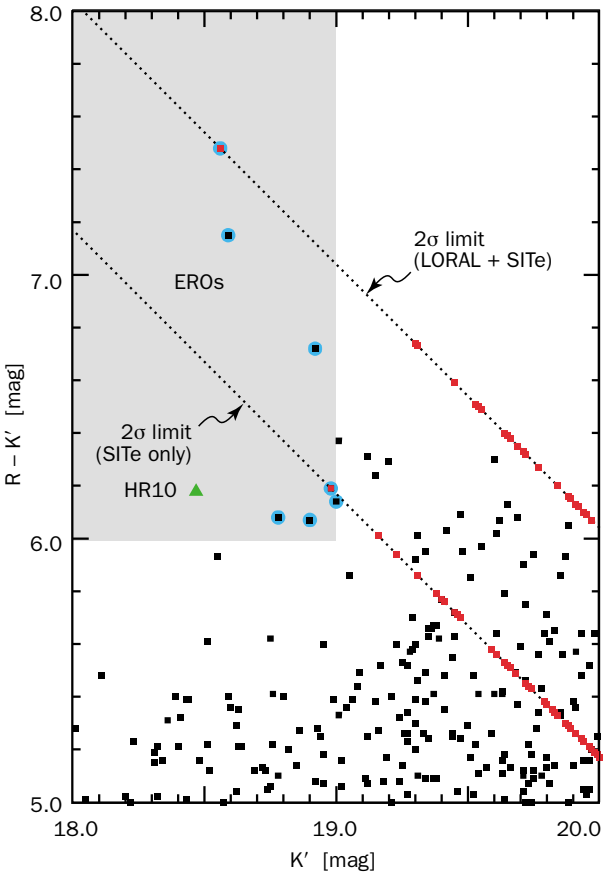

Figure IV.21: Colour diagram indicating the difference in the colours red minus infrared against the infrared brightness. The ERO candidates are located in the area of the top left.

with areas of 100 to 150 square minutes of arc each (corresponding to one quarter of the area of the full moon) through a series of colour filters. 10% of the total annual observation time on the 2.2 and 3.5 metre telescopes is made available for this ambitious project. However, the data which are already available are by no means solely restricted to use in the search for the youngest galaxies. Due to the large number of colour filter images they are also excellently suited to the search for objects with specific colour characteristics, including the EROs.

The astronomers obtained the images at wavelength 2.12 μm with the Omega Prime infrared camera at the prime focus of 3.5 metre telescope. To cover one of the CADIS fields entirely, four fields had to photographed and then mounted in the computer to create a mosaic with about 2500 × 2500 pixels on an area of 16 × 16 square minutes of arc. In the field comprising the central 160 square minutes of arc, the detection limit for pointlike sources was 20.5 mag. For extended objects it was about half a magnitude higher. By way of comparison, the same field was imaged in the red spectral range at a wavelength of 0.648 μm. For this purpose, the 2.2 metre telescope with the CAFOS camera and a CCD with 2049 × 2048 Pixels was available.

EROs should then become noticeable in a comparison of the two photographs because they are at least six magnitudes brighter on the infrared (2.12 μm) than on the red photograph. Moreover, they should be brighter than the 19th magnitude in the infrared. At this limit magnitude, the objects are still detectable with adequate significance (more than 2σ) on the one hand; and on the other, they are probably still just bright enough to enable subsequent spectral investigations on one of the largest telescopes such as the Keck telescope or the VLT.

In a colour diagram (Figure IV.21), eight objects met the criteria set for EROs. In subsequent observations, two of these proved to be very low mass, cool stars in our Milky Way. Five of the eight EROs were resolved on the photographs, so they did not appear to be stars. Their diameters (FWHM) are between 0.″9 and 2.″0. A sixth object is precisely at the resolution limit but this one does also appear to be extended.

One of the six remaining EROs shows an elongated structure with an extent of 1.″9 by 1.″1 (ERO 1 in Figure IV.22). A further ERO is located at a distance of only 2.″8 in the direction of the longitudinal axis. This could be a pair of interacting galaxies. From systems located closer to us, astronomers know that a major surge of star birth can commence in galaxies which fly past one another at close quarters or which penetrate each other. In this case, the term used is »starburst galaxies«. It is therefore obvious to suppose that the major infrared excess on ERO 1 is created by dust which reddens the light of newly formed stars. Moreover, objects ERO 1 and ERO 2 are only 39″ distant from one another and ERO 4 even has an ERO companion at a distance of 5″.

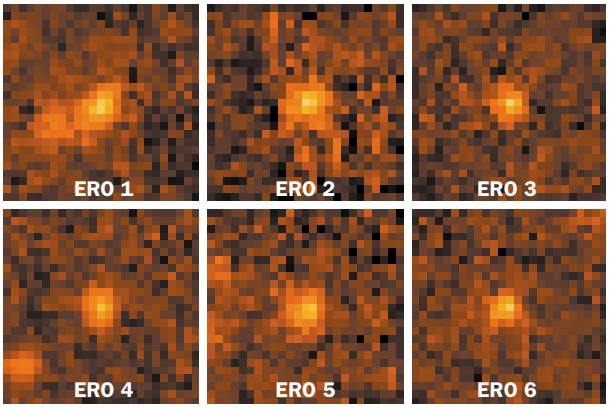

Figure IV.22: The photographs of some EROs show resolved objects, but no significant structures.

This could be an indication of a group or a cluster of galaxies.

Until spectral observations of these faint celestial objects are available, it is only possible to speculate about their distance. However, if these are indeed galaxies, as all the indicators would suggest, they should be located in a redshift range of between $z = 0.85$ and $z = 2$. This corresponds to stage of evolution when the universe had only reached between 20 and 40% of its present age. This statement not only applies to the possibility that these are elliptical galaxies with an old (red) star population but also to the possibility that they are starburst galaxies with heavy dust extinction. This estimate is obtained from typical values such as those which are known for near systems of this sort.

In the field of the sky which has been observed, the distance interval corresponds to a volume of $12.3\ 10^6$ ly^3. For the six EROs, this would yield a spatial density $2.4\ 10^{-4}$ per ly^3. This means that these objects are eight times more frequent than quasars in this distance range. In other words they represent a substantial population in this phase of the universe. If they are elliptical galaxies, they must be very massive according to their measured brightness. This would mean that such large star systems must have come into being in the cosmos relatively early. Perhaps they even mark the start of the formation of galaxy clusters. If the EROs are young star burst galaxies, their relatively high spatial density suggests that interactions between the galaxies must have occurred very frequently in the early phase of the universe.

In order to differentiate between both the possible interpretations – elliptical or starburst galaxies – further observations are necessary. On the one hand, spectroscopy with a large telescope would be very valuable. On the other hand, studies are already under way in the submillimetre range. These are used to estimate the dust masses in cases where the EROs are dust-rich starburst galaxies.

Cold dust in galaxies

Spiral galaxies are regularly formed systems in which stars, gas and dust are primarily arranged in the form of spiral arms. Our Milky Way is probably a member of this type, which is particularly fascinating. The stars contain by far the largest proportion of the visible mass in spiral galaxies. Their proportion is typically estimated at 90%. The interstellar gas accounts for just 10%, whereas the dust only contributes 0.1%. Nevertheless, the dust component is very important. This is because it contributes very effectively to the galaxy's energy irradiation: the dust particles absorb the short wave stellar light, which causes them to heat up and then to radiate in the long wave infrared range. In this way, the dust shields the interior of large clouds against energy-rich stellar radiation, and molecules can form under the protection of the absorbent dust. As has been known for a long time, new stars form in the interior of molecular clouds of this sort.

With existing infrared telescopes, however, it has only been possible to detect the relatively warm dust component with temperatures above about 20 Kelvin. Since the European Infrared Space Observatory (ISO) has been able to observe at wavelengths of some 200 μm for the first time, dust with temperatures as low as about 12 Kelvin has been made visible. For the first time, astronomers from the MPIA have been able to detect cold dust in the Andromeda galaxy (M 31) and in its companion galaxy, NGC 205, thanks to the ISOPHOT instrument on ISO.

Are spiral galaxies transparent?

Large dust clouds can be clearly discerned as dark areas on optical photographs of spiral galaxies. For this reason, several astronomers have already wondered whether the disks of spiral galaxies are possibly opaque. As long ago as the late 1950's, the astronomer Erik Holmberg conducted a study of more than 100 spiral galaxies with the result that these stellar systems are transparent. But in the 1990s, doubts arose in this regard, although it was impossible to resolve the issue.

Nevertheless, this problem is of great importance as regards to determining the mass and brightness of a spiral galaxy. If so much dust is present in the disks of the spiral galaxies that they are opaque, then – when viewed obliquely – the matter will conceal the stars located behind the disk, and the values derived for brightnesses and masses will turn out to be to low.

Beyond this, a major dust attenuation of the stellar light would have effects on the determination of distance. If, in fact, spiral galaxies are opaque, they appear proportionately fainter to us as their inclination in relation to the line of sight increases, and one would deduce too large a distance for them.

The question as to whether or not spiral galaxies are transparent is difficult to answer because observations in the visible range do not indicate whether any dust is present behind the visible stars. This will only become possible by measuring the far infrared emission, because the dust itself radiates here.

The Andromeda galaxy in the far infrared

At a distance of 2.3 million light years the Andromeda nebula is the nearest spiral galaxy to us. It is very similar to the Milky Way system in many of its characteristics, and is therefore also described as a sister galaxy. It is about 60% more massive than the Milky Way. Its galactic disk, with a diameter of about 160 000 light years, is tilted (Figure IV.23) at 13 degrees with respect to the viewing angle. Previous infrared observations with the IRAS satellite have shown that infrared intensity is increasing in the wavelength range from 60 μm to 100 μm. Accordingly, the maximum would have to be beyond 100 μm, that is to say in a range which would only be accessible with ISO.

In February 1997, astronomers at the MPIA and colleagues from the University of Helsinki prepared a complete map of the Andromeda galaxy at 175 μm (Figure IV.24). A deprojection of the disk by 78 degrees in the computer shows the distribution of the cold dust in plan view (Figure IV.25). About half of the total material is concentrated in a node-like ring with a width of 3200 light years and a radius 32 000 light years around the centre. However, the space within the ring is by no means totally dust-free. It is rather the case that a thin dust disk extends outwards from the centre and is limited by the ring. The ring therefore represents a local increase in the concentration of the dust. However, the greater brightness on the ISO photographs is not solely a consequence of the higher dust density, but is also due to the fact that warm star formation regions are located in the interior of the dust torus, and these excite their surroundings to shine.

In the south-western region (Figure IV.25, bottom right), the ring shows a cleavage. It is suspected that this is caused by a gravitational disturbance from the near companion galaxy M 32. Further outside, at a radius of 45 000 ly, a second fainter ring can be detected. Moreover several elongated dust regions appear within the bright ring, which may once have been part of a ring that used to be whole.

In contrast to the visible range, where the Andromeda galaxy shows its characteristic spiral structure, the dust is arranged in several concentric rings. These also occur on radio images which show the distribution of the molecular gas. Moreover, the only star formation regions worthy of mention are located in the bright ring.

This suggests the conclusion that in a few million's years time the Andromeda galaxy will have a closed

ring structure consisting of brightly shining young stars in addition to the spiral arms. Galaxies with rings of this sort are already known. In some cases they probably were created by another galaxy moving more or less perpendicularly through the disk of the spiral galaxy. As this happened, matter was compressed into a ring by the strong gravitational forces. This can be imagined as similar to a wave that is created when a stone is thrown into water.

In the case of the Andromeda galaxy, however, the visible companion galaxies are too low in mass to be able to provoke such an effect. Another supposition therefore tends towards the idea that the Andromeda galaxy previously had a central bar-shaped structure consisting of interstellar matter and stars. When this broke up, the matter within it was partly distributed in a central disk, and part of it was transported into the ring regions located further out, where it then gathered.

Based on the radiation fux measured with ISOPHOT at 175 μm and the fluxes known previously, which were supplied by IRAS, it is possible to build a model of the interstellar dust in the Andromeda galaxy. For this purpose it is sufficient to assume two components with temperatures of 45 K and 16 K (Figure IV.26). With certain assumptions about the characteristics of the dust particles (particularly their size and irradiation efficiency) the total mass of the cold dust can be calculated with the new data. This amounts to $3\ 10^7$ solar masses. This is not even 1% of the mass of the interstellar gas but it is ten times more than was expected on the bases of previous infrared measurements by the IRAS satellite. By way of comparison: the Milky Way system has

Figure IV.23: The Andromeda galaxy in visible light, taken with the Schmidt telescope on Calar Alto.

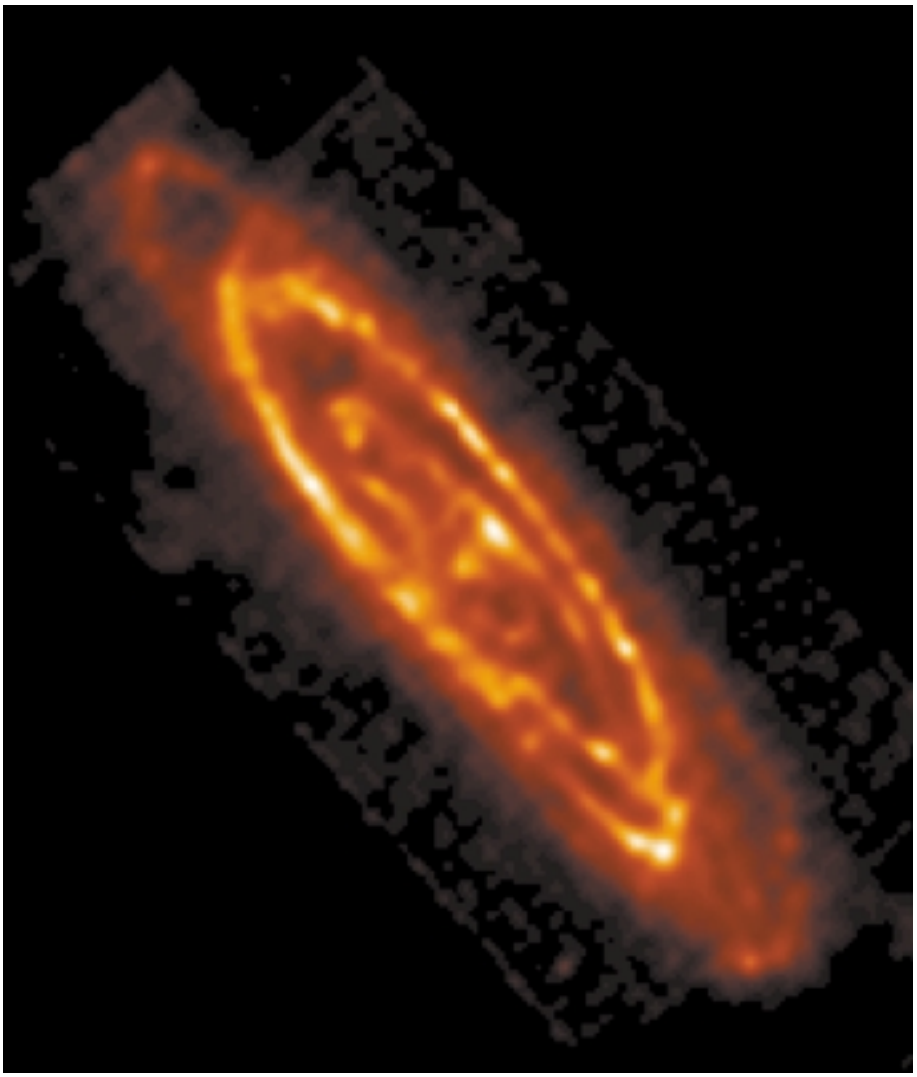

Figure IV.24: The Andromeda galaxy mapped with ISOPHOT in the far infrared at a wavelength of 174 μm.

about twice the mass of cold dust, although its total mass is about 60% less.

If the dust was distributed uniformly in a disk-shaped region within the bright ring, it would only absorb or scatter very little stellar light. In the ring, the dust attains a higher concentration, so that it attenuates the light of stars located behind it. However, this absorption, which is only locally strong, would not significantly attenuate the stellar light of the whole galaxy. The Andromeda galaxy is largely transparent.

We do not know whether the Andromeda galaxy can be regarded as representative of all spiral galaxies, but there is much to suggest this. If the other galaxy of this type also have similar quantities of dust, it maybe assumed that spiral galaxies in general are largely transparent.

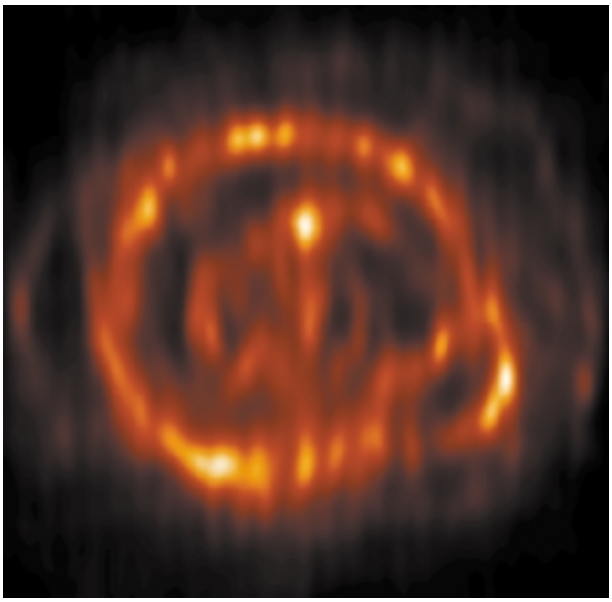

Figure IV.25: The deprojected far infrared image of the Andromeda galaxy clearly shows the ring-like arrangement of the cold dust.

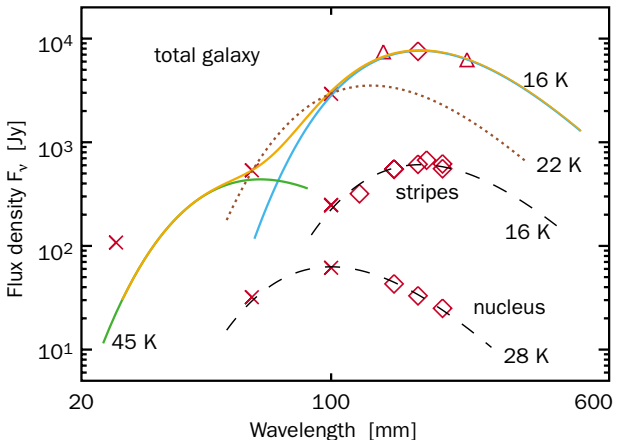

Figure IV.26: The intensity distribution of the Andromeda galaxy in the infrared can be explained by thermal radiation of dust at different temperatures.

The unusual dwarf galaxy NGC 205

The Andromeda galaxy is surrounded by a series of smaller star systems. The largest among these is the elliptical dwarf galaxy NGC 205 with a diameter of 4900 light years. One of the characteristics of elliptical galaxies is that they contain either no dust at all, or only very small quantities of dust, which is why no more stars can be created in them. NGC 205 was noticed due to the discovery of about a dozen of young and quite

Figure IV.27: Position of the two image elements of ISOPHOT on the galaxy NGC 205. The contour lines show the distribution of the atomic hydrogen and the shaded triangles identify regions in which radiotion of molecular CO can be detected.

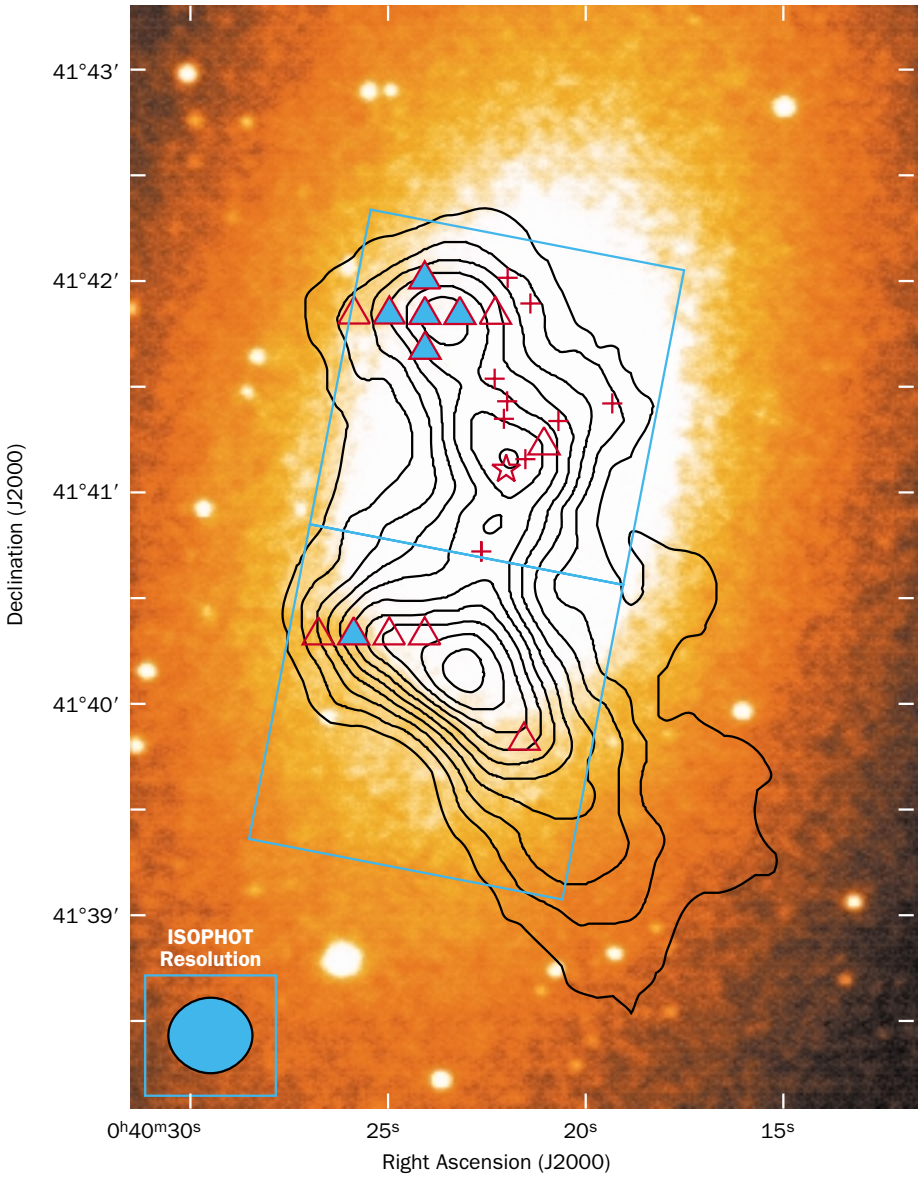

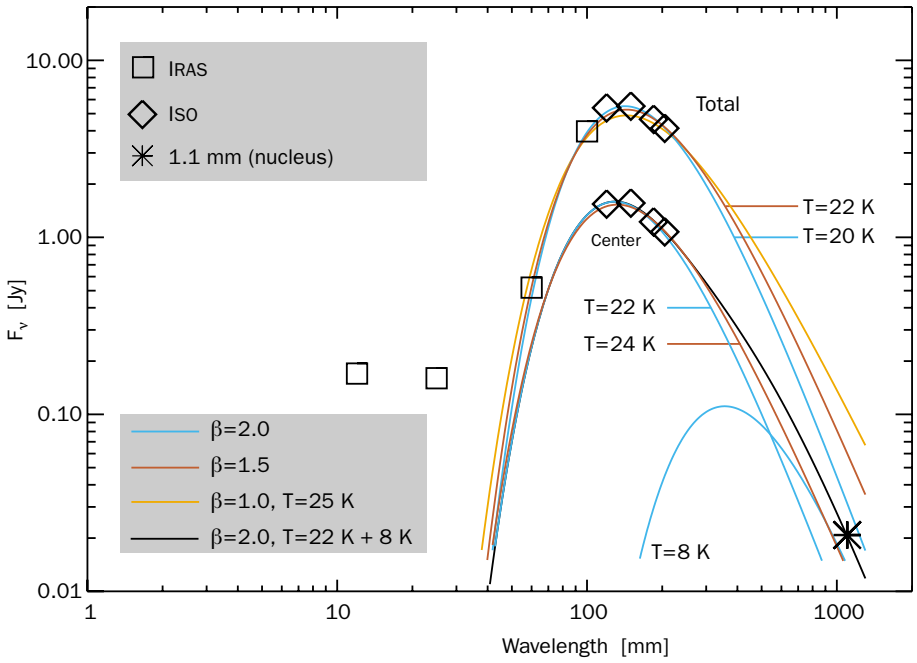

Figure IV.28: The spectral energy distribution of the galaxy NGC 205 in the infrared can be explained by thermal radiation of dust at about 22 K. It is possible to deduce a dust component with a temperature of only 8 K from submillimetre observations.

massive stars which may have formed there just a few million years ago. It was also possible to detect dust with IRAS, and later at a wavelength of 1.1 mm. This was the first time ever that an elliptical galaxy could be detected in the millimetre range. Hence, this unusual star system also suggested itself for observations with ISOPHOT in order to close the wavelength range between 100 μm and 1.1 mm which had been inaccessible until then.

The dwarf galaxy is so compact that it is impossible to make out any spatial details with ISO, as can be done in the substantially larger Andromeda galaxy. Even so, it was possible to separate the centre from the extended emission regions. Interestingly, the regions which are bright in the infrared coincide spatially with the regions featuring a higher concentration of atomic hydrogen gas (Figure IV.27). The ISO observations show that the maximum of the infrared radiation lies between 120 and 150 μm (Figure IV.28).

The measured values can be explained very well by two dust components at about 22 K (IRAS and ISO) and 8 K (millimetre observations). Dust as cold as this had never been observed before. The low temperatures below 10 K suggest extremely dense molecular clouds that are protected against stellar radiation which would heat them. This is a very unusual finding for elliptical galaxies. Normally, very little dust or none at all is to be found in these star systems. Why NGC 205 forms an exception is a question that has not been clarified. Some astronomers suppose that the galaxy has accreted dust from the nearby Andromeda galaxy or from its halo matter. This is a very unusual process, since it is normally the large galaxy which tears interstellar matter away from the smaller one in the case of a gravitational interaction.

IV.3 The Solar System

Asteroids as infrared standards

Standard light sources play a central role in astronomy. They are used as a reference for all types of measurements where the absolute value of physical variables is determined. For example, in order to determine absolute brightnesses or radiation powers, the star Vega is often used as a photometric standard in the visible range. Astronomical measurements have now become possible from the short-wave gamma range up to the long-wave radio range. For this range of electromagnetic radiation, extending over about 15 orders of magnitude, there is not just one sort of standard source. In fact, astronomers have to keep on defining new standards all the time.

Standard light sources for the infrared

The launch of the European Infrared Space Observatory, ISO, in November 1995 meant that the far infrared range up to a wavelength of 200 µm was opened up for the first time. This immediately led to a requirement for new standard objects. Astronomers at the MPIA, together with colleagues from the Astronomical Observatory in Uppsala, Sweden, and from the ISO Operations Centre in Villafranca, Spain, succeeded in establishing a set of asteroids as standards. For the first time, this provides a calibrating procedure (which has now been internationally recognised) for an extended wavelength range from the mid infrared to the submillimetre range. In order to achieve this, it was necessary to devise a thermal model for the asteroids. This also made it possible to derive further information from the ISO data concerning the nature of the surfaces of these small objects in our solar system.

Thomas Müller, who undertook fundamental work on this subject at the MPIA as part of his doctoral thesis, received a surprising honour for this: the International Astronomical Union gave asteroid number 8793 the name of Thomasmüller. It had already been discovered in 1979 by one of our Swedish colleagues, from whose group the suggestion for the name came.

There are only a few standards for the middle and far infrared range. Some bright stars, such as Alpha Bootis (Arcturus), Beta Pegasi or Gamma Draconis (Ettanin) are suitable for weak radiation flows above 50 µm, and the large planets Uranus and Neptune radiate very intensively above this wavelength (Figure IV.29). Asteroids suggest themselves as a third type of standard light source because they give off relatively intense thermal infrared radiation which can reach several hundred Jansky, starting from wavelengths of just a few micrometres. As compared with stars, asteroids have another advantage which distinguishes them as infrared standards. In general, stars are several magnitudes brighter in the visible range than in the infrared. This can lead to a technical measuring problem during infrared observations if the filters used in the visible range have small »leaks«, that is to say, if they are slightly permeable to visible light. In the case of asteroids, a leak of this sort does not have any serious effects because these small objects only give off a little visible light (reflected sunlight).

Nevertheless, these little objects in the solar system are not altogether ideal as standard light sources because their brightness varies on different time scales. They are not generally spherical – in fact, they are very irregular in form. Images from the Galileo space probe of Gaspra and Ida, and from NEAR showing Mathilde (Figure IV.30), have given direct evidence of this. Since the asteroids rotate, the cross-sectional area facing the observer also changes. This in turn means that the brightness changes with the rotation period, which is typically a few hours. Moreover, the distance of the earth from the asteroids fluctuates, leading to major brightness variations over the course of the year. If their orbits are heavily elliptical as well, the objects are heated to different degrees due to their varying distance from the sun. This fluctuation in the temperature of the asteroid shifts the emission maximum, thereby changing the form of the infrared spectrum in the course of one orbit by the asteroid.

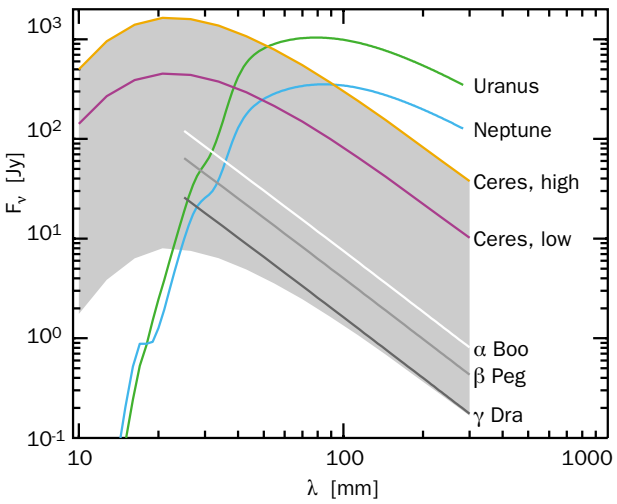

Figure IV.29: Brightness ranges for standard stars in relation to wavelength. The grey area indicates the area covered by asteroids.

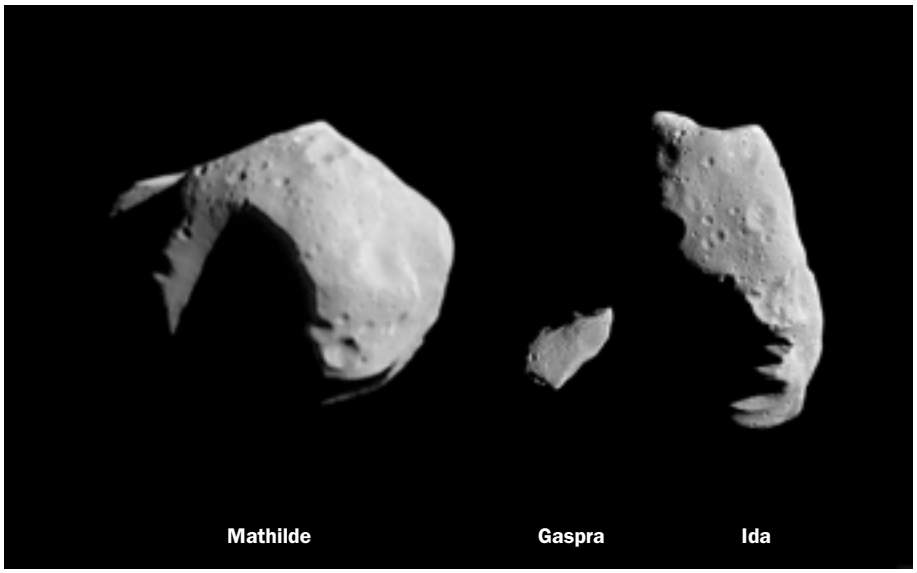

Figure IV.30: The individual asteroids of which detailed pictures are so far available: Mathilde, Gaspra and Ida (from left to right).

The thermal asteroid model and ISOPHOT data

It was therefore clear from the outset that asteroids can only be used as standards if there is a thermal model of these objects. Then, in fact, it becomes possible to calculate the infrared spectrum for every distance from the sun and the earth. The basis for this consisted of the observations with ISOPHOT, the photopolarimiter on board the ISO infrared observatory. Ten asteroids were selected according to the following criteria (Table IV.1):

- they are favourably placed in the sky for observations with ISO;
- the rotation behaviour (rotation period and form of the asteroids) allows observations without particularly large fluctuations in brightness; and
- the spectra do not feature any heavy lines in emission or absorption which might be attributable to divergences from the purely thermal spectrum.

Thermal models of asteroids have been in existence for a long time. However, the so-called Standard Thermal Model (and its modifications) assumes a spherical object which does not show any thermal inertia. Until now, this model has been suitable for numerous applications, but it proved inadequate for the problem to be solved, namely how to use asteroids as standard light sources. The new model takes account of the form of the asteroid, reproduced by a three-axis ellipsoid with axes a, b and c (Table IV.4) and its current axis of rotation in space. The model also includes important variables such as the heat conductivity and surface roughness of the asteroid. In qualitative terms too, the new model goes well beyond the existing one, since it casts more light on the physical processes which are the cause of thermal infrared radiation.

Table IV.1: The ten asteroids selected as infrared standards, and some of their properties. Uncertain values are in brackets.

Asteroid	largest diameter (km)	Period of Rotation (hours)	Axial ratios a/b	b/c
1 Ceres	959	9.07	1.00	1.06
2 Pallas	574	7.81	1.10	1.25
4 Vesta	578	5.34	1.03	1.22
532 Herculina	(263)	9.41	1.21	1.20
3 Juno	(290)	7.21	1.21	1.20
10 Hygeia	?	27.62	1.29	1.18
54 Alexandra	?	7.03	1.31	1.00
65 Cybele	(260)	6.18	1.04	1.00
106 Dione	(170)	13.92	1.00	1.34
313 Chaldaea	?	8.40	1.21	1.20

Tabelle IV.2: Parameters of the asteroids Hebe and Methis.

Asteroid	largest diameter (km)	Period of rotation (hour)	Axial ratios a/b	b/c
6 Hebe	187	7.28	1.14	1.1
9 Metis	190	5.08	1.30	1.24

The surface temperature of an asteroid is essentially calculated from the energy balance between absorbed solar radiation, emitted thermal radiation and thermal conduction into the interior of the object. The decisive factors for the radiation power of the object that is received on earth are its absolute size and its orientation and distance relative to the sun and the earth. Some of these sizes were known from earthbound observations. Thus it was possible to determine the diameters of Ceres, Pallas, Juno and Vesta, for example, with relative precision thanks to stellar occultation observations (where the occultation of a star by an asteroid is measured by several observers on the earth, and the size and shape of the asteroid is determined from these data). In addition, Vesta was photographed with the Hubble Space Telescope (Figure IV.31). The periods of rotation, the values for the ratios of the axes and the albedo (reflective capacity) can be determined from brightness observations (light curve). Other parameters such as thermal inertia, the »beaming« parameter and the wavelength-dependent emissivity were varied within plausible limits so that they optimally reproduced the infrared observations.

The beaming parameter, known for short as the beaming, identifies a characteristic of surfaces which is ascribed to roughness: accordingly, a sphere which is heated by the sun does not give off thermal emission uniformly in all directions, but instead radiates a larger proportion back in the direction of the sun (similarly to the opposition effect in the visible range). This effect is wavelength-dependent, and it is most strongly evident in the middle infrared. For example, at 10 μm, the excess radiation flow towards the sun is 20 to 40%, while it is less than 10% in the far infrared (Figure IV.32).

In practice, the astronomers proceeded in such a way as to introduce the most important parameters first (such as size and albedo). The »beaming« and the heat conduction were modelled after this. Finally, the emissivity was adjusted to the spectra.

To a very major extent, the new model is based on data which were obtained with the ISOPHOT instrument. For the ten asteroids in this case, the team of astronomers was able to have recourse to a total of 35 separate observations at wavelengths of between 50 and 200 μm. To cover an even larger wavelength range, they took further measurement data into consideration from four earthbound telescopes: the James Clerk Maxwell Telescope (JCMT, Hawaii), the United Kingdom Infrared Facility (UKIRT, Hawaii), the Infrared Telescope Facility (IRTF, Hawaii) and the Heinrich Hertz

Figure IV.31: Photographs of asteroid Vesta taken with the Hubble Space Telescope. (Photo: NASA/ESA)

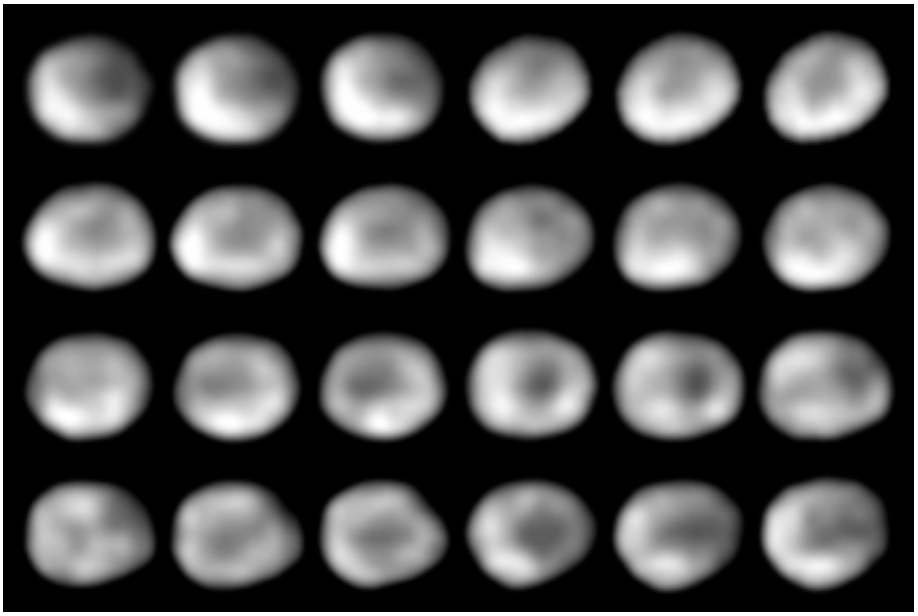

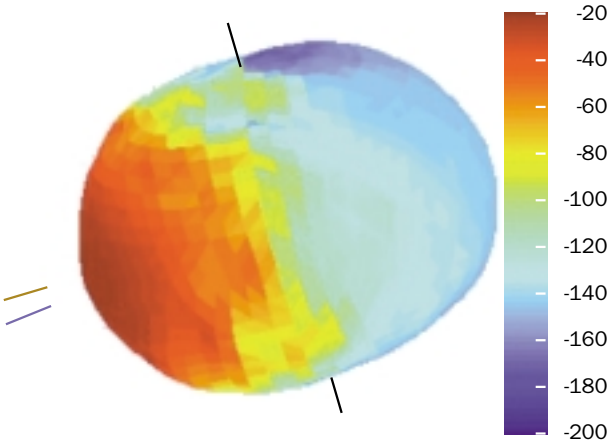

Figure IV.32: Thermal model of asteroid Vesta.

Telescope (HHT, Arizona), as well as IRAS, the predecessor of ISO. In this instance, great importance was attached to 167 infrared observations which they had obtained with the MAX infrared camera (built by the MPIA) on the UKIRT (see Chapter I).

With the help of this extensive set of data, the astronomers constructed a thermal model for each of the ten asteroids. The quality of these models was, of course, dependent on the precision of the initial parameters. For Ceres, Vesta, Pallas and Herculina, the best-measured asteroids, the team determined a precision of better than 10% for the prediction of the radiation fuxes in the wavelength range between 7 and 2000 μm. For the other asteroids, the precision should still be better than 15%. The precision with which the model reproduces the measured radiation fluxes on Herculina can be seen in Figure IV.33. This also clarifies how the thermal inertia is adapted to the model.

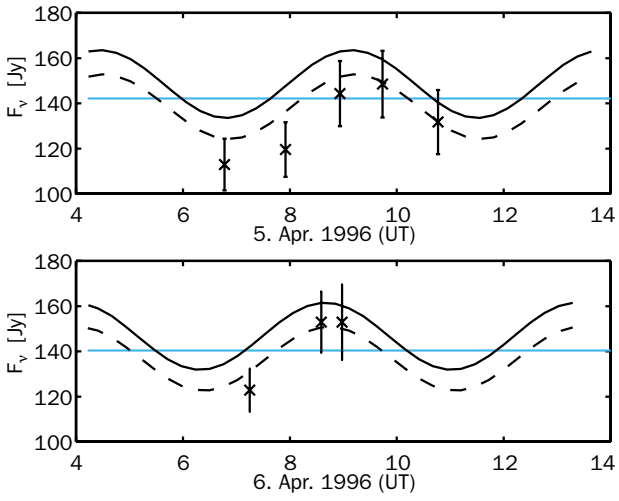

Figure IV.33: Model (lines) and observed light curve (crosses) of asteroid Herculina. The continuous curve is without assumed thermal inertia; the dotted curve is with assumed thermal inertia.

In this way, new standard light sources for the whole infrared range and the near millimetre range will be made available to astronomers all over the world in the future. This is because the new model now makes it possible to calculate the absolute radiation fluxes of these asteroids at every point in time and at every point in their orbits.

Except for Vesta, the asteroids that have been calibrated in this way belong to the C and S asteroid classes. C (carbonaceous) means rich in carbon, and S (silicaceous) means rich in silicon. Since a total of 90% of all known asteroids belong to these types, it may be supposed that the new thermal model can be transferred to most other asteroids as well, so that the number of standard light sources should increase even further in the future. Moreover, the incorporation of other ISOPHOT data which have not yet been analysed, as well as observations with infrared space telescopes which are still under construction at present, should enable the models to become even more accurate. Ultimately, the astronomers also intend to incorporate representatives of the metal-rich M asteroids in order to expand the collection of standard asteroids.

Polarisation measurements on asteroids

So far, it has only been possible to observe the surface of three asteroids directly. In 1991 and 1993, the Galileo Jupiter probe flew past the asteroids Gaspra and Ida, imaging their surfaces from a short distance. In 1997, the NEAR probe transmitted images of asteroid Mathilde to the earth. These three objects show crater-strewn surfaces which appear to be covered with a layer of dust. From the earth, no details can be discerned on these small celestial objects.

The most recently compiled thermal model not only enables us to calculate the absolute radiation flows of asteroids; it also opens up the possibility of obtaining more information about the nature of their surfaces. For this purpose, an attempt was made to measure a possible polarisation of the thermal infrared radiation on two asteroids.

It has already been known for some time that the heat radiation of solid celestial objects can be polarised; for example, polarized microwave emission from certain regions of the moon was detected in the 1960s, and from Mercury in the 1990s. In the 1980s, a polarization of 0.5 per cent was even measured in the infrared range on the largest known asteroid, Ceres. This effect is attributed to the fact that radiation from the interior of the object has to penetrate a layer of dust and rubble – the so-called regolith – close to the surface, before it escapes into space. The radiation is dispersed in this layer, during which a slight polarization occurs. In this case, the electrical vector is rotated into a plane which lies perpendicular to the surface and in the direction of propagation of the electromagnetic wave. Moreover, an

index of refraction can be assigned to the transition from the regolith into the vacuum.

If the asteroid is spherical and its surface cannot be resolved in the telescope, no overall polarization ensues because the polarized components located in various planes cancel one another out. It is only when an asteroid has an elongated form that net polarization should remain. The more elongated the object is, and the fewer and flatter are the craters which cover its surface, the higher the degree of polarization. It was hoped to measure an effect of this sort on asteroids Hebe and Metis with the ISOPHOT photopolarimeter on ISO. A favourable opportunity for this purpose arose in March and April 1998. This was the first ever attempt with asteroids in the far infrared. Both the asteroids are members of the so-called S class, whose main components are olivine, pyroxene and metals. They could therefore be the parent objects of the iron, rock and ordinary chondritic meteorites which are found on the earth.

After careful data evaluation, it was impossible to detect any significant polarization on either of the two asteroids. However, the upper limit value of 0.5 per cent made it possible to draw some conclusions about the surface roughness ϱ and the index of refraction n. The surface roughness ϱ is a measure of how extensively a surface element is strewn with craters and how deep the craters are. For example, the ratio of depth to diameter of the craters is incorporated into the calculation. From the observations, it was possible to derive a value for ϱ of between 0.4 and 0.7. By comparison, for the moon, a value of 0.4 is assumed, and for the asteroid Ceres, the latest ISO data yielded $\varrho = 0.7$. The index of refraction cannot be very high on account of the composition and porosity of the expected surface material. The typical value range (of the real component) of the index of refraction is $n = 1.2$ to 4.0 (Figure IV.34).

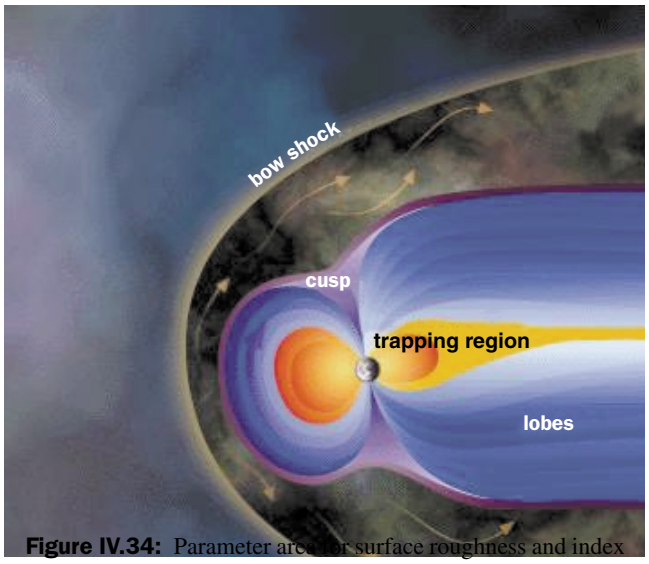

Figure IV.34: Parameter area for surface roughness and index of refraction. The grey area can be excluded for asteroid Metis, based on the model and the observations.

Variations in the solar wind

The solar wind, a cloud of particles which is constantly flowing away from the sun, fills the space between the planets with a finely dispersed plasma. This flowing plasma carries a magnetic field with it. The region filled by the solar wind is known as the heliosphere. The solar wind, with the magnetic field which it carries along, has various effects on our planet: it deforms the earth's magnetic field (Figure IV.35), heats up the outer layers of the atmosphere, leads to the familiar polar lights, and can even paralyse power supplies on the earth if severe »storms« occur. For more than twenty years, this flow of particles has been examined, mainly with space probes. In recent times, these have included the European space probe Ulysses, launched in 1990, and the Solar and Heliospheric Observatory, SOHO, built jointly by ESA and NASA, which was launched in 1995. New measurements from Ulysses have now caused astronomers at the MPIA and the Center for Astropysics and Space Sciences of the University of San Diego in California to evaluate old data from the Helios solar probe. This set of data is unique in that it comprises the entire solar activity cycle from 1975 to 1986. The new evaluation showed that the solar wind had risen more than expected at the activity maximum.

Coronal holes and mass eruptions

The sun irradiates the majority of the energy produced in its interior into space, in the form of visible radiation. However, our daytime star is by no means just a source of electromagnetic radiation. Hot particles evaporate from the outermost layer of its atmosphere, the corona (the temperature of which is between one and two million degrees), and they fly out into space in the solar wind, at speeds of several hundred kilometres per second. Every second, the sun loses more than a million tons of matter (almost exclusively consisting of atomic nuclei of hydrogen (protons) and helium) in this way. Measured by its total mass, this is a minute proportion – the loss of mass is only $2.2\ 10^{-14}$ solar masses per year, or to put it another way, at a constant rate, our central star has lost only one ten thousandth of its total mass since it was created 4.6 billion years ago. This loss of mass probably only exerts a minor influence on the evolution of the sun. More massive stars, however, develop a substantially more powerful particle wind with quite major mass loss rates (cf. Chapter IV.1 »Eta Carinae«).

Investigation of this phenomenon is highly important for various reasons. For example, the solar wind acts on the planets and also on the earth. The particle flow and the magnetic field carried along with it encounter the earth's magnetic field and press it in on the »windward«

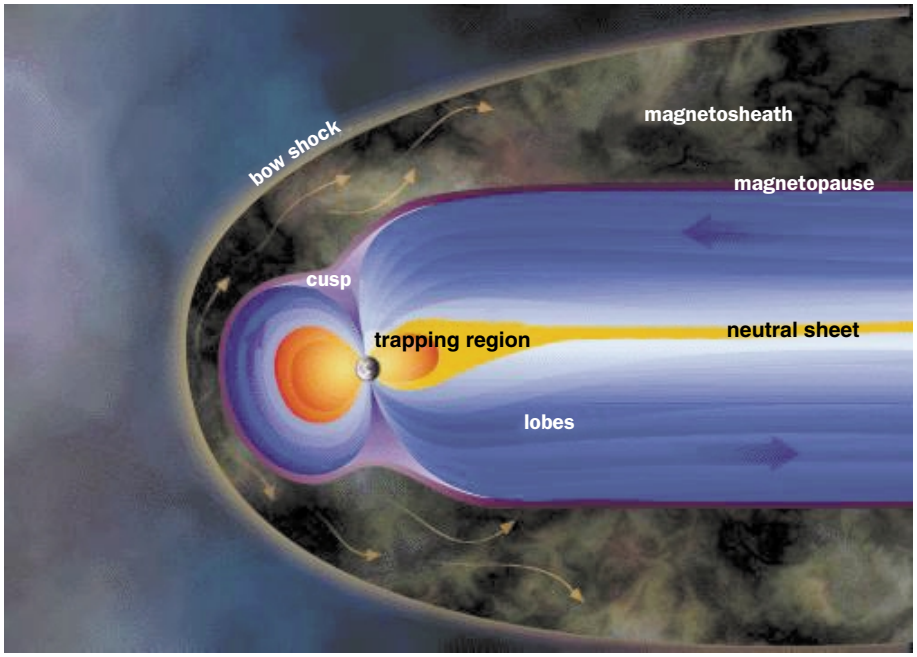

Figure IV.35: Illustration of the magnetosphere which is compressed by the solar wind on the left and is drawn out lengthwise into a trail on the right.

side, while they pull it lengthwise on the »leeward« side (the side facing away from the wind) like a flag. Heavy »gusts« in the solar wind can shake the earth's magnetic field up to quite a considerable extent. In these cases, a complicated system of electrical flows is induced in the magnetosphere, and in turn, these can induce heavy currents in electrical lines on earth. In extreme cases, this can even cause a collapse of the power supply, as happened in Canada in March 1989. Other influences on our technological world also occur: for example, the induced currents can evidently increase the corrosion of pipelines. The question as to whether long-term variations in the solar wind (possibly dependent on solar activity) influence the earth's climate still remains largely unclear. Research into solar-terrestrial relations is still in its infancy. Most recently, it has been advanced considerably by the launches of several satellites which are tracking the solar wind in various ways, and are searching for possible correlations with processes and events on the sun.

From the astronomical viewpoint, this makes it all the more unsatisfactory that the cause of the particle acceleration in the corona is still not fully understood. Even so, it is now certain that there is more than one mechanism. In actual fact, at least two mechanisms go into action, and their intensity fluctuates with the phase of the activity cycle.

Over the course of the last 20 years, the solar physicists have discovered that some characteristics of the solar wind change with the sun's activity phase, and that the cause of this is to be sought in various acceleration mechanisms. During the activity minimum, about 60 per cent of all particles originate from so-called coronal holes. These are dark areas in the upper corona which are easily recognizable in UV and X-ray light. In these areas, the atmospheric density is less than in the surroundings, and magnetic field lines project openly from them into the far reaches of interplanetary space, whereas they are usually closed. The particles of the solar wind are accelerated outwards along these open field lines.

However, coronal holes of this sort only occur rarely during the activity maximum, so that the proportion of the particle flow coming from them falls sharply. In this phase, strong magnetic fields build up, extending from the surface up to about 35 degrees of solar latitude and contributing towards the particle acceleration. In addition, coronal mass eruptions take place frequently – giant gas clouds of several 10^{13} kilograms which build up locally and shoot explosively into space at high speeds (Figure IV.36). Investigations to date have shown that these mass eruptions contribute about 16% to the total solar wind in periods of maximum activity.

Old HELIOS data newly analysed

However, this estimate – made only a few years ago – is based on one single piece of work. Verification using other methods was therefore extremely desirable. This possibility was afforded by older data.

Since the start of the 1980s, various measurements suggest that throughout the activity cycles there is a connection between the proton density n and the par-

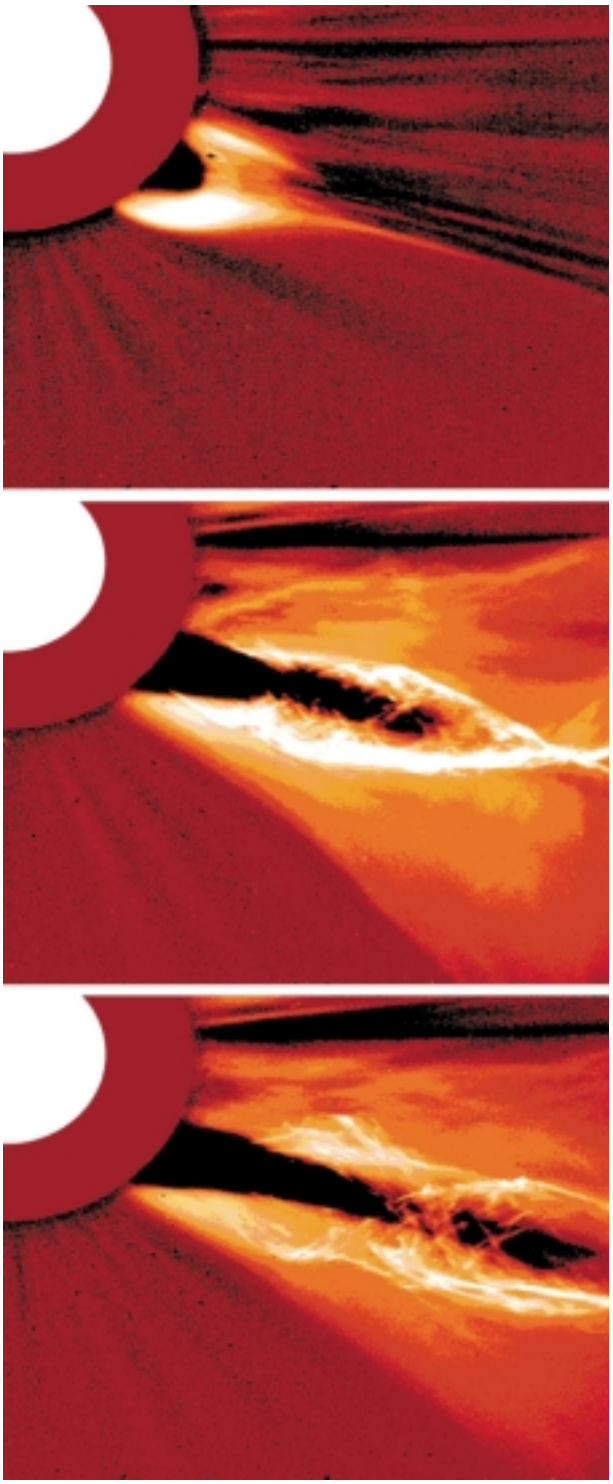

Figure IV.36: A coronal mass eruption on the sun, observed with the LASCO instrument on the SOHO space observatory. (Photo: MPAe, ESA/NASA)

ticle speed v of such a sort that the monumentum flux density remains constant ($n \times v^2$ = constant). Most recently, results from the Ulysses solar probe indicate that this physical variable also remains virtually unchanged, regardless of the solar latitude.

Observations from the 1980s showed that the wind velocity over the solar poles fell substantially during the maximum. From this, it should follow – if the law of preservation of monumentum flux density applies – that the flow of matter must have increased substantially during this period. In order to test this hypothesis, older data were subjected to a new analysis. On the one hand, the set of data from the Helios probes was available for this purpose. The two German-American probes Helios 1 and 2 were launched into orbits in 1974 and 1976 and approached to within 43 million kilometres of the sun. Up to 1981 and 1986 respectively, the instruments had recorded the density and speed of the particles in the ecliptic.

At the same time, radio telescopes on earth were used to measure fluctuations in the solar wind speed, in relation to the heliographic latitude. These observations are based on the so-called interplanetary scintillation effect. For this purpose, pointlike radio sources were observed with several telescopes. In these cases, the radio signal shows flickering which can be attributed to the fact that the radio waves are deflected by the plasma of the solar wind as they pass through interplanetary space. (The stars flicker in the sky at night for a similar reason.) In this way, inhomogeneities of density in the solar wind can be registered with extents of a few hundred kilometres. These data showed unambiguously that the solar wind speed from polar regions fell from about 600 km/s to 400 km/s from the activity minimum to the maximum (Figure IV.37).

By combining these two sets of data, the researchers compiled a global density model of the solar wind which varies with the activity cycle. The constancy of the monumentum flux density was assumed here. In addition, they used data from the Zodiacal light photometer on board the Helios probes – this instrument had been built by the MPIA at the time. The photometer on Helios 1 registered the brightness of the Zodiacal light in three areas: 16°, 31°and 90° south of the ecliptic, while the instrument of identical design on Helios 2 recorded the area north of the ecliptic (Figure IV.38). The two photometers covered more or less the same area as the scintillation observations.

Apart from an annual fluctuation in brightness, the Helios data also indicated short-term variations within one day. The causes of these variations lay in plasma clouds which were flowing more or less radially away from the sun. The Helios measurements can therefore also be used to register fast phenomena such as the coronal mass eruptions.

This set of data was now introduced into a model of the solar wind which was based on two main assumptions: the density drop of the solar wind plasma occurs in inverse quadratic proportion to the solar distance, and the monumentum flux density is constant.

In a first step, only the data from Helios 1 were included, and they were averaged over half a year. In

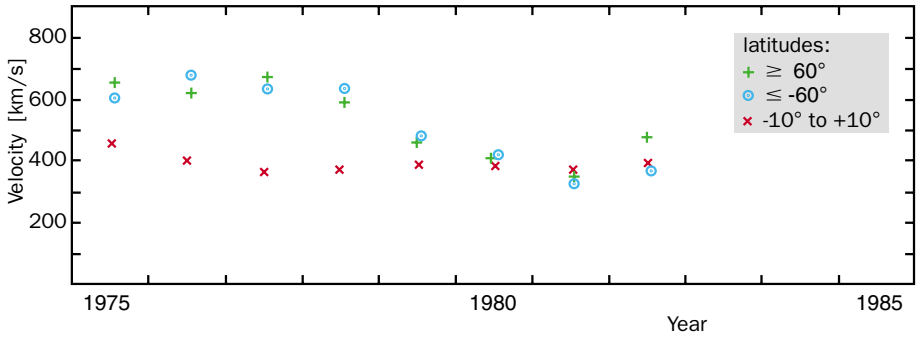

Figure IV.37: Speed variations in the solar wind between 1975 and 1982.

this instance it emerged that during the activity maximum, the brightness of the Zodiacal light above the solar poles was up to 18% above the value expected by the model (Figure IV.39). The authors suspect that these increased brightness values were caused by brief »gusts« in the solar wind. However, they are not recorded individually when the data are averaged. If the Helios 2 data are taken as well, although they only cover the period from 1976 to 1979, then an even greater discrepancy of up to 70 % emerges between the model and the measurement data. Several years ago, a more accurate data analysis had already shown that eleven coronal mass eruptions had occurred just in the period between april 17 and may 27, 1979 – considerably more than usual. This confirmed the extremely large proportion of solar wind particles which reach the planetary system due to these explosive processes.

Finally, the model made it possible to calculate the mass, monumentum and energy flow. It became apparent that the mass flow from activity minimum to maximum rose from 1.2 10^{12} g/s to 1.7 10^{12} g/s. In the phase of the Helios 1 data, the coronal mass eruptions contributed 18% at the maximum, and in the short phase of

Figure IV.38: Schematic representation of the Helios probe on its orbit round the sun and observation directions of the solar wind with Helios and with earthbound radio telescopes.

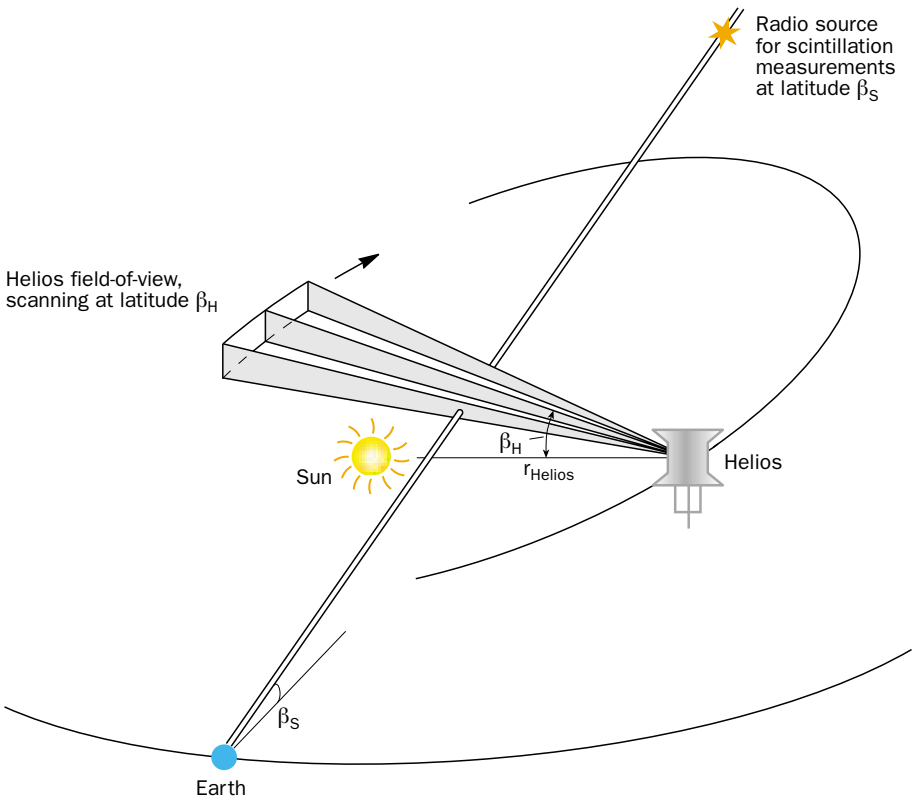

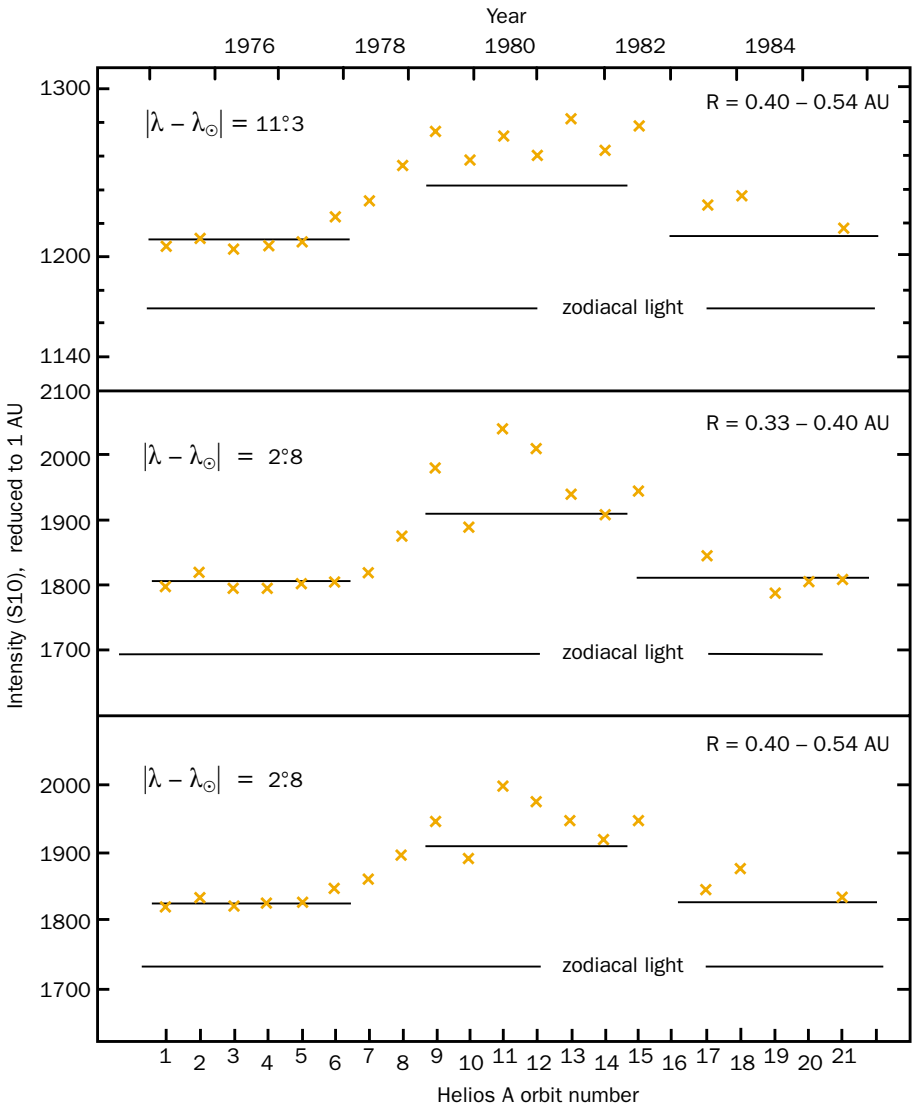

the Helios 2 data the figure was actually about 50%. The kinetic energy of the wind, on the other hand, remains almost constant, with 2 10^{20} W at the minimum and 1.8 10^{20} W at the maximum.

This result therefore underscores the importance of the coronal mass eruptions for the solar wind in times of heavy activity, and the numbers confirm the only investigation of this aspect of the solar wind which has so far been undertaken. Future research will show whether the solar wind reaches interplanetary space solely through coronal holes and coronal mass eruptions, or whether other mechanisms are also at work.

Figure IV.39: Comparison of observed brightness increases (crosses) during the solar maximum with predictions (continuous lines). The predictions are based on the assumption of a constant monumentum flux density for the solar wind. The two lower diagrams show the conditions for observation over the solar south pole, and the upper diagram refers to a direction of observation to the east and west of this.

Staff

In Heidelberg

Directors: Appenzeller (temporary, Acting Director as from 1.8.), Beckwith (Acting Director until 31.8.)

Scientists: Ábrahám, Bailer-Jones (as from 27.7.), Barrado-Navascues (bis 31.12.), Beetz, Birkle (as from 1.7.), Burkert, Fried, Graser, Haas, Herbst, Herbstmeier (until 30.6.), Hippelein, Huang, Huth (until 10.7.), Kalas (until 14.11.), Klaas, Kunkel (until 30.9.), Leinert, Lemke, Lenzen, Ligori (as from 15.5.), Mac Low, Marien, Meisenheimer, Th. Müller (until 30.9.), Mundt, Neckel, Pitz (until 31.3.), Radovich (as from 15.9.), Röser, Schmidtobreick (as from 1.8.), Slyz (as from 12.10.), Staude, Stickel, Thompson (until 13.11.), Tusche, R. Wolf.

Ph. D. Students: Baumann, Berkefeld (until 30.11.), Eckardt, Fockenbrock (until 30.4.), Heitsch (as from 1.7.), Hetznecker (as from 15.3.), Hotzel (as from 15.1.), Jester (as from 15.9.), Kasper (as from 15.8.), Kessel, Klessen (until 30.6.), Kranz (as from 1.12.), Naab (as from 1.6.), Petr (until 30.6.), Phleps (as from 1.10.), Schuller (as from 15.2.), Seidel, v. Kuhlmann, Woitas, Wolf, Chr.

Diploma Students: Kranz (until 30.1.), Krause (as from 1.11.), Naab (until 31.5.), Phleps (until 1.9.). Von der FH Mannheim: Hipp (until 31.3.), Lehmitz (until 31.3.), Marx (until 30.6.), Sebb (1.3.–31.8.), Steckel (as from 1.9.), Thomas (as from 1.9.), Wackermann (as from 1.10.).

Scientific Services: Bizenberger, Hille (until 31.3.), Hiller, Khan (as from 1.5.), Ortlieb, Quetz, Rohloff.

Computers, Data Processing: Brüge (until 31.7.), Briegel (as from 1.11.), Engelhardt (until 17.11.), Hippler, Rauh, Storz, Tremmel, Zimmermann.

Elektronics: Becker, Ehret, Grimm, Grözinger, Klein, Ridinger, Salm, Unser, Wagner, Werner, Westermann, Wrhel.

Fine Mechanics: Bellemann (until 31.5.), Benesch, Böhm, Ebert (until 12.9.), Franke, Heitz, Meister, Meixner, Morr, Münch, J. Pihale, Sauer.

Photo Shop: Anders-Özcan, Neumann (bis 31.7.).

Graphic Artwork: Meißner-Dorn, Weckauf.

Administration, Secretariate: Behme, de Mooij (as from 1.11.), Fink, Flock, Gieser, Hartmann, Heißler, Heukäufer (as from 6.12.), Janssen-Bennynck, Kellermann, Papousado, Rushworth, Schleich, Schürmann (until 30.11.), Zähringer.

Technical Services: Gatz, O. Götz, Klingmann, Lang, Nauss (ab 1.10.), B. Witzel, F. Witzel, Zergiebel.

Trainees: (Fine mechanics) Fabianatz, Greiner, Geuer, Haffner (as from 1.9.), Jung, Wesp (as from 1.9.).

Free Collaborator: Dr. Bührke.

Scholarship Holders: Andersen (until 30.4.), Bate (until 30.9.), Berkefeld (as from 1.12.), Mori (as from 24.8.), Fockenbrock (as from 1.5.), Heraudeau, Kania (until 30.11.), Klessen (1.7.–31.8.), Maciejewski (as from 9.11.), Nelson (as from 15.9.), Patsis (until 31.5.), Petr (1.7.–31.8.), Porro, Robberto, Surace (until 14.11.), Thiering (as from 1.5.), Toth.

Guests: Dr. Allard, Kansas (Aug.); Dr. Bodenheimer, Santa Cruz (Nov.); Dr. Cao, Peking (Jan.); Dr. Hozumi, Shiga (Juni); Dr. Ida, Tokyo (Aug.–Okt.); Kelly, Los Angeles (Juni–Sept.); Kiss, Budapest (Sept.–Dez.); Dr. Larwood, London (Juli–Dez.); Dr. Luu, Cambridge, Mass. (März); Dr. Richards, Chilton (Juli–Sept.); Dr. Richichi, Florenz (Nov.).

Due to the regular meetings of the ISOPHOT Co-investigators associated to other Research Institutes and industrial Firms in Germany and fro abroad, numerous guests were at the MPIA for short times, who are not mentioned here individualy.

Co-operative Students: Krause (until 31.8.), Mayer, Kunkel, De Vos (2.3.–29.5.).

Calar Alto/Almeria:

Local Director: Birkle (until 30.6.), Gredel (as from 1.5.), Vives.

Astronomy, Night Assistants: Aceituno (as from 15.4.), Aguirre, Alises, Frahm, Hoyo, Montoya (as from 15.4.), Quesada (beurlaubt), Thiele.

Telescope Techniques: Capel, de Guindos, Garcia, Helmling, Henschke, L. Hernández, Lingenfelder (until 31.5.), Raúl López, Morante, W. Müller, Nuñez, Parejo, Schachtebeck, Usero, Valverde, Wilhelmi.

Technical Services: A. Aguila, M. Aguila, Ariza, Barón, J. Braun, Carreno, Dominguez, Gómez, Góngora, Manuel Hernández, Klee, Rosario López, Marquez, Martinez, Puertas, F. Restoy, Romero, Sáez, Sanchez, Schulz, Tapias.

Administration, Secretariate: Magdalena Hernández, M.J. Hernández, M.I. López, C. Restoy.

Working Groops and Scientific Collaborations

Instrumentation Projects

ALFA
Stefan Hippler, M. Kasper, P. Kalas, R.-R. Rohloff, K. Wagner, P. Bizenberger and all technical Departments of MPIA and Calar Alto Observatory in collaboration with
MPI für extraterrestrische Physik, Garching
University of Massachusetts, Amherst, USA.

CONICA
Rainer Lenzen, W. Benesch, P. Franke, M.A. Khan, N. Münch, N. Ortlieb, R.-R. Rohloff, C. Storz, A. Tusche, K. Wagner, in collaboration with:
MPI für extraterrestrische Physik, Garching.

MAX
Tom Herbst, S.V.W. Beckwith, M. Robberto, P. Bizenberger, C. Birk.

MIDI
Christoph Leinert, U. Graser, B. Grimm, T. Herbst, St. Hippler, R. Lenzen, R. Ligori, R. Mundt, R. Lenzen, N. Ortlieb, E. Pitz, I. Porro, M. Robberto, R.-R. Rohloff, K. Wagner in collaboration with:
Kiepenheuer-Institut, Freiburg,
Thüringer Landessternwarte, Tautenburg,
Amsterdam University, Sterrewacht Leiden,
Observatoire de Meudon, Observatoire de Nice.

MOSCA
Joseph Fried, W. Benesch, P. Franke, N. Münch, N. Salm, B. Grimm, K. Marien, K. Zimmermann, A. Brüge, B. v. Kuhlmann.

OMEGA Cass
Rainer Lenzen, T. Herbst, H. Bellemann, P. Bizenberger, P. Franke, C. Storz.

PACS für FIRST
Dietrich Lemke, S. Eckardt, U. Grözinger, U. Klaas, H. Krause, in collaboration with:
MPI für extraterrestrische Physik, Garching
and DLR, Berlin.

ISO-Datenzentrum
Dietrich Lemke, ISOPHOT-PI, and the ISO-Group at MPIA: P. Ábrahám, J. de Mooij, S. Eckhardt, U. Grözinger, M. Haas, P. Heraudeau, U. Herbstmeier, S. Hotzel, U. Klaas, T. Kranz, M. Kunkel, T. Müller, M. Radovich, A. Rushworth, L. Schmidtobreick, M. Stickel, C. Surace, L.V. Toth.

Observations:

Asteroids
Thomas G. Müller, Ulrich Klaas in collaboration with:
Astronomisches Observatorium Uppsala,
ISO Science Operations Center und ISO Datenzentrum, Villafranca, Five College Radio Astronomy Observatory, Amherst, USA,
Institut für Planetenerkundung, DLR, Berlin.

Solar Wind
Christoph Leinert Leinert in collaboration with:
Center for Astropysics and Space Sciences, University of San Diego, USA.

Brightness Fluctuations of the Zodiacal Light
Christoph Leinert, U. Herbstmeier, P. Ábrahám, D. Lemke, C. Surace, M. Kunkel, in collaboration with:
Konkoly-Observatorium Budapest,
Helsinki Observatory,
ISO Science Operations Center, Villafranca.

Jets from Joung Stars
Reinhard Mundt in collaboration with:
Thüringer Landessternwarte, Tautenburg.

Double Stars
Monika Petr, Ch. Leinert, S.V.W. Beckwith, J. Woitas, in collaboration with:
Observatoire de Paris-Meudon,
Osservatorio Astrofisico di Arcetri, Florenz,
MPI für Radioastronomie, Bonn,
Astrophysikalisches Institut Potsdam.

Circumstellar Discs
Peter Ábrahám, Ch. Leinert, U. Klaas, D. Lemke, I. Heinrichsen, in collaboration with:
Konkoly Observatorium, Hungary,
Universitäts-Sternwarte, Jena,
Thüringer Landessternwarte, Tautenburg.

CADIS
Klaus Meisenheimer, H.-J. Röser, H. Hippelein, S.V.W. Beckwith, J. Fried, R. Fockenbrock, C. Leinert, E. Thommes, Ch. Wolf.

Young Galaxies and EROs
Steve V.W. Beckwith, D.Thompson in collaboration with: CAISMI-CNR, Florence,
California Institute of Technology, Pasadena,
Goddard Space Flieght Center, Greenbelt, USA.

Quasars
Joseph Fried

ISO Serendipity Survey
Manfred Stickel, S. Bogun, D. Lemke, U. Klaas, L.V. Toth, U. Herbstmeier in collaboration with:
ISO Science Operations Center, Madrid,
Univ. Budapest, Hungary,
Astrophysikalisches Institut Potsdam,
California Institute of Technology, Pasadena,
Imperial College, London.

Theoretical Studies

Photoevaporation of Protostellar Disks
Olaf Kessel in collaboration with:
Astronomisches Institut der Universität Würzburg.

Ionizing Radiation in Smooth Particle Hydrodynamics
Olaf Kessel, A. Burkert.

Thermal Instabilities in Gaseous Clouds
Andreas Burkert in collaboration with:
Lick Observatory, Santa Cruz, USA.

Formation of Double Stars
Matthew R. Bate in collaboration with:
Institute of Astronomy Cambridge, UK
MPI für Radioastronomie, Bonn.

Eta Carinae
M.-M. Mac Low in collaboration with:
MPI für Astrophysik, Garching
Astronomisches Institut – UNAM, Mexico City.

Evolution of Dwarf Galaxies
Andreas Burkert, Mordecai-Marc Mac Low, Olaf Klessen in collaboration with:
MPI für Astrophysik, Garching,
Institut für Astrophysik der Universität Heidelberg,
Osservatorio Astrofisico di Arcetri, Florence,
Tokio University, Japan.

Dynamics of Spiral Galaxies
Panos Patsis in collaboration with:
ESO, Chile, Universität Athen.

Formation of Elliptical and S0-Galaxies
Thorsten Naab, Andreas Burkert.

Density Profiles at the Centres of Galaxies
Andreas Burkert in collaboration with:
Shiga University, Kyoto University, Japan.

Formation and thermal Instabilities of clumpy Clouds
Andreas Burkert in collaboration with:
Lick Observatory, Santa Cruz, USA.

Collaboration with Industrial Firms

Calar Alto Observatory
Carl Zeiss, Jena und Oberkochen

ALFA
AOA Inc., Cambridge, Mass, USA
Berliner Institut für Optik, Berlin
Cambridge Innovations, Farmingham, Mass, USA
Microgate S.r.l., Bozen, Italien,
MIT/Lincoln Laboratory, Lexington, Mass, USA
Univ. of Massachusetts, Amherst, Mass., USA

Wide Field Imager
Faulhaber Motoren
Fisba Optik, St. Gallen,
Linos Photonics, Göttingen,
Omega, Vermont, USA,
Schott, Mainz,
Stegmann

MIDI
Cherent, Dieburg
CME CompuMess Elektronik, Unterschleißheim
CREASO, Gilching
Cryophysics, Darmstadt
Dell Computer, Langen
EBV-Elektronik, München
Edwards Hochvakuum, Marburg
esd electronic system design, Hannover
Halfmann Teleskoptechnik, Neusäß-Voglsang
HaSoTec, Rostock
Infrared Optical Products, USA
Jenaer Meßtechnik, Jena
Kniel System Elektronik, Karlsruhe
Laservision, Forchheim
Leybold Vakuum, Köln
LOT-Oriel, Darmstadt
Messer-Griesheim, Darmstadt
NESLAB Instruments, Frankfurt
OWIS, Staufen
Pfeiffer Vakuum, Wiesbaden
Polatec, Waldbronn
Raytheon, USA
Sun Microsystems, Grasbronn
VAT Vakuumventile, Schweiz
VSYSTEMS Electronic, München

Omega Cass
Barr, Westford, Mass., USA
Carl Zeiss, Jena
Infrared Laboratories, Tucson, AZ, USA

Conica
Barr, Westford, Mass., USA
Carl Zeiss, Jena
Janos, Townshend, Vermont, USA
Linos Photonics, Göttingen
Leybold, Hanau
Möller, Wedel
Omega, Vermont, USA
Pörschke, Höchst
Präzisionsoptik, Gera
Queensgate, Barkshire, GB
Richardson Grating, Rochester, USA
Vitron, Jena

Kamera MAX
Boeing, Kalifornien, USA
Gatir, Florida, USA
Infrared Laboratories, Tucson, AZ, USA
Janos, Townshend, Vermont, USA
Kevin Hanna, Florida, USA

PACS
ANTEC, Kelkheim
IMEC, Leuven

CCD Technology
Dataman, Pliezhausen
EEV Ltd., GB
Haefele, Schriesheim.
Heraeus, Hanau
Lockheed Martin Fairchild Syst., USA
New Focus, Santa Clara, USA
Philips, Eindhoven, Niederlande
Roth, Karlsruhe
SITe Corp., Beaverton, Oregon, USA
Steward Observatory, Tucson, Arizona, USA
Tafelmeier, Rosenheim

Computers
AKRO, UNterschleißheim
Additive, Friedrichsdorf
Creaso, Gilching
Draco, Hamburg
Edo, Hockenheim
PROUT, Darmstadt
ProMedia, Oftersheim
Seicom, Ismaning
Sun, Langen
Transtec, Tübingen

Mechanics and Electronics
Adam + Hecker, Wiesloch
Almet-AMB, Mannheim

Amphenol-Tuchel Electronics, Heilbronn
APE Elektronik, Kuppenheim
AVNET EMG, Braunschweig
Best Power Technology, Erlangen
Binder Magnete, Villingen-Schwenningen
Börsig, Neckarsulm
Bubenzer Bremsen, Kirchen-Wehrbach
Bürklin, München
Cadillac-Plastic, Viernheim
Carl Roth, Karlsruhe
Cherry Mikroschalter, Auerbach
Com Pro, Stuttgart
Compumess Electronik, Unterschleissheim
Conrad Electronic, Hirschau
CTS Microelectronics, Chicago, Ill., USA
CTS Microelectronics, West Lafayette, Ind., USA
Dalektron, Dreieich
Dannewitz, Linsengericht
Dürkes & Obermayer, Heidelberg
Dyna Systems NCH, Mörfelden-Walldorf
EBJ, Ladenburg
EBV-Electronik, Leonberg
EC Motion, Mönchengladbach
Edsyn Europa, Kreuzwertheim
Eldon, Büttelborn
Elna Transformatoren, Sandhausen
elspec, Geretsried
ELV Electronik, Leer
ERNI, Adelberg
eurodis Enatechnik, Quickborn
Euromicron, Mittenaar
EWF, Eppingen
Farnell Electronic Components, Deisenhofen
Farnell Electronic Services, Möglingen
FCT Electronic, München
Fischer Elektronik, Lüdenscheid
Fritz Faulhaber, Schönaich
Future Electronics Deutschland, Unterföhring
Gould Nicolet Meßtechnik, Dietzenbach
Hartmann + Braun, Alzenau
Helukabel, Hemmingen
Herz, Leister Geräte, Neuwied
Hewlett-Packard Direkt, Böblingen
Holz Electronik, Kirchheim
Hommel-Hercules Werkzeughandel, Viernheim
Horst Göbel, Ludwigshafen
Horst Pfau, Mannheim
HOT Electronic, Taufkirchen
HTF Elektro, Mannheim
Huber + Suhner, Taufkirchen
IBF Mikroelektronik, Oldenburg
Inkos, Reute/Breisgau
iSystem, Dachau
Jacobi Eloxal, Altlussheim
Jarmyn, Limburg
Kniel, Karlsruhe
Knürr, München
Lambda Electronics, Achern
Lemo Electronik, München
LPKF CAD/CAM Systeme, Garbsen
Macrotron, München
Matsuo Electronics Europe, Eschborn
Matsushita Automation, Holzkirchen
Maxim Ges. f. elektronische integrierte Bausteine, Planegg
Menges electronic, Dortmund
Metrofunkkabel-Union, Berlin
MSC Vertriebs-GmbH, Stutensee
MTI, Baden-Baden
Nanotec, Finsing
Nickel Schalt- und Meßgeräte, Villingen-Schwenningen
Niebuhr Optoelectronik, Hamburg
Nies Electronic, Frankfurt
Nova Electronik, Pulheim
Otto Faber, Mannheim
pbe Electronic, Elmshorn
Phytec Meßtechnik, Mainz
Plastipol, Runkel
PSI Tronix, Tulare, Cal., USA
Püschel Electronik, Mannheim
R.E.D. Reg. Electronic Distrib., Rodgau-Jügesheim
Radiall, Rödermark
Rau-Meßtechnik, Kelkheim
Reinhold Halbeck, Offenhausen
Retronic, Ronneburg
Riekert & Sprenger, Wertheim
Rittal-Werk, Herborn
Roland Häfele, Schriesheim
RS Components, Mörfelden-Walldorf
Rufenach Vertriebs-GmbH, Heidelberg
Rutronik, Ispringen
Sasco, Putzbrunn
Scantec, Planegg
Schaffner Elektronik, Karlsruhe
Schuricht, Fellbach-Schmiden
SCT Servo Control Technology, Taunusstein
SE Spezial-Electronic, Bückeburg
Siemens IC-Center, Mannheim
Spindler & Hoyer, Göttingen
Spoerle Electronic, Dreieich
Synatron, Hallbergmoos
TMS Test- und Meßsysteme, Herxheim/Hayna
Tower Electronic Components, Schriesheim
TreNew Electronic, Pforzheim
TS-Optoelectronic, München
TWK-Elektronik, Karlsruhe
Vacuumschmelze, Hanau
Vero Electronics, Bremen
W. & W. Schenk, Maulbronn
Wikotec, Bramsche
Wilhelm Gassert, Schriesheim
WS CAD Electronik, Berk Kirchen

Teaching Activities

(Winter Term 97/98 and Summer Term 98)

Lectures

Ch. Leinert, D. Lemke: Introduction to Astronomy and Astrophysics, I

I. Appenzeller: Instruments and Observational Methods

A. Burkert und R. Wehrse (ARI): Structure, Formation, and Evolution of Galaxies in the Early Universe

Ch. Leinert und D. Lemke: Introduction to Astronomy and Astrophysics, II

I. Appenzeller:Physics of the Planetary System

R. Mundt: The Search for Extrasolar Planets

Seminars and Colloquia

R. Mundt, H.P. Gail (Univ. Heidelberg), H. Schwan (ARI), W.M. Tscharnuter (Univ. Heidelberg): Seminar: Introduction to Astronomy and Astrophysics, III

K. Meisenheimer und H.J. Röser: Seminar: Measuring the Structure of the Universe

I. Appenzeller, B. Baschek (Univ.Heidelberg), R. Wehrse (ARI), B. Wolf (Landessternwarte): Seminar: Non-spherical and Variable Winds of Luminous and variable Stars

K. Meisenheimer, H.J. Röser: Seminar: Reduction und Analysis of Optical Observations in Astronomy

Public Lectures

S. Beckwith: »Young Stars and Planetary Systems«, Aspen, USA (January), Einstein-Forum in Potsdam (May), Siemens-Stiftung (July); »Formation of Structure in the Universe«, Symposion of the Max-Planck-Gesellschaft, Berlin (December).

H. Elsässer: »Dangers from Space?«, November 13., Mannheim Planetarium

D. Lemke: »The ISO Mission and its Results«, Annual Meeting of the Math.-Nat. Teachers in Heidelberg (September) und in Nordenham (October).

A.M. Quetz: live interview at the TV channel Sat 1 about Perseids.

J. Staude gave several lectures at High Schools about Young Stars and Extrasolar Planets in occasion of the annual meeting of the Max Planck Society in Weimar (June), as well as in the Starkenburg Observatory, Heppenheim (August).

Meetings and Invited Talks

The Calar Alto Colloquium with more than 20 contributions was held at Königstuhl on March 16. and 17.

Talks given in Research Institutions and at international Meetings

Solid Interstellar Matter – The ISO Revolution, Les Houches, January: P. Ábrahám

Meeting of the AAS, Washington, January: A. Burkert

The Magellanic Clouds and Other Dwarf Galaxies, Graduiertenkolleg Bonn, January: M. Haas, M.-M. Mac Low

ISO Detector Workshop, ESA Villafranca, Januar: D. Lemke

Conference on Interstellar Turbulence, Puebla, Mexico, January: M.-M. Mac Low

Worshop on Gas Flows in Barred Galaxies, Herdfordshire, G,B., Januayr: P.A. Patsis

Conference on »Universal Star Formation«, Aspen, Colorado, Januar: S. Beckwith

Conference on »Instrumentation for Large Optical Telescopes«, Keck Observatory (Hawaii,USA), February: S. Beckwith

Conference on Neural Networks, Brisbane, Australia, Februar: C.A.L. Bailer-Jones

Colloquium at the Universitäts-Sternwarte Göttingen, February: H.-J. Röser

SPIE Conference on »Astronomical Instrumentation«, Kona, Hawaii, March: T. Herbst, U. Klaas, D. Lemke, R. Lenzen, M. Stickel

SPIE Conference on »Astronomical Interferometry«, Kona, Hawaii, March: U. Graser, Ch. Leinert, I. Porro

Conference on »Dwarf Galaxies«, Les Arcs, Frankreich, März: A. Burkert

Colloquium »Observing the First Galaxies: The CADIS Survey«, Baltimore, USA, April: S. Beckwith

Colloquium »Observing Primeval Galaxies«, MIT, Cambridge (Mass.), April: S. Beckwith

Seminar »Infrared Searches for Primeval Galaxies«, Harvard, Cambridge (Mass.), April: S. Beckwith

Colloquium »Circumstellar Disks and Extrasolar Planet Formation«, Harvard, Cambridge (Mass.), April: S. Beckwith

EGS XXIII General Assembly, Nice, April: P. Ábrahám, Th. Müller

UK National Astronomy Meeting St. Andrews, UK, April: C. Bailer-Jones

Conference on »Very Low Mass Stars and Brown Dwarfs in Stellar Clusters«, La Palma, May: C. Bailer-Jones, Ch. Leinert, R. Mundt

Conference on Variable and Non-Spherical Winds in Luminous Hot Stars, Heidelberg, May: M.-M. Mac Low

IAP Colloquium »Widefield Surveys in Cosmology«, Paris, May: Ch. Wolf

Conference on Star Formation, Heraclion, Creta, June: S. Beckwith

Conference on »Science with the NGST«, Liège, Belgien, Juni: S. Beckwith, T. Herbst

Physikalisches Kolloquium, Jena, June: K. Meisenheimer

Conference on »Protostars and Planets«, Santa Barbara, Calif., July: A. Burkert

Workshop on Space Cryogenics, ESA, Noordwiyk, Juli: D. Lemke

Summer School du ESO/OHP, Obs. de Haute-Provence, July: H.-J. Röser

Conference on »New Perspectives on the Interstellar Medium«, Pentincton, Canada, August: M.-M. Mac Low

ESO/OSA Meeting on Astronomy with Adaptive Optics, Sonthofen, September: M. Kasper

AG-Tagung Heidelberg, September: Ábrahám, Lemke, Haas, Héraudeau, Herbst, Hotzel, Klaas, K. Meisenheimer, Müller, I. Porro, Tóth, Woitas,

Conference on »Galaxy Evolution«, Paris, September: S. Phleps

Conference »The Universe as seen by ISO«, Paris, October: D. Lemke

Optical/Infrared Interferometry Workshop, Flagstaff, Arizona, October: Rohloff

ESFON Meeting, Heidelberg, October: A. Burkert, Woitas

GAIA Science Workshop, ESTEC, Leiden, November: C. Bailer-Jones

Washington Area Astronomy Meeting, Laurel, MD, USA, November: S. Beckwith

Service in Committees

*K. Birkle und .R. Mundt*were in the Calar Alto Program Committee.

A. Burkert was Chairman of the European Network for Star and Planet Formation

A. Burkert represented the MPIA Staff in the Chemisch-Physikalisch-Technische Sektion of the Max Planck Society

H. Elsässer was elected Chairman of the Section Astronomy/Astrophysics und Member of the Senate of the Deutsche Akademie der Naturforscher Leopoldina

U. Klaas represented the MPIA at the ISO Post Operational Meetings about Data Archives

Ch. Leinert was member of the Interferometric Sccience Advisory Committee (ESO) and the Organizing Committee of the IAU Commission 21 (Light of the Night Sky), Executive Committee of Division III (Planetary System Sciences)

D. Lemke ,as Principal Investigator, was member of the ISO Science Team

D. Lemke was member of the Experts Panel »Verbundforschung« of the Federal Ministery of Science and Technology

M.-M. Mac Low was member of the Space Telescope Time Allocation Committee, Subcommittee Hot Stars

R. Mundt was member of the Advisory Committee about the future use of the Calar Alto Observatory

R. Mundt was was member of the Habilitation Committee of the Faculty of Physics and Astronomy

I. Porro collaborated with JOTA

Publications

Ábrahám, P., Ch. Leinert, A. Burkert, D. Lemke and Th. Henning: Search for cool circumstellar matter in the Ursae Majoris group with ISO. Astron. Astrophys. **338**, No.1, 91–96 (1998)

Ábrahám, P., Ch. Leinert, D. Lemke, A. Burkert, and T. Henning: Far infrared photometry of circumstellar matter around intermediate mass stars. In: ISO's view on Stellar Evolution. ESA Proceedings, Noordwijkerhout, Netherlands 1997.Astrophys. & Space **255**, 45–51 (1998)

Ábrahám, P., Ch. Leinert and D. Lemke: Interplanetary dust as observed by ISOPHOT. AG Abstract Series **14**, 47 (1998)

Anders, S., N. Thatte, L.E. Tacconi-Garman, A. Eckart, W. Hackernberg, T. Ott, R. Genzel, S. Hippler, R.-R. Rohloff and S.V.W Beckwith: Diffraction limited spectroscopy with 3D and ALFA – First results. AGM Abstr. Ser. **14** I02A (1998)

Bailer-Jones, C.A.L., M. Irwin and T. von Hippel: Semi-automated Extraction of Digital Objective Prism Spectra. Mon. Not. R. Astron. Soc. **298**, 1061 (1998)

Bailer-Jones, C.A.L., M. Irwin and T. von Hippel: Automated Classification of Stellar Spectra. II: Two-Dimensional Classification with Neural Networks and Principal Components Analysis. Mon. Not. R. Astron. Soc. **298**, 361 (1998)

Bailer-Jones, D.J.C. MacKay, T.J. Sabin and P.J. Withers: Static and Dynamic Modelling of Materials Forging. Proc. 9th Australian Conference on Neural Networks. In: T. Downs, M. Frean, M. Gallagher (eds), **21** (1998)

Bailer-Jones, C.A.L., D.J.C. MacKay and P.J. Withers: A Recurrent Neural Network for Modelling Dynamical Systems. Network: Computation in Neural Systems, **9** (4), 533 (1998)

Bailer-Jones, C.A.L., D.J.C. MacKay, T.J. Sabin and P.J. Withers: Static and Dynamic Modelling of Materials Forging. In: Australian Journal on Intelligent Information Processing Systems Networks, **5** (1), 10 (1998)

Bate, M.: Brown Dwarfs and Extrasolar Planets. In: The Mass-Ratio Evolution of Accreting Protobinary Systems: Implications for Brown Dwarfs in Binaries. ASP Conf. Proc. **134**, 273 (1998)

Bate, M.R.: Collapse of a Molecular Cloud Core to Stellar Densities: The First Three-Dimensional Calculations. Astrophys. J. **508**, 95. (1998)

Bate, M.R., C.J. Clarke and M.J. McCaughrean: Interpreting the mean surface density of companions in star-forming regions. Mon. Not. R. Astron. Soc. **297** (4), 1163–1181 (1998)

Beckwith, S.V.W.: Star Formation and the NGST. Science with the NGST. Eds. E. Smith and A. Koratkar, ASP Conference Series, **133** (1998).

Beckwith, S.V.W., D. Thompson, F. Mannucci and S. G. Djorgovski: An Infrared Emission Line Galaxy at z = 2.43. Astrophys. J. 504, 107–112 (1998).

Birkle, K., O. Ryan, H. Böhnhardt, Z. Sekanina, D. Engels, P. Keller and M. Jäger: Dust Tail Striae in Comet Hale-Bopp. Astron. Ges. Abstract Ser. **14**, 100 (1998)

Bizenberger, P., M.J. McCaughrean, C. Birk, D. Thompson and C. Storz: Omega Prime: The Wide-Field Near-Infrared Camera for the 3.5 m telescope of the Calar Alto Observatory. In: A.F. Fowler (ed): Infrared Detectors and Instrumentation in Astronomy, Proc. SPIE **3354**, 825–832 (1998)

Bonnell, I.A., M. Bate, and H. Zinnecker: The Formation of Massive Stars. Mon. Not. R. Astron. Soc. **298**, 93 (1998)

Brandner, W., M. Kunkel, Ch. Leinert, R. Kohler, H. Zinnecker and A. Moneti: The Low-Mass Stellar Content of the Scorpius-Centaurus OB Association. Bull. Amer. Asron. Soc. **193**, 7310B

Burkert A., P. Abraham, Ch. Leinert, D. Lemke, and Th. Henning: Far-Infrared Photometry and Mapping of Herbig Ae/Be Stars with ISOPHOT. Abstract Series **14**, 128 (1998)

Burkert A. and C. R. O'Dell: The Structure of Cometary Knots in the Helix Nebula. Astrop. J. **503**, 792 (1998)

Burkert, A. and J. Silk: Dark Baryons and Rotation Curves. In: Galactic Halos: ASP Conf. Ser. **136**, 397 (1998)

Eislöffel, J. and R. Mundt: Imaging and Kinematic Studies of Young Stellar Object Jets in Taurus. Astron. J. **115**, 1554–1575 (1998)

Castro-Tirado, A.J., J. Alberto, J. Gorosabel, Javier, Benitez, Narciso, Ch. Wolf, R. Fockenbrock, E. Martinez-Gonzalez, H. Kristen, A. Broeils, H. Pedersen, J. Greiner, E. Costa, M. Feroci, L. Piro, F. Frontera, L. Nicastro, E. Palazzi, C. Bartolini, A. Guarnieri, N. Masetti, A. Piccioni, M. Mignoli, M. Wold, M. Lacy, K. Birkle, T. Broadhurst, S. Brandt and N. Lund: Photometry and Spectroscopyof the GRB 970508 Optical Counterpart. Science **279**, 1011 (1998)

Castro-Tirado, A.J., J. Gorosabel, N. Benitez, C. Wolf, R. Fockenbrock, E. Martinez-Gonzaléz, H. Kristen, A. Broeils, H. Pedersen, J. Greiner, E. Costa, L. Piro, K. Birkle, et al.: Photometry and Spectroscopy of the GRB 970508 Optical Counterpart, Science **279**, 1011–1914 (1998)

Davies, R.I., W. Hackenberg, T. Ott, A. Eckart, H.-C. Holstenberg, S. Rabien, A. Quirrenbach and M. Kasper: ALFA: First Operational Experience of the MPE/MPIA Laser GuideStar System for Adaptive Optics. Proc. SPIE **3353** (1998)

Eislöffel, J. and R. Mundt: Imaging and Kinematical Studies of Young Stellar Objects in Taurus. Astron. J. **115**, 1554 (1998)

Elsässer, H.: Results of the Heidelberg Void Program Proceedings: Supernovae and Cosmology, Eds: L. Labhardt et al. Astron. Institut der Univ. Basel 119–125 (1998)

Felli, M., G.B. Taylor, Th. Neckel, and H.J. Staude: The ionized wind of IRAS 08159-3543. Astron. Astrophys. **329**, 243–248 (1998)

Fernández, M. and L. F. Miranda: Spectroscopy of low mass pre-main sequence stars: photospheric spots and chromospheric activity. Astron. Astrophys. **332**, 629–642 (1998)

Fischer, O., B. Stecklum and Ch. Leinert: 2D Speckle polarimetry of Z Canis Majoris. Astron. Astrophys. **334**, 969–975 (1998)

Fried, J.W.: Faint galaxies around quasars at z = 1 and gravitational lensing of distant objects. Astron. Astrophys. **331**, L73–76

Garcia-Berro, E., S. Torres, J. Isern, A. Burkert: Monte Carlo Simulation of disc white dwarf population. Mon. Not. R. Astron. Soc. **302**, 173–188

Garcia-Segura, C., N. Langer, M. Rozyczka, M.M. Mac Low and J. Franco: The Effects of Rotation and Stellar Magnetic Field in the Nebular Shapes: LBV Nebulae and PNe. Rev. Mex. Astron. Astroph. Conf. Ser. **7**, p. 50

Gorosabel, J., A. J. Castro-Tirado, C. J. Willott, H. Hippelein, J. Greiner, A. Shlyapnikov, S. Guziy, E. Costa, M. Feroci, F. Frontera, L. Nicastro and E. Palazzi: Detection of the near-infrared counterpart of GRB 971214 3.2 hours after the gamma-ray event. Astron. Astrophys. Lett. **335** (1998), 5–8

Gorosabel, J., A.J. Castro-Tirado, C. Wolf, J. Heidt, T. Seitz, E. Thommes, C. Barolini, A. Guarnieri, N. Masetti, A. Piccioni, S. Larsen, E. Costa, M. Feroci, F. Frontera, E. Palazzi and N. Lund: An optical study of the GRB 970111 field beginning 19 hours after the gamma-ray burst, Astron. Astrophys. **339**, 719–728 (1998)

Graser, U. and Ch. Leinert: MIDI – the Mid infrared interferometric instrument for the VLTI. AG Abstract Ser. **14**, 91 (198).

Grosbøl, P. J. and P. A. Patsis: Stellar disks of optically flocculent and grand design spirals. Decoupling of stellar and gaseous disks. Astron. Astrophys. **336**, 840 (1998)

Haas, M.: Very cold dust in the peculiar dwarf elliptical galaxy NGC205. Astron. Astrophys. **337** (1998)

Haas, M., R. Chini, K. Meisenheimer, M. Stickel, D. Lemke, U. Klaas and E. Kreysa: On the Far-Infrared Emission of Quasars. Astrophys. J. **503**, 109–113 (1998)

Haas, M., D. Lemke, M. Stickel, H. Hippelein, M. Kunkel, U. Herbstmeier and K. Mattila: Cold dust in the Andromeda Galaxy mapped by ISO. Astron. Astrophys. **338**, No. 1, L33 (1998)

Heinrichsen, I., H.J. Walker and U.Klaas: Infrared Mapping of the dust disc araund Vega. Mon. Not. R. Astron. Soc. **293**, L78–82 (1998)

Henning, Th., A. Burkert, R. Launhardt, Ch. Leinert and B. Stecklum: Infrared imaging and millimetre continuum mapping of Herbig Ae/Be and FU Orionis stars. Astron. Astrophys. **336**, 565–568 (1998)

Herbst, T.M.: A Micropupil-Based Near Infrared Imaging Spectrograph. SPIE Proc. **3324**, p. 720 (1998)

Herbstmeier, U., P. Ábrahám, D. Lemke, R. J. Laureijs, U. Klaas, K. Mattila, Ch. Leinert, C. Surace and M. Kunkel: Small-scale structures in the far-infrared background. Astron. Astrophys. **332**, 739 (1998)

Herbstmeier, U. and A. Wennmacher: ISOPHOT observations of a cold filament in the local hot bubble. In: The Local Bubble and Beyond, (Eds.) D. Breitschwerdt, M.J.Freyberg, J. Trümper. Proc. IAU Colloquium 166, Lecture notes in Physics, vol. 506, pp. 117–120. Springer-Verlag, Berlin (1998)

Hippelein, H., S. Beckwith, R. Fockenbrock, J. Fried, U Hopp, Ch. Leinert, K. Meisenheimer, H.-J. Röser, E. Thommes and C. Wolf: The Calar Alto Deep Imaging Survey. In: New Horizons from Multi-Wavelength Sky Surveys. Proc. 179th Symposium of the International Astronomical Union, Baltimore, Kluwer Academic Publishers 1998, 179, p. 293–295

Hippler S., A. Glindemann, M. Kasper, P. Kalas, R.-R. Rohloff, K. Wagner, D. P. Looze and W. Hackenberg: ALFA:The MPIA/MPE Adaptive Optics with a Laser for Astronomy Project. SPIE Proc. Vol. **3353**, 1998, 44–55.

Huang, J.-S., L. L. Cowie and G. A. Luppino: Morphological Classification of the Local I-and K-Band Galaxy Sample. Astrophys. J. **496**, 31

Jackson, B. V., P. Hick, C. Leinert, A. Yokobe: Helioshperic modeling used to map global solar wind flows. Astron. Astrophys. Suppl. **192**, (1998).

Kessel, O., Yorke, H. W. and S. Richling: Photoevaporation of protostellar disks III. The appearance of photoevaporating disks around young intermediate mass stars. Astron. Astrophys. **337**, 832 (1998)

Kiss, C., A. Moór, and L.V. Tóth: Revised Catalogue of IRAS Loops in the IInd Galactic Quadrant. In: the Astract Book of the 3rd Cologne-Zermatt Symposium. (Ed.) V. Ossenkopf, Shaker-Verlag, 1998.

Klaas, U., R.J. Laureijs and J. Clavel: Far-infrared polarisation of the quasar 3C 279. AG. Abstract Series **14**, E03 (1998)

Klaas, U., D. Lemke, T. Kranz, R. J. Laureijs, Ch. Leinert, J. Schubert, M. Stickel and L. V. Tóth: Infrared straylight measurements of the ISO telescope. In: Infrared Astronomical Instrumentation. Proceedings of the SPIE 3354-111, (Ed.) A.M. Fowler, Bellingham 1998, 996–1004

Klessen, R.S., A. Burkert and M. R. Bate: Fragmentation of Molecular Clouds: The Initial Phase of a Stellar Cluster. Astrophys. J. Lett. **501**, 205–208 (1998)

Klessen, R.S. and P. Kroupa: Dwarf Spheroidal Satellite Galaxies Without Dark Matter: Results From Two Different Numerical Techniques. Astrophys. J. **498**, 143–155 (1998)

Köhler, R., Ch. Leinert: Multiplicity of T Tauri stars in Taurus after ROSAT. Astron. Astrophys. **331**, 977–988 (1998)

Köhler, R., Ch. Leinert and H. Zinnecker: Multiplicity of T Tauri Stars in Different Star-Forming Regions. AG Abstrac Ser. **14**, 17 (1998)

Kranz, T., D. Lemke, L. V. Thot, U. Klaas, Ch. Leinert and R. J. Laureijs: ISO/ISOPHOT straylight caused by Sun, Moon and Earth. AG Abstract Ser. **14**, 127 (1998)

Lehtinen, K. D. Lemke, K. Mattila and L. Haikala: Far-infrared ISOPHOT observations and the enrgy balance of a quiescent globule. Astron. Astroph. **333**, 702 (1998)

Leinert, Ch. and Th. Encrenaz: ISO Observations of the Solar System. In. Highlights of Astronomy XI/ Highlights of the IOS Mission, (1998), vol. 11, 1151

Leinert, Ch. F. Allard, A. Richichi and H. Jahreiß: The low-mass companions in the nearby triple system LHS 1070. In: Brown dwarfs and extrasolar planets, eds. F. Rebolo, E.L. Martin, M.R. Zapatero-Osorio, ASP Conf. Ser. Vol. 134, p. 203

Leinert, Ch., S. Bowyer, L.K. Haikala, M.S. Hanner, M.G. Hauser, A.-Ch. Levasseur-Regourd, I. Mann, K. Mattila, W.T. Reach, W. Schlosser, H.J. Staude, G.N. Toller, J.L. Weiland, J.L. Weinberg and A.N. Witt: The 1997 reference of diffuse night sky brightness. Astron. Astrophys. Suppl. 127, 1-100 (1998)

Leinert, Ch. and U. Graser: MIDI – the Mid-infrared interferometric instrument for the VLTI. SPIE Conference on Astronomical Interferometry, Kona, Hawaii, March 1998. SPIE 3350-108, (1998)

Leinert, Ch. and B. V. Jackson: Global Solar Wind Changes Over Solar Cycle 21: a Combination of Helios Photometer, In-situ and IPS Data. Astrophys. J. *505*, 984–992 (1998)

Leinert, Ch. and K. Mattila: Natural Optical Sky Background. Eds. S. Isobe and Derek McNally, ASP Conf. Ser., Vol. 139, p. 17 (1998)

Leinert, Ch., Woitas, F. Allard, A. Richichi, and H. Jahreiss: The Low-Mass Companions in the Nearby Triple System LHS 1070. In: Rebolo, R., Martin, E.L., Zapatero Osario, M.R.: Brown Dwarfs and Extrasolar Planets. Astr. Soc. Pac. Conf. Series, **134**, 203–209.

Lemke, D. Astronomie mit Weltraumteleskopen. In: Jahresbericht des Physikalischen Vereins Nr. 169. Frankfurt am Main 1998, 45–52.

Lemke, D., L. Barl, S. Eckardt, O. Frenzl, U. Grözinger, L. Hermans, G. Jakob, R. Katterloher, A. Poglitsch, J. Seijnaeve and J. Wolf: FIRSA - the demonstrator array of the FIR camera for the photoconductor instrument PACS on ESA's FIRST satellite. Proceedings of the SPIE Infrared Astronomical Instrumentation Conference, SPIE 3354-137 (1998), (Ed.) A.M. Fowler, Bellingham, 1998, 1185–1191.

Lemke, D., U. Klaas, P. Ábrahám, J.A. Acosta Pulido, H. Castaneda, L. Cornwall, C. Gabriel, U. Grözinger, M. Haas, I. Heinrichsen, U. Herbstmeier, J. Schubert, B. Schulz, M. Stickel and L.V. Tóth: ISOPHOT - Inflight performance report. Proceedings of the SPIE Infrared Astronomical Instrumentation Conference, SPIE 3354-46 (1998), (Ed.) A.M. Fowler, Bellingham 1998, 627–636.

Lemke, D., K. Mattila, K. Lehtinen, R. J. Laureijs, T. Liljeström, A. Léger and U. Herbstmeier: Detection of UIR bands in an isolated local interstellar cirrus cloud. Astron. Astrophys. **331**, 742 (1998).

Lenzen, R., R. Hofmann, P. Bizenberger and A. Tusche: CONICA: The high resolution near-infrared camera for the ESO VLT. SPIE 3354-44, 606–614 (1998)

Lenzen, R., P. Bizenberger, N. Salm and C. Storz: Omega-Cass: A new multi-mode NIR-imager/spectrometer for the Calar Alto Observatory. SPIE 3354, 493–499 (1998)

Levine, D.A., C.J. Lonsdale, R. Hurt, H.E. Smith, G. Helou, C. Beichmann, C. Cesarsky, D. Elbaz, U. Klaas, R. Lauejis, D. Lemke, S.D. Lord, R.G. McMahon, M. Moshir, G. Neugebauer, B.T. Soifer, D. Van Buren, A. Wehrle, and R.D. Wolstencroft: First Results from the ISO-IRAS Faint Galaxy Survey, Astrophys. J. **504**, 64–76 (1998).

Lipovetsky, V., D. Engels, A. Ugryumov, U. Hopp, G. Richter, Y. Izotov, A. Kniazev and C. Popescu: Hamburg/SAO Survey of Emission-Line Galaxies. In: New Horizons from Multi-Wavelength Sky Survey, IAU Symp. No. 179, Eds. B.J. McLean, D.A. Golombek, J.J.E. Hayes, H.E. Payne, Kluwer Dordrecht, 1998, 299–301

Maciejewski, W., D.P. Cox: Supernova Remnant in a Stratified Medium: Explicit, Analytical Approximations for Adiabatic Expansion and Radiative Cooling. Astrophys. J. **511**, 792–797

Mac Low, M.-M.,: Wolf-Rayet and LBV Nebulae as the Result of Variable and Non-Spherical Stellar Winds. In: Variable and Non-Spherical Stellar Winds in Luminous Hot Stars. Ed. B.Wolf, Springer-Verlag, Heidelberg, IAU Coll. 169, 59 (1998)

Mac-Low, M.M., T.H. Chang, Y.-H. Chu and S.D: Points: ROSAT observations of the giant HII complex N 11 in the LMC. In: Magellanic Clouds and Other Dwarf Galaxies. Richtler T. and J. Brown (eds.), Shaker Verlag, Aachen, p. 269 (1998)

Mac Low, M.-M., T.H. Chang, Y.-H. Chu, S. D. Points, R.C. Smith and B.P. Wakker: X-Rays from Superbubbles in the Large Magellanic Cloud. V. The H II Complex N11. Astrophys. J. **493**, 260–273 (1998)

MacLow, M.M. and A. Ferrara: Starbursts in Dwarf Galaxies: Bown out or blown away. In: Magellanic Clouds and Other Dwarf Galaxies. Richtler T. and J. Brown (eds.), Shaker Verlag, Aachen, p. 177–180 (1998)

MacLow, M.M. and A. Ferrara: Superbubbles in Dwarf Galaxies: Blown out or blown away. In: Lecture Notes in Physics. **596**, 559–562 (1998)

Mac Low, M.M., R. Klessen, V. Ossenkopf, A. Burkert, M.D. Smith and M. Norman: Turbulence in Molecular Clouds. AG Abstract Series **14**, 122 (1998)

Mac Low, M.-M., R.S. Klessen, A. Burkert and M.D. Smith: Kinetic Energy Decay Rates of Supersonic and Super-Alfvénic Turbulence in Star-Forming Clouds. Phys. Rev. Lett. **80** (13), 2754–2757 (1998)

Mannucci, F., D. Thompson, S.V.W.Beckwith and G.M.Williger: Infrared Emission-line Galaxies Associated with Damped Ly and Strong Metal Absorber Redshifts. Astrophys. J. **501**, L11 (1998)

Mattila, K., K. Lehtinen and D. Lemke: Detection of widely distributed UIR band emission in the disc of NGC891. Astron. Astroph. **342**, 643–654 (1998)

Meisenheimer, K., S. Beckwith, R. Fockenbrock, J. Fried, H. Hippelein, J. Huang, Ch. Leinert, S. Phleps, H.-J. Röser, E. Thommes, D. Thompson, C. Wolf, F. Chaffee: The Calar Alto Deep Imaging Survey for Galaxies and Quasars at $z > 5''$. In: The young universe: Galaxy formation and evolution at intermediate and high redshift. S. D'Oderico, A. Fontana, E. Giallongo (eds.), ASP Conf. Series **146**, 134 (1998)

Meyer, M. R., S. E. Edwards, K. Hinkle and S. E. Strom: Near-Infrared Classification Spectroscopy: H-band Spectra of Fundamental MK Standards, Astrophys. J. Vol. **508**, Issue 1, pp. 397-409

Mori, M., Y. Yoshii and K. Nomoto: Dissipative Process as a Mechanism of Differentiating Internal Structures between Dwarf and Normal Elliptical Galaxies in a CDM Universe. Astrophys. J. Vol. **511**, Issue 2, pp. 585–594

Moritz, P., A. Wennmacher, U. Herbstmeier, U. Mebold, R. Egger and S.L. Snowden: X-ray shadows of the Draco nebula – A new method to determine neutral hydrogen column densities. Astron. Astroph. **336**, 682 (1998)

Müller, T. G. and J. S. V. Lagerros: Asteroids as far-infrared photometric standards for ISOPHOT. Astron. Astrophys. **338**, No. 1, 340–352 (1998)

Müller, T.G. and J.S.V. Lagerros, M. Burgdorf, T. Lim, P. Morris, A. Salama, B. Schulz and B. Vandenbussche: Fundamental thermal emission parameters of Ceres – derived from ISO observations. AG Abstract Series **14**, E13, (1998)

Mundt, R. and J. Eislöffel: T Tauri Stars Associated with Herbig-Haro Objects an d Jets. Astron. J. **116**, 860–867 (1998)

Natta, A., M. R. Meyer and S. V. W. Beckwith: Circumstellar Discs Around Pre-Main Sequence Stars: What ISO Can Tell Us. In: Star Formation with the Infrared Space Observatory. Eds. J. Yun and R. Liseau. ASP Conference Series, **132**, 265 (1998)

Nikoli S., C. Kiss, L.E.B. Johansson and L.V. Tóth: HCN and HNC distributions in the L1251 dark cloud. In: the Abstract Book of the 3rd Cologne-Zermatt Symposium. (Ed.) V. Ossenkopf, Shaker-Verlag, 1998

Ossenkopf, V., F. Bensch, M.M. Mac Low and J. Strutzki: Molecular Cloud Structure Analysis by Direct Simulation. In: The Physics and Chemistry of the Interstellar Medium, Abstract Book of the 3rd Cologne-Zermatt Symposium, Shaker-Verlag, Aachen 103 (1998)

Pedersen, H., A.O. Jaunsen, T. Gray, R. Østensen, M.I. Andersen, M. Wold, H. Kristen, A. Broeils, M. Näslund, C. Fransson, M. Lacy, A.J. Castro-Tirado, J. Gorosabel, J.M. Rodriguez Espinosa, A.M. Pérez, C. Wolf, R. Fockenbrock, J. Hjorth, P.Muhli, P. Hakala, L. Piro, M. Feroci, E. Costa, L. Nicastro, E. Palazzi, F. Frontera, L. Monaldi and J. Heise: Evidence for diverse optical emission from gamma-ray burst sources. Astrophys. J. **496**, 311–315 (1998)

Petr, M. G., V. Coudé du Foresto, S. V. W. Beckwith, A. Richichi and M. J. McCaughrean: Binary Stars in the Orion Trapezium Cluster Core. Astrophys. J. **500**, 825–837 (1998)

Phleps, S., K. Meisenheimer, B. Fuchs, C. Wolf and H. Jahreiss: Structure of the Galaxy Studied with CADIS Deep Star Counts. In: Galaxy Evolution: Connecting the Distant Universe with the Local Fossil Record. Paris-Meudon Observatory. Conf. Proc. p. 58 (1998)

Popescu, C.C., U. Hopp, H.-J. Hagen, H. Elsässer: Search for emission-line galaxies towards nearby voids, Astron. Astrophys. Suppl. Ser. **133**, 13–24 (1998)

Porro, I. L., W.A. Traub, N.P. Carleton: Importance of telescope alignment for the erformance of a stellar interferometer. SPIE Conference, Kona, March 1998, SPIE Conf. Proc. 3350 (1998)

Rebolo, R., E.L. Martin and M.R. Zapatero Osorio:Brown dwarfs and extrasolar planets. ASP Conf. Ser. Vol. **134** (1998)

Richichi, A., S. Ragland, B. Stecklum and Ch. Leinert: Infrared high angular resolution measurements of stellar sources. IV. Angular diameters and effective temperatures of fifteen late-type stars. Astron. Astrophys. **338**, 527–534 (1998)

Richichi, A., B. Stecklum, T.M. Herbst, P.-O. Lagage and E. Thamm: The Carbon Star IRAS 06088+1909". Astron. Astrophys. **334**, 585 (1998)

Robberto, M. and T. M. Herbst: Warm dust around Blue-Hypergiants: Mid-IR Imaging of the Luminous Blue Variable HD 168625. Astrophys. J. **498**, 400 (1998)

Robberto, M. and T.M. Herbst: MAX: The New MPIA Thermal Infrared Imager. SPIE Proc. **3354**, p. 711 (1998)

Sabin, T.J., S.M. Roberts, P.J. Withers and C.A.L. Bailer-Jones: Gaussian Process Modelling of the Evolution of Microstructure in Cold-Worked Aluminium-Magnesium Alloys. Conference on Forging and Related Technologies. In: Professional Engineering Publishing Ltd., Bury St. Edmunds, Conf. Transactions 1998-3, 411–420 (1998)

Sandquist, E., R.E. Taam, D.N.C. Lin and A. Burkert: Planet Consumption and Stellar Metallicity Enhancements. Astrphys. J. **506**, 65 (1998)

Sandquist, E., R. E. Taam, D.N.C. Lin and A. Burkert: Double Core Evolution X. Through the Envelope Ejection Phase. Astrphys. J. **500**, 909 (1998)

Schulte-Ladbek, R.E., U. Hopp: The Stellar Content of 10 Dwarf Irregular Galaxies. Astron. J. **116**, 2886–2915 (1998)

Stickel, M., S. Bogun, D. Lemke, U. Klaas, L.V. Tóth, U. Herbstmeier, G. Richter, R. Assendorp, R. Laureijs, M.F. Kessler, M. Burgdorf, C.A. Beichman, M. Braun, M. Rowan-Robinson and A. Efstathiou: The ISOPHOT far-infrared Serendipity north ecliptic pole minisurvey. Astron. Astrophys. **336**, 116–122 (1998).

Stickel, M., D. Lemke, S. Bogun, U. Klaas, M. Kunkel. L. V. Tóth, S. Hotzel, U. Herbstmeier, M. F. Kessler, R. Laureijs, M. Burgdorf, C. A. Beichman, M. Rowan-Robinson, A. Efstathiou, G. Richter and M. Braun: The ISOPHOT Far-Infrared Serendipity Sky Survey.In: Observatory Operations to Optimize Scientific Return. Proceedings of the SPIE Infrared Astronomical Instrumentation Conference, SPIE 3349-48 (1998), (Ed.) P.J. Quinn. SPIE, Bellingham 1998, 115–125.

Stickel, M., D. Lemke, K. Mattila, L. K. Haikala and M. Haas: Far-Infrared Emission of Intracluster Dust in the Coma Galaxy Cluster. Astron. Astrophys. **329**, 55 (1998).

Stickel, M., D. Lemke, M. Haas, K. Mattila, and L.K. Haikala: Far-Infrared Emission of Intracluster Dust in the Coma Cluster. In: A New Vision of an Old Cluster: Untangling Coma Berenice. Proceedings of the Rencontres Astrophysiques International Meeting, Marseille, (Eds.) A. Mazure, F. Casoli, F. Durret, D. Gerbal. World Scientific Publishing Co., 1998, 183.

Surace C. and G. Comte: The Marseille Schmidt Survey for active star forming galaxies: Data on 92 emission line objects in two fields. Astron. Astrop. Suppl. **133**,171.

Thommes, E.: Galaxies at High Redshifts - Observing Galaxies in the Cradle. Proc.Ringberg Workshop »From Galaxies to the Universe«, astro-ph/9812223

Thommes, E., S. Beckwith, R. Fockenbrock, J. Fried, H. Hippelein, U. Hopp, Ch. Leinert, K. Meisenheimer, S. Phleps, H.-J. Röser, D. Thompson, C. Wolf: First Results of the Calar Alto Deep Imaging Survey. Proc. 12th Potsdam Cosmology Workshop. In: ed. V. Müller et al., World Scientific, p. 9–12, 1998

Thommes, E., K. Meisenheimer, R. Fockenbrock, H. Hippelein, H.-J. Röser, S. Beckwith: Detection of candidate Lyα-emitting galaxies at redshift 5.″7, Mon. Not. R. Astron. Soc. **293**, L6-L12 (1998)

Thommes, E., K. Meisenheimer, R. Fockenbrock, H. Hippelein, H.-J. Röser: Search for Primeval Galaxies with the Calar Alto Deep Imaging Survey in The Evolving Universe. Proc. Ringberg Workshop, Kluwer Academic Publishers 1998, p. 419

Thommes, E., K. Meisenheimer, R. Fockenbrock, H. Hippelein and H.-J. Röser: The Calar Alto Deep Imaging Survey. First Results. In: New Horizons from Multi-Wavelength Sky Surveys. McLean B.J., D.A. Golombek, J.J.E. Hayes and H.E. Payne (eds.). Proceedings of the 179th Symp. of the IAU, held in Baltimore 1996, Kluwer Academic Publishers, (1998) p. 296

Thommes, E., K. Meisenheimer, H.-J. Röser, F. Chaffee, S. Beckwith, R. Fockenbrock and H. Hippelein: Candidate Ly - emitting galaxies at z = 5.7 revised. Mon. Not. R. Astron. Soc., **239**, L6 (1998)

Thompson, D. J. and S .V .W: Beckwith: Seeing Red:Extremely Red Objects from the CADIS K' Survey. In: Eds. V. Mueller, S. Gottloeber, J. P. Muecket, J. Wambsganss: Large Scale Structure: Tracks and Traces. World Scientific, p. 13–14 (1998)

Tóth, L.V., M. Kun,and L. Szabados (Eds.): The Interaction of Stars with their Environment. Communications from the Konkoly Observatory of the Hungarian Academy of Sciences, No. 100, Vol. 12 Part 2 (1998)

Tóth, L.V., D. Lemke, O. Krause, S. Hitzel and M. Stickel: Detection of Cold Interstalla Clouds by the ISOPHOT Serendipity Survey. AG Abstract Series **14**, E12 (1998)

Vives, T.: La Edad del Universo. Tribuna de Astronomía No. 146, 20–25 (1998)

Vives, T.: Los enigmas y misterios de la astronomía actual. Univeso No. 36, 20–27 (1998)

Wehrse, R., Ph. Rosenau, A. Survernev, J. Liebert and Ch. Leinert: ISOPHOT's observations of 3 M Dwarfs. Astrophys. & Space Science **255**, 127 (1998).

Williger, G., A. Smette, C. Hazard, J. Baldwin and R. McMahon: Large Scale Structure in the Ly Forest. In: New Horizons from Multi-Wavelength Sky Survey, IAU Symp. No. 179, Eds. B.J. McLean, D.A. Golombek, J.J.E. Hayes, H.E. Payne, Kluwer, Dordrecht, 1998, 329–331

Wirth, A., J. Navetta, D. Looze, S. Hippler, A. Glindemann and D. Hamilton: Real-time modal control implementation for adaptive optics. Appl. Optics Vol. 37 (21), 4586-4597.

Woitas, J. and Ch. Leinert: HV Tauri C - Herbig-Haro flow or stellar companion with strong forbidden emission lines? Astron. Astrophys. **338**, 122-126 (1998)

Woitas, J. and Ch. Leinert: How frequent are substellar companions in T Tauri binary systems? AG Abstract Ser., **14**, p.17 (1998)

Wolf, Ch., et al.: Wide Field surveys in Cosmology, Conf. Proc. p. 173 (1998)

Wolf, Ch., R. Mundt, D. Thompson, F. Chaffee, S.V.W. Beckwith, R. Fockenbrock, J. Fried, H. Hippelin, J.-S. Huang, B. von Kuhlmann, Ch. Leinert, K. Meisenheimer, S. Phleps, H.-J. Röser and E. Thommes: Discovery of three very distant M and L dwarfs. Astron. Astrophys. **338**, 127–131 (1998)

Wolf, Ch., S.V.W. Beckwith, F.H. Chaffee, R. Fockenbrock, J. Fried, H. Hippelein, J.-S. Huang, B. von Kuhlmann, Ch. Leinert, K. Meisenheimer, H.-J. Röser, S. Phleps, E. Thommes and D. Thompson: CADIS multicolor approach finds more $z >$ 2.2-QSOs. Proc. of IAP 1998, p. 173

York, D.G., M.M. Mac Low, B. Brown, L.M. Franco, L.M. Rebull, C. Graziani and J. Lauroesch: DuSable High School Internet Project and its influence in connecting Chicago Public Schools to the Internet. Bull. Amer. Astron. Soc. 30 (1998)

Diploma Thesis

Kranz, Th: Measurement of the Straylight from Sun, Moon and Earth within the ISO Space Telescope Heidelberg University, 1998

Doctorate Theses

Berkefeld, T.: Studies about Measurement and Correction of the Contributions of Individual Atmospheric Layers to Wavefront Distortion. Heidelberg 1998

Fockenbrock, R.: Spatial Distribution, Luminosity Function and Statistics of Emission Line Galaxies at $0.2 < z < 1.2$. Heidelberg 1998

Klessen, R.: Fragmentation of Molecular Clouds: The Initial Phases of a Stellar Cluster. Heidelberg

Petr, M.: Binary Stars in the Orion Trapezium Cluster: A High Angular Resolution Near-Infrared Imaging Study. Heidelberg 1998

Theurer, J.: Generation and Propagation of Acoustic Wave Spectra in Late-Type Stellar Atmospheres. Heidelberg 1998

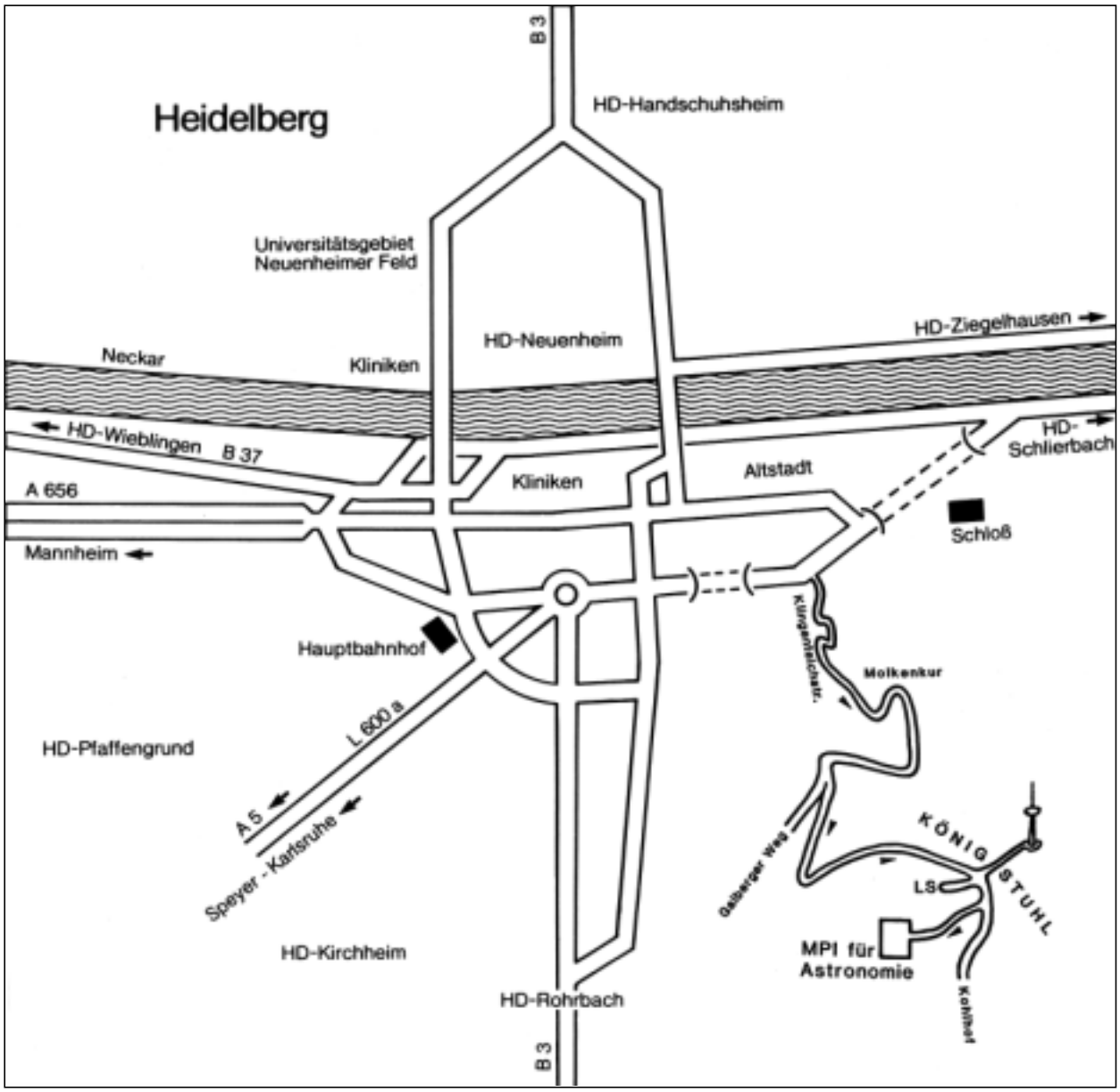

Heidelberg – City map